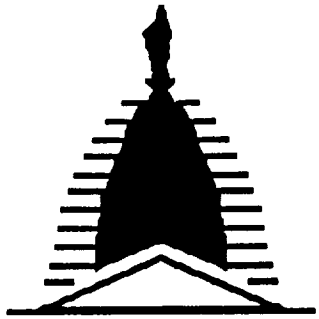

UNIVERSITY of
NOTRE DAME

NASA/USRA UNIVERSITY ADVANCED DESIGN PROGRAM 1989-1990

UNIVERSITY SPONSOR
BOEING COMMERCIAL AIRPLANE COMPANY

FINAL DESIGN PROPOSAL

THE DRAG-n-FLY

A Proposal in Response to a Low Reynolds Number Station Keeping Mission

May 1990

Department of Aerospace and Mechanical Engineering
University of Notre Dame
Notre Dame, IN 46556

Drag - n - Fly

A Proposal in Response to a Low Reynolds Number Station Keeping Mission

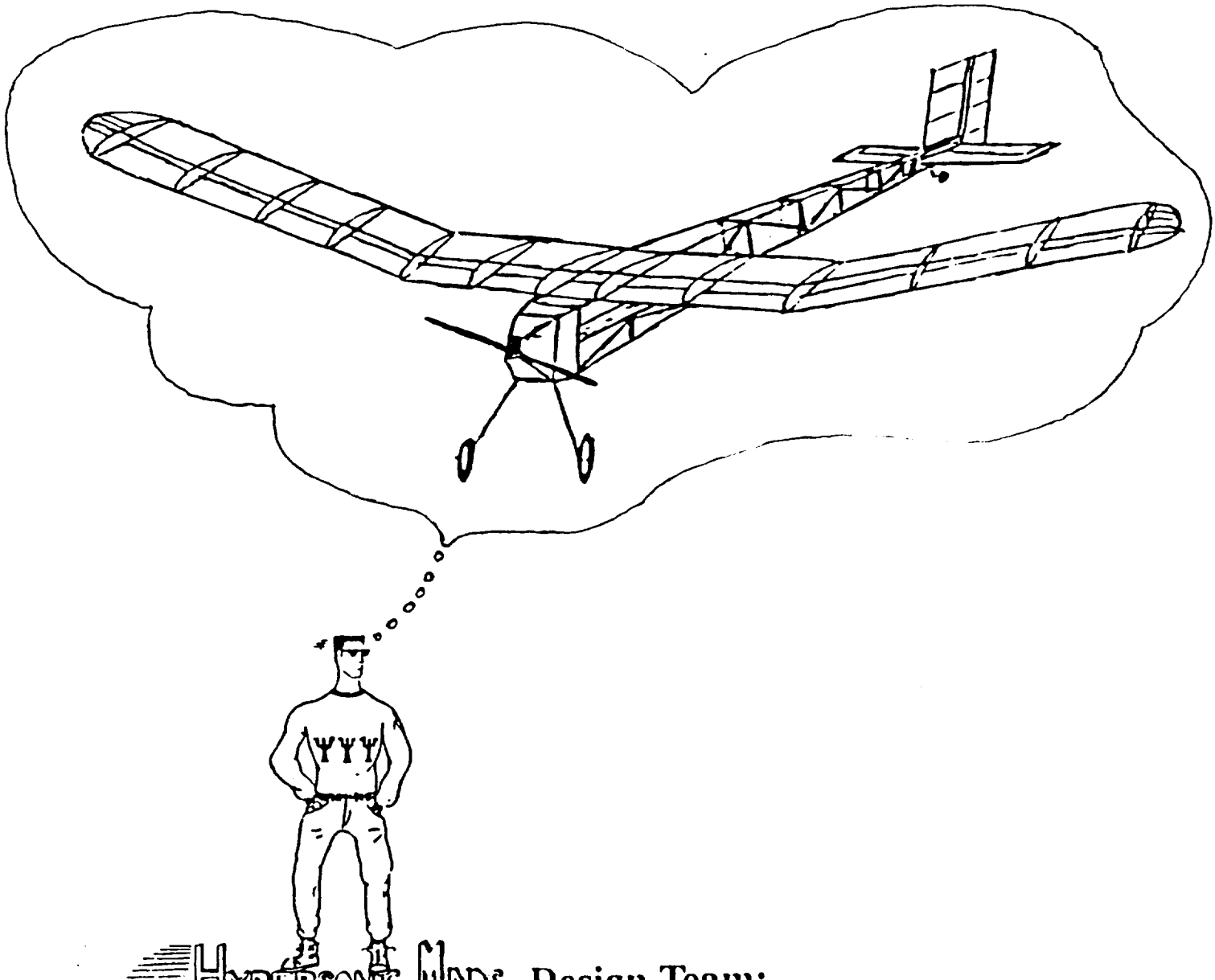

HYPERSONIC MINDS **Design Team:**

Mark Foohey
John Niehaus
Jenny Neumann
Pat Deviny
Jerry Zurovchak
Joey Brenner
Peter Gendron

Submitted May 7, 1990

Table of Contents

EXECUTIVE SUMMARY

The Drag-n-Fly is a remotely piloted, low Reynolds number vehicle. It was designed to maintain level controlled flight and fly a closed course at flight speeds corresponding to Reynolds numbers of less than 2×10^5 and as close to 1×10^5 as possible. The success of the mission will be associated with achieving the lowest mean chord Reynolds number possible and maximizing loiter time on the course.

A three-view drawing and specifications summary follow this executive summary.

The flight plan for the Drag-n-Fly calls for the vehicle to ascent to a cruise altitude of 25 ft. Once achieved, the Drag-n-Fly will demonstrate it's maneuverability by flying within a restricted altitude range on a figure "8" course with a spacing of 150 feet between the markers which define the course. The Drag-n-Fly will complete three laps and then a final oval to bring the RPV back around in preparation for landing.

The airfoil selected for the Drag-n-Fly is a Spica chosen for its high lift coefficient at low Reynolds number. The actual lifting surface for the Drag-n-Fly is a 8.5 foot long wing with total surface area of six square feet and aspect ratio of 12. There is no sweep or twist associated with the wing and the taper ratio is 1.0. During the flight the lifting surface expects a wing loading of approximately 7.1 $0z/ft^2$.

The propulsion system for the Drag-n-Fly consists of a 10" diameter propeller mounted on the front of the vehicle. The propeller, the Zinger 10-6, is driven by the ASTRO 05 electric motor and eight 500 MAH Nickel Cadmium batteries. This motor/battery combination was selected not only because it is capable of providing the thrust needed to accomplish the mission, but also because of its lightweight nature. An electronic speed control will also be utilized to maintain altitude through the turns.

Structural support for the Drag-n-Fly comes from four box beams running the length of the fuselage. These box beams will be constructed of Balsa wood. The strongest part of the aircraft is the front fuselage, since the motor and avionics are located in this region. This area will be reinforced by panels to increase the strength of the front fuselage. The spars of the wing will be made of spruce and the ribs will be formed of Balsa wood.

The tail and horizontal stabilizers are located for aft of the lifting surface in order to assure proper static stability. The vertical tail area is 0.5 square feet and the horizontal tail area is 1.05 square feet. Two movable control surfaces are used to maneuver the Drag-n-Fly during the figure eight course. A rudder will be implemented to control yaw and an elevator to control the pitch during the flight course, and both control surfaces will be actuated by mirco-servos. The roll stability will be handled by dihedral angle of 10.5 degrees.

The present design for the Drag-n-Fly will meet the criteria for the present mission. Some areas of concern are in the construction of the dihedral angle on the wing when it is mounted to the fuselage,control of the aircraft once in flight (will the control surfaces deflect enough to maneuver the aircraft), and the fact that no one in Design Group A has any prior experience in building. While there are areas of concern, this design group is very confident that this aircraft will be a highly-maneuverable RPV with the capability to fly at low Reynolds number regimes.

SPECIFICATIONS	VALUES
Reynolds number	112,000
Flight Velocity	25 ft/s
Engine Type Engine Power	ASTRO 05 90 Watts @ 7200 RPM
Endurance	193 seconds
Range	4831 feet
Propeller	Zinger 10-6
Take-off distance	31 feet
Landing distance	133 feet
Fuselage Average Diameter	4.67 inch
Fuselage Length	41 inches
Wing Surface Area	6 ft^2
Wing Root Chord	8.5 inch
Wing Taper Ratio	1.0
Wing Span	8.5 feet
Wing Aspect Ratio	12
Wing Max Lift Coefficient	1.0
Wing Dihedral	10.5 degrees
Wing Angle of Incidence	5 degrees
Vertical Tail Area	0.5 ft^2
Horizontal Tail Area	1.05 ft^2

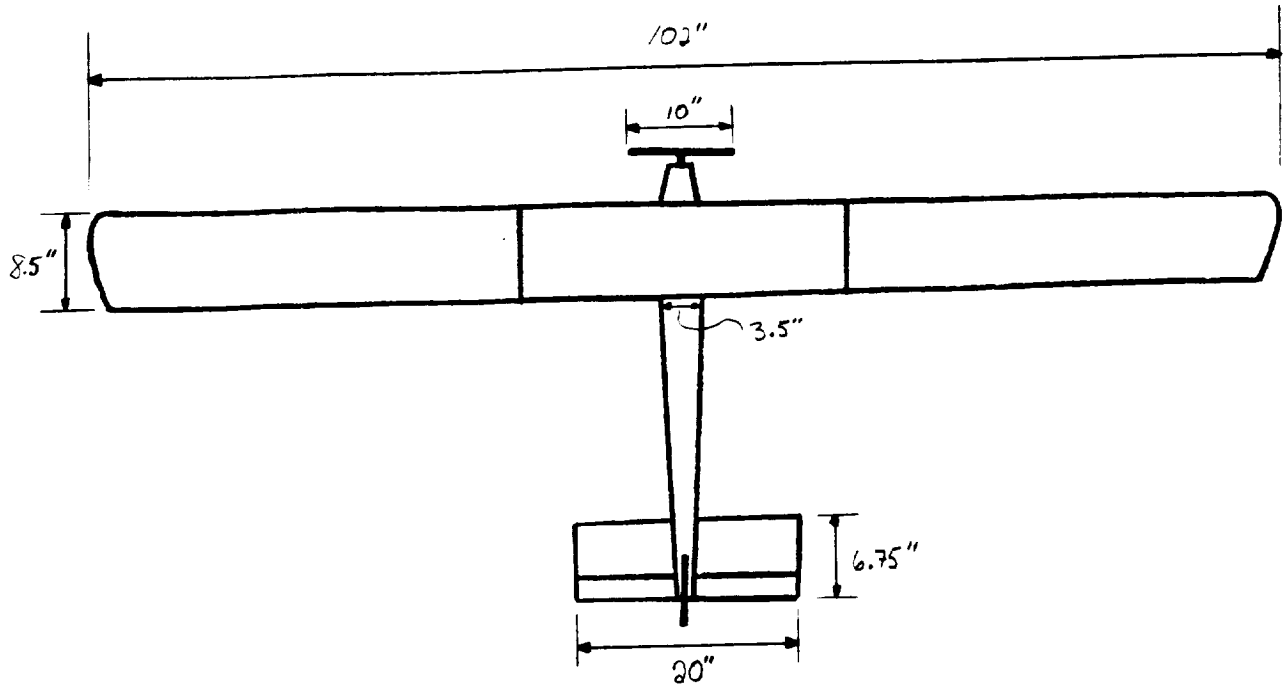

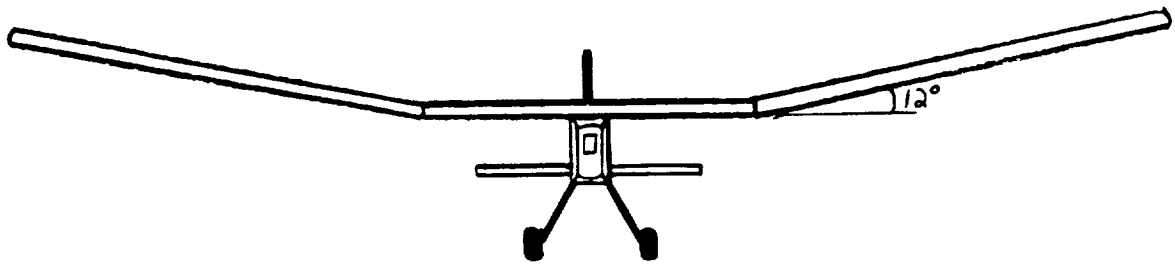

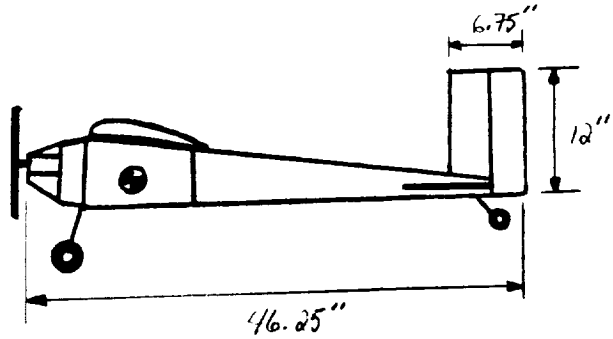

DRAWN TO SCALE

1 PRELIMINARY CONCEPT DESIGN

1.1 MISSION REQUIREMENTS AND OBJECTIVES

1.1.1 MISSION DEFINITION

The objective of this mission is to develop a remotely piloted vehicle (RPV) which will maintain level controlled flight and fly at speeds corresponding to Reynold's numbers less than 2×10^5 and as close to 1×10^5 as possible. This mission is defined with the following requirements and constraints. The RPV is required to fly a closed figure eight pattern within a restricted air space. The course envelope is constrained by the dimensions of the flight arena (Loftus Center) and two pylons spaced 150 feet apart. The maximum allowable altitude is 25 feet, and the RPV must never exceed this height at any point on the course. The RPV must take-off from the pit area, complete three figure eight laps, and finally, return to the pit area for landing. The greatest measure of merit is awarded for accomplishing this mission with the lowest mean chord Reynold's number in conjunction with maximizing the loiter time on the closed course.

MISSION REQUIREMENTS
- Maintain level flight at $1 \times 10^5 \leq Re < 2 \times 10^5$.
- Fly within a restricted airspace, (Loftus Center).
- Follow a closed figure eight pattern.
- Never exceed altitude of 25 feet.
- Take-off and land in pit area.

1.1.2 AIRCRAFT DESIGN

The proposed aircraft design must satisfy the following requirements and constraints. Only those propulsion systems, which have non-airbreathing engines and do not emit any mass, may be used. The RPV must take-off from the ground, and land on the ground, and do so within the designated 150 foot pit area. It must be able to be remotely controlled, with ample maneuverability and control, so that it can be flown within the limited airspace by a pilot with minimal flying experience. The aircraft must be of adequate strength and size in order to carry an instrument package payload which has a weight of two ounces and

dimensions of 2" x 2" x 2". In addition, the complete aircraft must be able to be disassembled to fit within a 2' x 2' x 4' container for transportation and storage.

DESIGN CONSTRAINTS
- Non-Airbreathing engines only.
- Take-off and land from the ground.
- Must be remotely controlled.
- Fit in a 2'x 2'x 4' storage container when dismantled.
- Carry a 2 ounce , 2"x 2"x 2" payload.

1.1.3 DESIGN OJECTIVES

The mission and system were further fixed by the design objectives and goals set by the design team. These objectives and goals were determined independent of the RPV configuration.

1.1.3.1 TAKE-OFF

The first phase of the mission is the take-off and climb stage. The main objective of the take-off phase is to have the airplane achieve lift off and reach a cruise altitude of 15 feet by the end of the 150 foot pit area. This goal, in turn, determined the ground roll distance and ascent angle. In order to reach the desired altitude of 15 feet by the end of the 150 foot pit area, a maximum ground roll distance of approximately 30 feet with an ascent angle of 10 degrees and a rate of climb of approximately 3.1 feet per second is necessary. The landing gear will be a permanently attached system with no assisting launch device being implemented. Wheel control will not be used since the rudder will provide sufficient control to steer the plane while taxiing.

1.1.3.2 CRUISE

Once altitude has been reached, a banking maneuver must be performed immediately, in order to perform the required turn. A large turn radius is desired to maximize the loiter time through a turn. This corresponds to a longer flight distance as well as a lower bank angle. The lower bank angle reduces the power needed to propel the RPV through each turn. The targeted radius is 55 feet, allowing five feet on the outside to compensate for pilot error and response time. The turn will encompass 190 degrees. The remaining

portion of the flight lap consists of two straight flight sections of equal length, connecting the two turns as shown in figure 1.1-1.

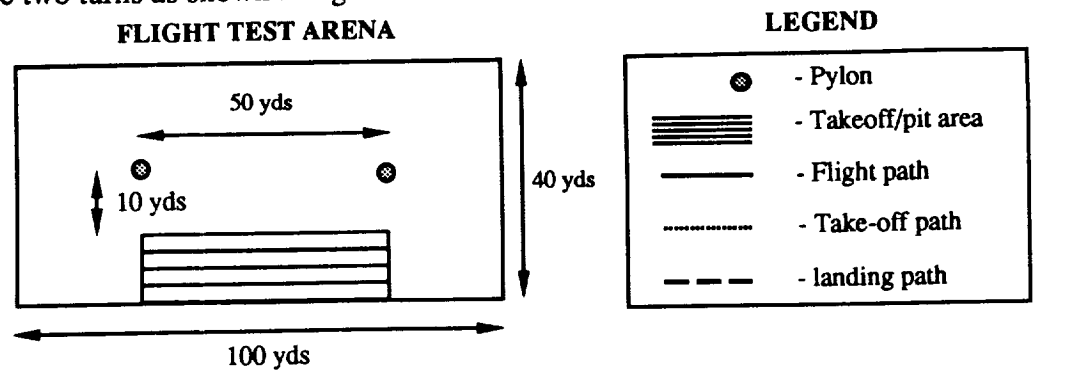

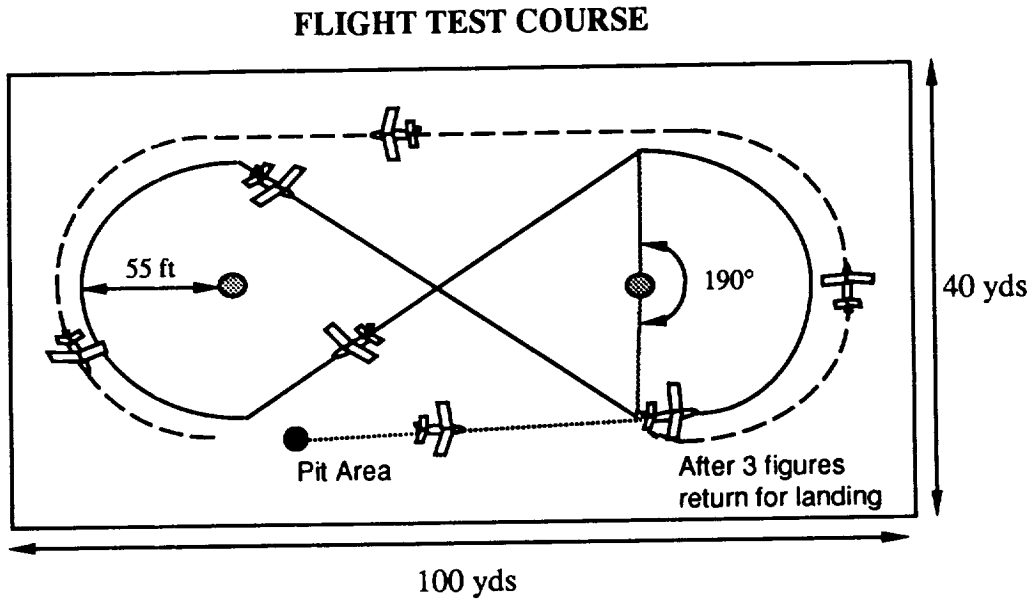

Figure 1.1-1

1.1.3.3 TURNS

During each turn, the RPV will bank at an angle of approximately 20 degrees and experience a wing loading of 7.1 ounces per square foot. It is desired to roll the RPV to the necessary bank angle in a minimum of two seconds, requiring a roll rate of 10 degrees per second. Turn maneuvers will be performed by deflecting the rudder and elevators.

Two control channels will be used to control these deflections. A third control channel will employ a speed control device to ensure level turns throughout the flight, as a result, the speed will not remain fixed during the flight. Although the speed will vary, a target value of 25 feet per second was set as the cruise velocity.

1.1.3.4 FLIGHT PATH / LANDING

The RPV flight path for the entire mission includes a 30 foot ground roll, a 10 degree ascent to an altitude of 15 feet, three figure eight laps, and a final sweep around the course to bring the RPV into position for landing. The total distance of this flight corresponds to a range of 4830 feet and an endurance of 193 seconds. The RPV will descend as it approaches the pit area for landing. The descent angle will not exceed 10 degrees, or go below the minimum glide angle of three degrees. Upon touchdown, the engine will be shut off. It will be possible to switch the engine on and off via a remote control. Since no brakes will be used, a landing distance of 64 feet is needed to bring the plane to a complete stop.

1.1.3.5 GENERAL CONFIGURATION REQUIREMENTS

The final area of design to be addressed are general configuration requirements which will affect any particular design chosen. The RPV weight shall remain constant during all phases of the flight with the target weight being three pounds. A maximum lift coefficient of 1.2 is desired. A color scheme will be chosen such that the RPV will be highly visible to the pilot and design team, but basic, so as not to require an additional weight penalty.

1.2 CONCEPT SELECTION

Initially, from the seven concepts that were produced by each member there were two basic types of aircraft that were being considered to complete the mission. The first was an unconventional tandem/joined-wing aircraft with the wings joined at a point about three-quarters out on the semi-span. The other six being the more conventional wing-tail-fuselage type aircraft with the primary differences in the tails. These seven concepts were reduced to three such that they could be compared and one could be selected for the design.

The first candidate was the tandem/joined-wing aircraft as shown in Figure 1.2-1 a,b, and c. The front end of the fuselage was expected to be quite large tapering down to a small circular back end. The propeller was placed at the rear end of the aircraft creating a pusher type aircraft. One possible advantage of this aircraft was a reduction in weight because the joined wing reduces the wing bending and because only two channels of control were needed. Also, the double wing would disperse the surface area necessary for flight allowing decreases in weight possibly leading the aircraft to fly at slower speeds which would provide merit for this mission. Another appealing factor of this aircraft was the originality and uniqueness of designing and building a different type of aircraft.

The second concept which was considered was a conventional aircraft with a high wing, low horizontal tail and twin vertical tails; one each on the tips of the horizontal tail. This aircraft would have three channels of control; rudder, elevator and speed. Roll maneuvers would be achieved from a combination of the rudder and a dihedral angle. The anticipated advantage of the twin vertical tails was the extra rudder control power (without an excessively large rudder) needed to travel the figure eight course with no ailerons. For ease of construction, the fuselage cross section was square in design and the wing had no taper. In addition the wing had a high aspect ratio for better lift and drag characteristics.

The third concept was essentially the same as the second concept except for the tail design. Only one vertical tail was proposed in this design, but again, the horizontal tail would be a low tail. The other primary difference being that this aircraft would have ailerons and thus require one more channel of control. One further difference was that the fuselage was round in order to decrease body drag. This concept included wing taper for reducing drag.

To help in the selection process, the two more conventional designs were combined into one concept boasting some advantages of each and then this concept was compared with the tandem wing design. The conventional aircraft that was considered is shown in Figures 1.2-2 a,b, and c. It included a high, tapered wing with dihedral. Taper was considered to decrease drag and the dihedral and high wing were presumed necessary to achieve roll maneuvers and increase roll stability. The wing had a high aspect ratio (about 9) for better lift and drag characteristics. The horizontal tail was low to keep it out of the wake of the wing and there were two vertical tails to provide sufficient rudder size for roll and yaw control and sufficient tail area for acceptable roll stability. There were three channels of control, speed, rudder and elevator. Roll maneuvers were expected to be achieved through a healthy dihedral angle and rudder deflection. The fuselage was rounded with a three inch

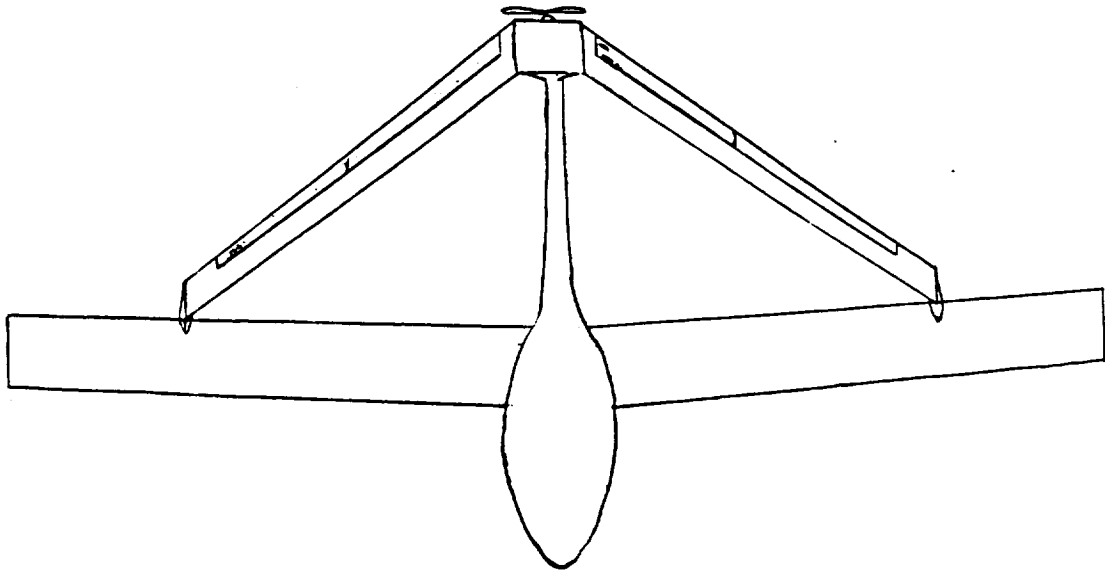

TOP VIEW

Figure 1.2-1 a

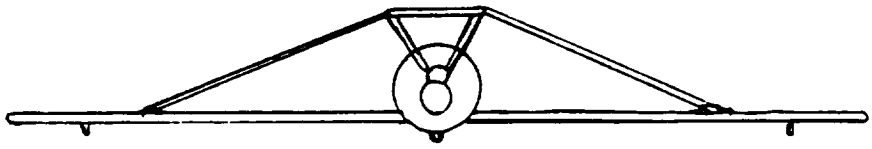

FRONT VIEW

Figure 1.2-1 b

SIDE VIEW

Figure 1.2-1 c

TOP VIEW

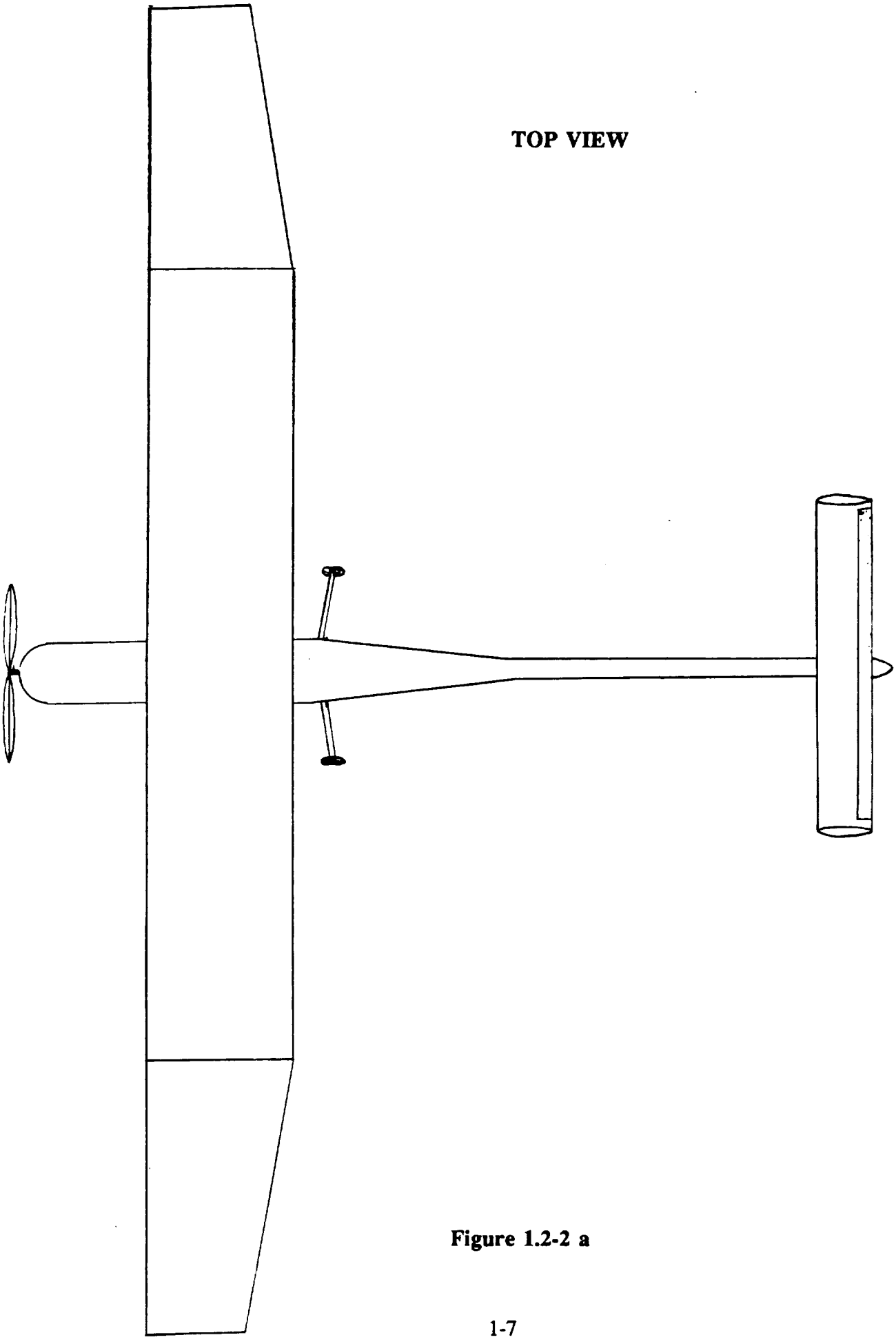

Figure 1.2-2 a

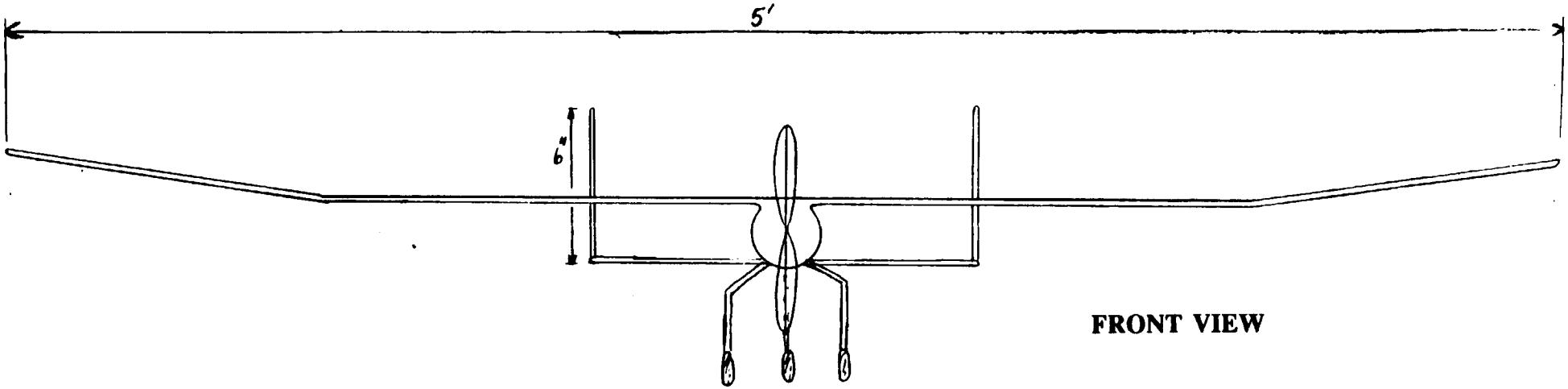

FRONT VIEW

Figure 1.2-2 b

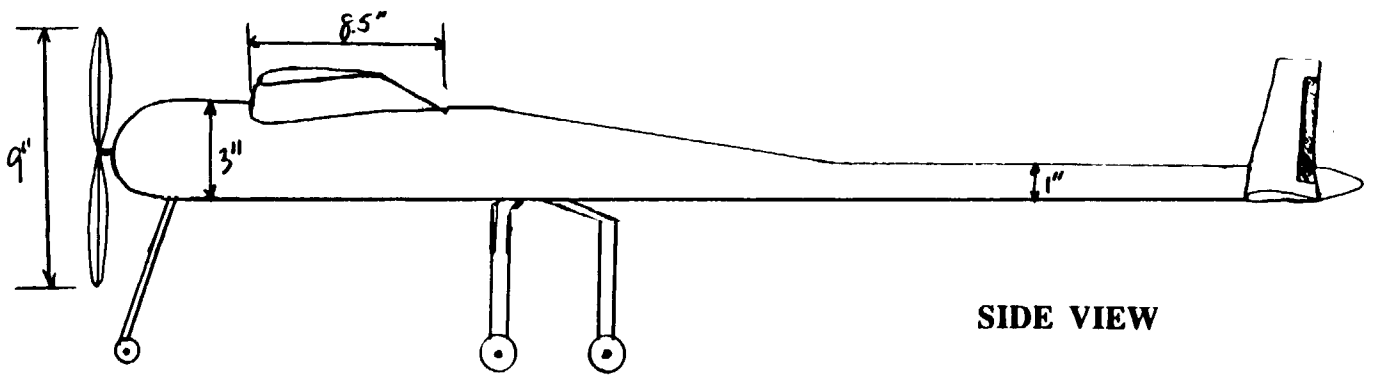

SIDE VIEW

Figure 1.2-2 c

diameter in the forward section, just large enough to hold the payload. It tapered down to one inch at the tail. The fuselage size was minimized and its shape rounded in order to reduce drag. The proposed landing gear was tricycle type.

Advantages of the conventional type aircraft included the following.

- There was a large database on this type of aircraft giving typical trends for RPV aircraft based on reference areas.
- With a large data base the design team could concentrate on problems associated with low Reynolds number and not primarily on problems dealing with a new type of design.

The other concept competing with the semi-conventional RPV was the tandem/joined-wing plane. This concept is shown in Figures 1.2-1 a,b, and c as was noted previously. As shown in the diagram, the wings are connected at about three-quarters of the semi-span of the main wing. The secondary wing includes what would be called ailerons but they could act as ailerons, rudder, and elevator since they are at an angle with reference to the horizon. There is also a small rudder as the anticipated yaw control with the ailerons was not assumed sufficient. The ailerons would be one channel of control, although it must include a mixer, and the rudder another channel. The fuselage is large in the front since it was anticipated that most of the payload and batteries could be stored in this area. The landing gear was again tricycle type. The advantages of this concept are as follows.

- A possible reduction in weight of the aircraft.
- Large wing areas, including both wings, without large, heavy, and multiple spars.

The weight reduction could not be proven but it was speculated that the joined tandem wings could strengthen the aircraft in the wings and back end of the fuselage and as a result less structural support would be needed allowing a reduction in weight. One further appealing factor of this concept was the originality.

With the advantages came some disadvantages of the tandem/joined-wing design.

- Their was no database for this type of aircraft.
- Control surface mechanisms may be difficult to integrate into the design.
- The tandem/joined-wing configuration may pose difficulties in longitudinal static stability due to the odd horizontal tail or second wing.

The lack of a database would make it difficult to validate a lot of the results. The difficulties with the control mechanisms may be just one of the many construction difficulties in this design.

Measuring the advantages and the disadvantages, the semi-conventional wing, fuselage, tail aircraft was selected. The primary reasons being the data base availability and the uncertainty of whether speed and weight could be reduced with the tandem wing aircraft. Structural study and research of the tandem/joined-wing aircraft produced no positive results as the whether the advantages could actually be materialized. Also, the advantage of a data base for the concept selected made the initial design phase simpler allowing more time for the higher level design.

Several changes in the original concept took place as more detailed analysis was done. Reducing the twin vertical tail to a single vertical tail was one major change. The necessary size of the vertical tail for roll control was not as large as anticipated. In addition, attaching twin vertical tails would have required adding structure outboard on the horizontal tails thus adding weight. Another change was the the size of the fuselage. As a truss style fuselage was decided upon to minimize weight, the height of the fuselage was increased. The increase created a larger moment of inertia, thus lowering the bending moments. The height changed from 3 to 6 inches and the width to 3.5 inches at the wing, tapering down to a 2 inch width and height at the tail. To simplify construction of the truss fuselage, the shape was changed from round to rectangular. Another simplification to ease construction was the elimination of taper of the wing. Studies on the effect of taper on the program LinAir demonstrated only small drag decreases that would be non-rewarding for the time spent making every airfoil of the wing a different size. The aspect ratio was also increased to even a higher value of 12. This change allowed more surface area without increasing the mean aerodynamic chord and Reynolds number. Despite the large increase in the span of the wing, the aircraft roll rate was still adequate and the structural support was still expected to be sufficient to hold the wing. The plane could then produce three pounds of lift with a coefficient of lift of 0.67. The current status of the design is as shown in Figures 1.2-3 a,b, and c.

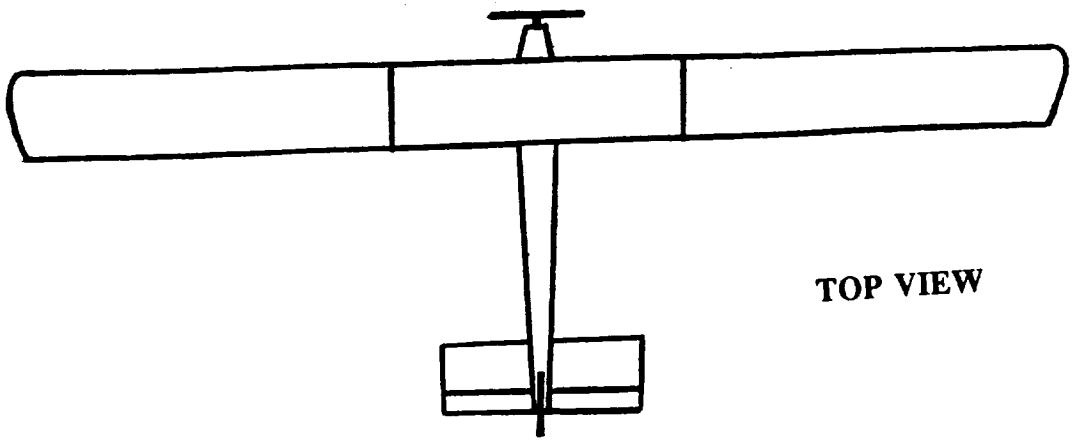

TOP VIEW

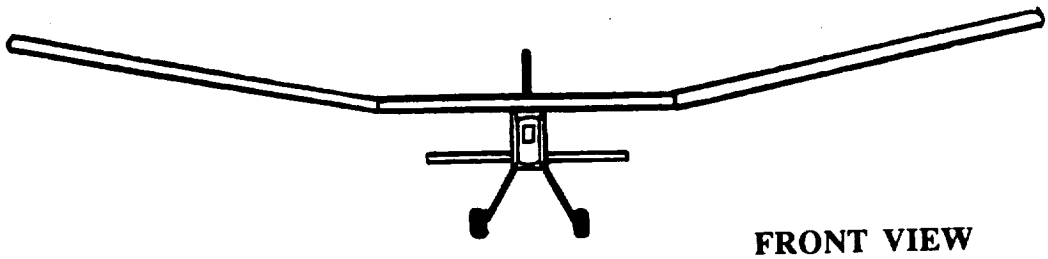

FRONT VIEW

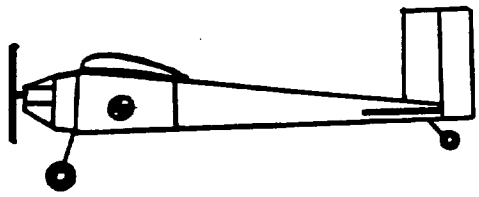

SIDE VIEW

Figure 1.2-3

2 CONCEPT DESIGN

2.1 AERODYNAMIC DESIGN

This section discusses the wing and airfoil selection, and drag estimation method used for the DRAG-n-FLY. Included in this section is the lift curve for the aircraft, as well as its drag polar.

2.1.1 WING DESIGN

The wing sizing and design was one of the more flexible areas in the overall design. Initially, a rectangular, one-piece, high aspect ratio wing was selected for the RPV. The original surface area estimates came from an aircraft weight estimation, and the lift required to support that weight both at takeoff and at cruise. A high aspect ratio was chosen to have the necessary lifting surface area while minimizing the wing chord (and thus, the minimum chord Reynolds number).

The selected airfoil is the SPICA, chosen from a number of other airfoils as the subject of an airfoil trade study. Once the airfoil was chosen, preliminary estimates of the available lift pushed surface area and wingspan up. The propulsion team, analyzing power required and power available curves, determined that a higher surface area was needed. Table 1 demonstrates the jump in sizing over the course of the design period, from February 1 to March 22, 1990.

Table 2.1-1 Changes in Wing Sizing

Parameter	**2/1/90**	**3/1/90**	**3/22/90**	**final concept**
AR	9.0	10.0	12.0	12.0
S (ft2)	3.4	5.0	6.0	6.0
b (ft)	5.4	7.07	8.5	8.5

Several wing parameters remained unchanged from the start. A taper study showed that the positive effects of taper, such as decreased drag, were not substantial enough to outweigh the difficulties in constructing a wing with rib lengths changing with spanwise distance, a

task requiring accurate placement and the ability to hold it all in place. Twist was never added for similar construction difficulties. Sweep is not needed at low speeds.

Dihedral, however, was added to make effective turning possible without the use of ailerons. Rather than set the entire wing with dihedral, two outboard sections with dihedral were built. This part of the design was driven by control analysis.

The final wing configuration is shown in Figure 2.1-1 and has the following characteristic as seen in Table 2.1-2.

Table 2.1-2: Final Wing Characteristics

Surface Area ,S	6 ft^2
Wingspan, b	8.5 ft
Chord, c	8.5 in
Aspect Ratio, AR	12.0
Airfoil section	SPICA
Incidence angle	5°
Dihedral:	0° from fuselage to 1.2 ft along the span
	12° from 1.2 ft spanwise to tip
Taper	None
Twist	None

3-D View of Left Wing

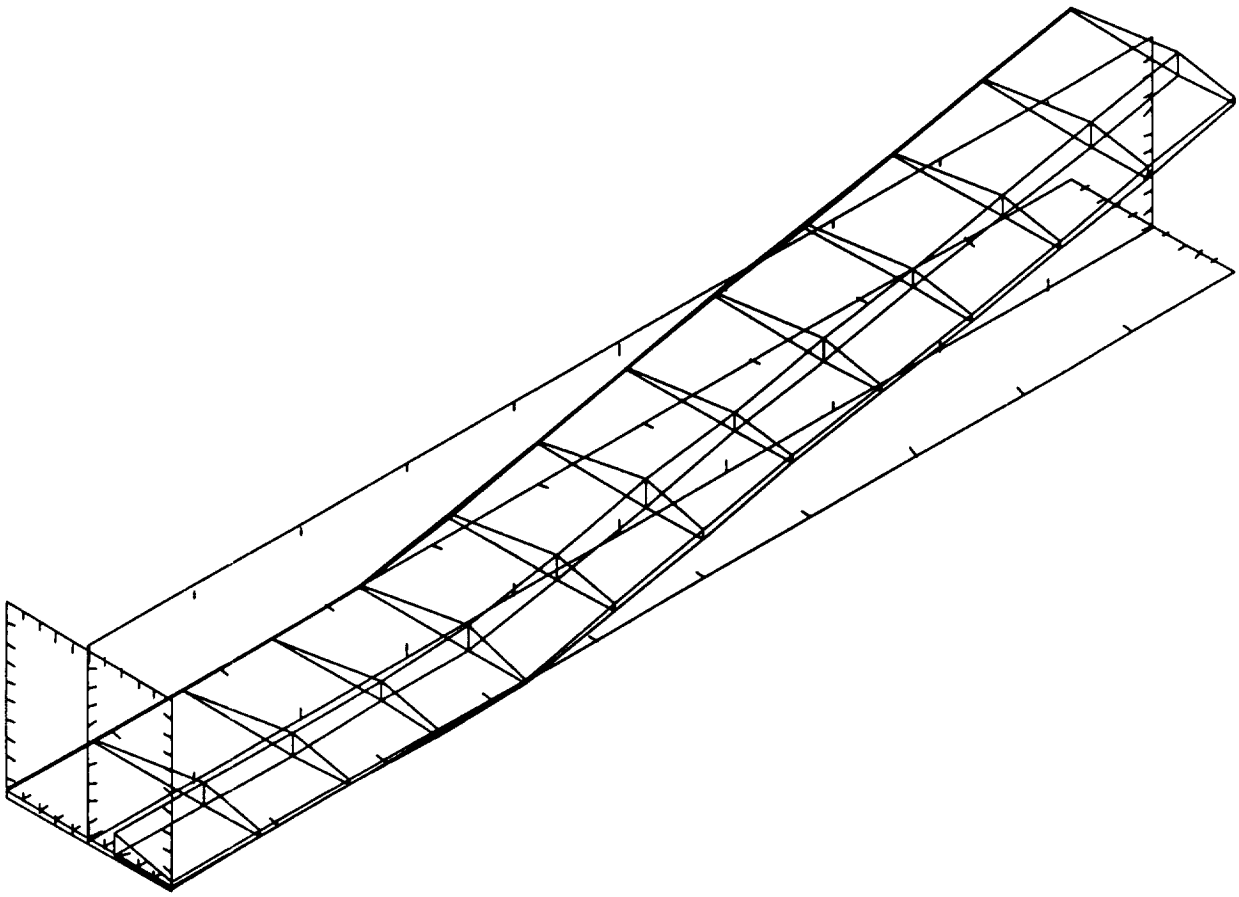

Figure 2.1-1

2.1.2 AIRFOIL SELECTION

Due to the complications associated with low Reynold's flight, such as laminar flow separation, selecting the proper airfoil became a crucial part of the system design. As a result, a study was performed to determine which airfoil section best met the needs of the mission. Since the RPV will fly at a low Reynold's number (Re=100,000), only those airfoils that performed at well in low Re flight were considered. This, however, still left several airfoil sections to choose from. To solve this, a list of criteria was established in order to select the proper airfoil from those available. The criteria took into account the airfoil thickness, aerodynamic characteristics, and the shape of the airfoil.

2.1.2.1 AIRFOIL THICKNESS

Thickness is an important factor in the selection of the airfoil for two reasons, strength and weight. Since a cantilevered wing is desired, the airfoil section needs to be thick enough (at least 10 % of the chord[1]), to adequately support the main wing spar without the use of external bracing. However, because a low weight vehicle is desired, the airfoil section should not be so thick that it adds unnecessary weight. It has been found that the structural support gained by sections of thickness greater than 15% is very small compared to the additional weight gains.[2] Therefore, only those airfoils that fell in the medium thickness range, or those with a thickness of 10 to 14 percent of the chord, were considered.

2.1.2.2 AIRFOIL SELECTION DATA AND CRITERIA

Once the thickness range was selected, aerodynamic characteristics of the remaining airfoils were studied and compared. This was accomplished using experimental test data given on airfoils. The mission goal of a low Reynold's number flight, however, limited the data that could be used, because, as the Reynold's number decreased, so did the airfoil performance. At low numbers, (such as 100,000), it becomes difficult to keep the flow attached to the airfoil, and as a result laminar flow separation occurs. Because of this, the only data used, was that which was obtained at a Reynold's number similar to what was trying to be achieved.

---

[1] Korff, Walter H., Lightplane Design, C. A. Steele Publishers, Mt. Vernon, Illinois, 1935.
[2] Ibid.

Using lift curve slopes and drag polars[3] , the airfoils were examined for high lift (C_{Lmax}), the lowest drag, and a gentle stall behavior (as opposed to an abrupt stall), and a high stall angle (α_{CLmax}), according to the criteria below. The design team felt that this criteria was the minimum the airfoil would need, based upon the mission and design objectives. In addition, the data was also studied for separation bubbles. Only those airfoil sections with the best combination of the criteria listed below, and those that did not appear to have a separation bubble, were examined further.

AIRFOIL SELECTION CRITERIA

- $C_{Lmax} \geq 1.0$
- Low drag
- Gentle Stall behavior
- $\alpha_{CLmax} \geq 10°$
- No separation bubbles

2.1.2.2.1 STALL BEHAVIOR

Although a low drag is desired, it is also important to keep stall behavior in mind. For instance, some of the lowest drag airfoils have the worst stall characteristics. Even though it may have the lowest drag, an airfoil that stalls abruptly is undesirable because, with such an airfoil, lift is lost without warning when the wing stalls. As a result more altitude is lost in trying to recover after the stall, then might have been gained from the marginally lower drag.

2.1.2.2.2 STALL ANGLES

Along with a gentle stall, airfoils with large stall angles were desired. Large stall angles allow for larger margins of safety which are desirable in the event that one of the parameters should vary from what is expected. Suppose, for instance, the friction from the ground causes the RPV to roll for take-off at a slower velocity than expected. The lower velocity would require a higher C_L value in order to achieve the lift necessary for take-off. For example, using the equation below, a three pound aircraft (W), with a six square feet wing area (S), would need a lift coefficient of about 0.87, to take-off at 20 ft/s (V).

---

[3] Selig, Michael S., Donovan, John F., and Fraser, David B., Airfoils at Low Speeds, H. A. Stokely, Publisher, Virginia, 1989.

$$L=W = 1/2\ \rho\ V^2\ S\ C_L$$

If the ground was so rough that it only allowed the plane to reach a velocity of 20 ft/s, the lift coefficient would need to be at least 1.0 to achieve lift-off. An increase in C_L, such as this, could put the plane at, or very near its C_{Lmax} value for some of the airfoils, as can be seen in Figure 2.1-2. Because stall occurs near C_{Lmax}, the plane might be trying to take-off at its stall velocity, and as a result, it will never lift-off. In this case, however, an airfoil with a large stall angle would have a better chance at still being able to take off.

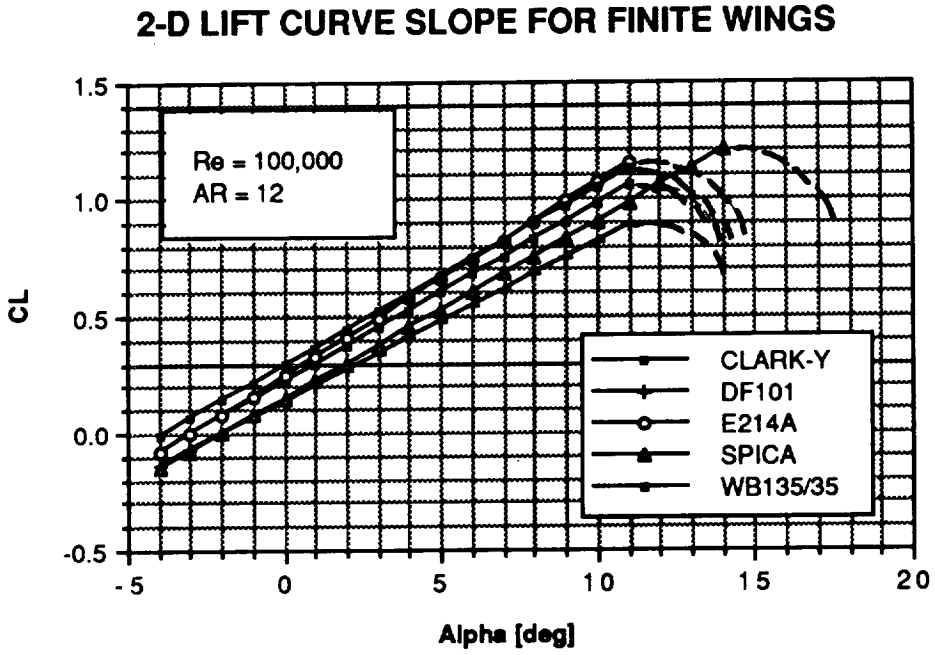

Figure 2.1-2

The graph above shows the lift curve slopes for the final five airfoil sections considered. The data shown in this plot is the for a two dimensional finite wing. It was found by correcting the infinite wing data for aspect ratio (AR = 12) using the equation below.[4]

$$a = a_0 / [\ 1 + a_0/(\pi\ AR\ e)]$$

[4] Anderson, John D., Jr., Introduction to Flight, McGraw-Hill, Inc., U. S. A. 1985.

The infinite data needs to be corrected because the slope of the lift curve for a finite wing (a), is less than that for an infinite wing (a_o). The span efficiency factor (e), used in the above calculation was 0.87. A further discussion on how the span efficiency was estimated can be found in section 2.1.3.

2.1.2.2.3 AIRFOIL SHAPE

The final criteria used to select an airfoil was its shape. In order to make construction of the wing as easy as possible smooth and simple shapes were chosen. Those sections with complicated shapes (such as those with high camber or very thin trailing edges), were excluded. As a result of this evaluation, the SPICA airfoil was chosen.

2.1.2.3 THE SPICA AIRFOIL

The SPICA is a flat bottom airfoil, with a thickness of 11.72 % (of the chord), and a camber of 4.75 % (See Figure 2.1-3). The high lift coefficients produced, combined with its gentle stall behavior, improve its chances for tight, low level turns. After the data was corrected for the aspect ratio, it was found that the SPICA has a zero lift angle of -2.0 degrees, and could achieve a C_{Lmax} of 1.2 at about a 14 degree angle of attack, as shown in Figure 2.1-2.

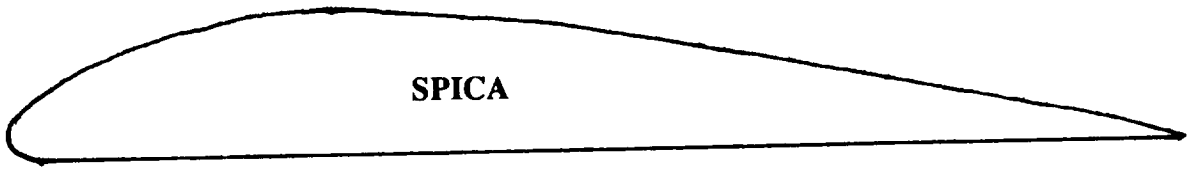

- 11.74 % thickness
- 4.47 % chord
- $C_{Lmax} = 1.2$
- $\alpha_{CLmax} = -2.0°$
- $\alpha_{L=0} = 14°$

Figure 2.1-3

The three dimensional lift generated by the wing was produced using the lifting line program [5] found in Appendix C. Assuming that the lift from the fuselage and tail surfaces would not be significant compared to the that of the wing, the lift generated from the wing

[5] Nelson, Robert C., Atmospheric Flight Mechanics, University of Notre Dame, Indiana, 1989.

was taken to be the lift of the entire airplane. The lift at various attack angles was found using the program. This data was then used to create the three dimensional lift curve slope shown in Figure 2.1-4. From this graph the attack angles needed for a specific lift coefficient were estimated.

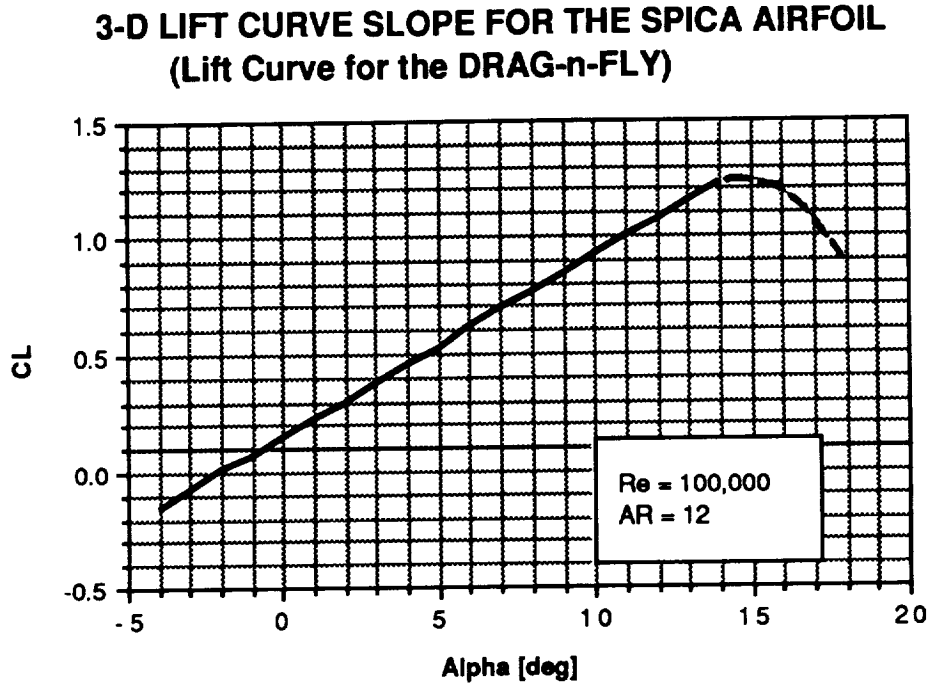

Figure 2.1-4

It is important to note that the stall data, (given in dashed lines) in Figures 2.1-2 and 2.1-4 was not calculated as was the data given by the solid lines. Since the correction methods used (aspect ratio and lifting line program), are based upon the constant slope portion of the infinite wing lift curve, the stall behavior for the two and three dimensional finite wings could not be found using these methods. In spite of this, an estimation of stall behavior was made based on the data given for the infinite wing.

2.1.3 DRAG ESTIMATION

Overall drag is one of the key parameters limiting the design and performance of the aircraft. In spite of its importance the techniques used to estimate drag are approximate at best. The following areas are discussed: usefulness of drag analysis; estimation of parasite

drag; estimation of induced drag; drag polar approximation. Included in the discussion are the methods used in the analysis.

In general, the primary force resisting the passage of an aircraft through the atmosphere is drag. The effects are felt in every aspect of design: power plant selection, wing sizing, and stability and control. Thus one of the primary concerns is building an aircraft that minimizes the negative effects of drag. Drag directly determines the power required to remain in the air. Basic power requirements motivate the selection of propeller and engine which must perform through takeoff loads, cruise, and landing. Power requirements also limit range and endurance. Wing sizing and airfoil selection come into play; the price of lift is a component of drag induced by the lift.

2.1.3.1 PARASITE DRAG

The drag estimate is broken down into two areas: parasite drag and induced drag. Parasite drag, also known as profile drag, is the airplane drag at zero lift. It represents the effects of shear stress at the surface over the entire plane, the fluff body drag of a body moving through a fluid, boundary layer separation, and other effects. Clearly, since an analytical solution to the problem is unavailable (if not impossible), the parasite drag must be estimated empirically. One method analyzes the plane by dividing the plane into its components.[1] The drag on each component is then estimated experimentally. The parasite drag coefficient can then be estimated by summing the individual parts using

$$C_{Do}=\Sigma\,(C_{Di}\,A_i / S_{ref})$$

S_{ref} is taken to be the wing surface area. A_i is the area on which the individual drag coefficient is based. Table 2.1-3 presents the drag estimated for each part. The end result is a value for the parasite drag coefficient, as shown below.

$$C_{Do}=0.018$$

This value compares favorably with the estimates from previous year's RPVs.

---

[1] Nelson, Robert C., Atmospheric Flight Mechanics, University of Notre Dame, Indiana, 1989.

Table 2.1-3: Parasite Drag component contributions

Component	CDi	Ai
Wing	0.007	Wing planform area
Fuselage	0.110	Max frontal area of fuselage
Tailplane	0.0080	Horiz. or V_{ref} area
Interference	Add 5% to C_{Do}	
Roughness/ Protuberances	Add 10% to C_{Do}	
Landing gear	Add 0.0170	

2.1.3.2 INDUCED DRAG

The induced drag would occur even if fluids were frictionless, since it is a component of the inclined lift vector. C_{Di}, the induced drag coefficient, is approximated using the following equation.

$$C_{Di} = C_L^2 / (\pi \, AR \, e)$$

The induced drag is a function of the coefficient of lift, the aircraft aspect ratio, the Oswald efficiency factor. The induced drag varies throughout the flight, changing as the square of the lift coefficient. C_L is known from airfoil selection and angle of attack (as was discussed in the previous section 2.1.2). The only unknown parameter is e, the Oswald efficiency factor. This factor must also be determined from experimental data. The method is based on a breakdown of the contribution of the wing, the fuselage, and a miscellaneous term for the rest of the body.[2] The efficiency is given by the following equation.

$$1/e = 1/e_{wing} + 1/e_{body} + 1/e_{other}$$

The wing efficiency contribution can be found from experimental data correlating the aspect ratio and the wing efficiency. Using Figure 2.1-5, this value (e_{wing}) was found to be 0.0.75 when the aspect ratio (AR) is equal to 12.

---

[2] Jensen, Daniel T., Drag Prediction Methodology for Low Reynolds Number Flight Vehicles, University of Notre Dame, Indiana, 1989.

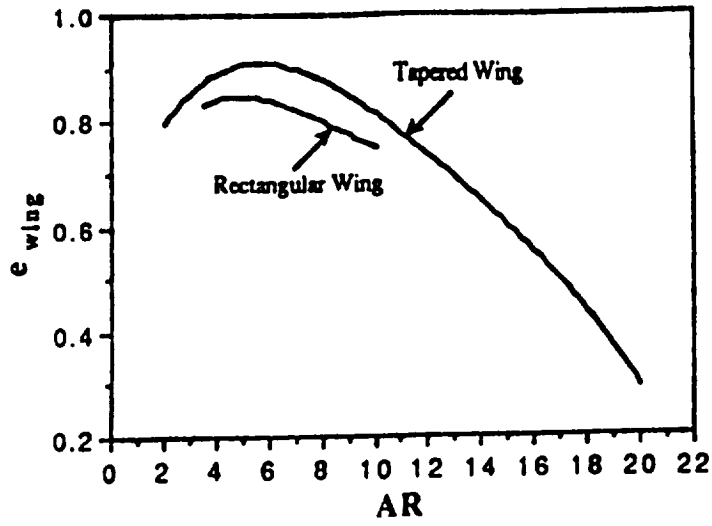

Figure 2.1-5

The fuselage contribution can be found from the body efficiency factor, $E_{fuselage}$. It is the body efficiency (e_{body}), scaled by the cross-sectional area of the body, relative to the wing area. The value of $E_{fuselage}$, which equals 0.6, was found using Figure 2.1-6, with the aspect ratio equal to 12.

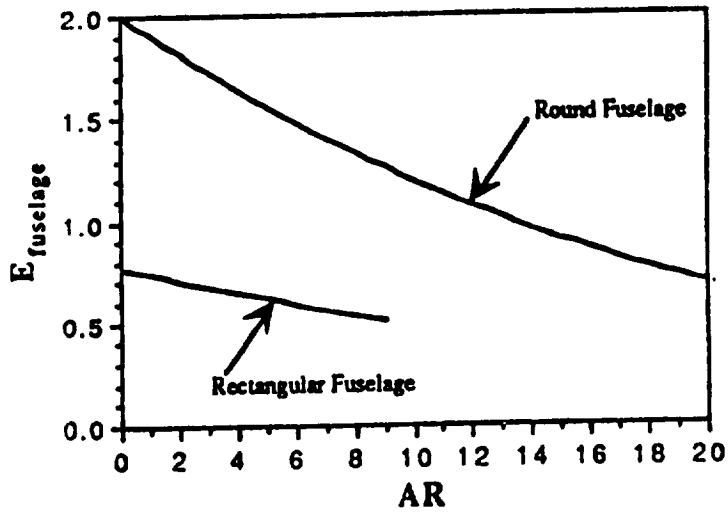

Figure 2.1-6

$$e_{body} = E_{fuselage} S_{ref} / S_{body}$$

Once $E_{fuselage}$ is found, e_{body} can then be calculated using the equation above, where S_{ref} is the wing area, and S_{body} the maximum fuselage cross sectional area. Knowing all of the efficiencies, the Osward efficiency (e) was then found using the equation aforementioned.

$$e = 0.868$$

From the estimated values of C_{Do} and the Oswald efficiency, the aircraft drag polar was then compiled.

$$C_D = C_{Do} + C_L^2 / (\pi\, AR\, e)$$

$$C_D = 0.018 + .0378\, C_L^2$$

This plot (Figure 2.1-7) represents the total aircraft drag coefficient at the trimmed condition. The drag polar is of typical parabolic form, plotting the coefficient of drag versus the coefficient of lift for the entire aircraft. At the bottom of the 'drag bucket', where $C_{L=0}$, the parasite drag, C_{Do}, can be read directly from the graph.

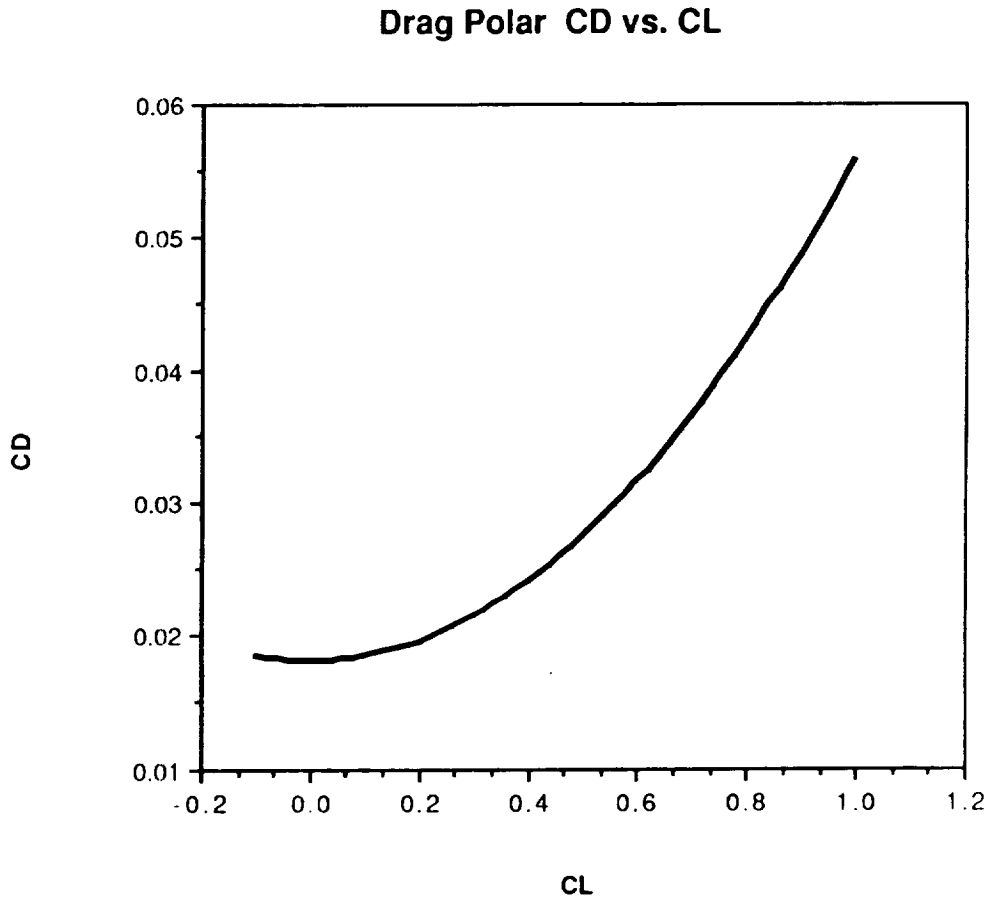

Figure 2.1-7

2.2 PROPULSION SYSTEM

2.2.1 SYSTEM SELECTION

In deciding upon the propulsion system best suited for this mission, we determined four important objectives which we needed our propulsion system to accomplish to satisfy the requirements of the mission. Therefore, the selection of the system was dictated by its ability to meet the following objectives:

- provide necessary power for 3 full laps and return to landing area
- maximize flight time
- provide sufficient take-off power
- be as lightweight as possible

Initially, two methods of propulsion were considered. Because the system was required to be non-airbreathing and not emitting any mass (i.e. rocket, etc.), our options were limited to either rubber band power or an electric propulsion system. Analyzing the rubber band power alternative, we found that it would be difficult to obtain the necessary endurance to complete the entire course. Furthermore, the use of rubber bands would prevent us from having any speed control over the vehicle, since once the rubber bands are released, they cannot be stopped. However, in researching electric propulsion, it was found that an electric motor would be suitable to meet these requirements, as well as the objectives specified above. Thus, an electric propulsion system was selected for this mission.

Next, the proper electric motor needed to be selected. After an initial analysis of the power required for the mission dictated that approximately 10 Watts of power are required during cruise (see section 3.3), it was decided that three motors would be analyzed: the ASTRO 035, ASTRO 05 and ASTRO 15 motors. First, data was obtained for each of these motors. A propeller was selected with a known efficiency versus advance ratio relationship (namely the Zinger 10-6) to provide a starting point for the comparison of motors. Then, a computer program was written that provided power available data at various RPM settings (see Appendix A-1 for listing and output of program). Next, the data for each motor was input into the program and the resulting power available data was analyzed. In looking at the ASTRO 035 motor system, it was found that this motor could provide up to 55 Watts of power once airborne and would have no problem keeping the aircraft in the air. However, in looking at the power required at take-off, it was found that the ASTRO 035 would require approximately 96 feet to take-off, thus using almost 65% of the runway

simply for ground roll and exceeding the amount of runway that we wanted to use for take-off. Furthermore, this motor would require the use of a smaller propeller, thus diminishing the thrust available. Therefore, the ASTRO 035 was eliminated from consideration.

The ASTRO 05 and ASTRO 15 were then analyzed in a similar fashion as the ASTRO 035. In looking at the two motors, it was found that each system would provide sufficient thrust both during cruise and in meeting the required take-off distance (see table 2.2-1). It was also found that the ASTRO 15 produced a significant amount more power than the ASTRO 05. However, not only does the ASTRO 05 (6.5 oz.) weigh less than the ASTRO 15, but it also requires fewer batteries for operation and a much lighter total system weight. Since the additional power of the ASTRO 15 would be of no benefit because of the nature and goals of this mission, it was decided that the lighter-weight motor should be selected. Thus, the ASTRO 05 will be used to power the vehicle.

Table 2.2-1

MOTOR	MOTOR WT. [oz.]	BATTERY WT. [oz.]	SYSTEM WT. [oz.]	Max. Power Out [W]	TAKE-OFF DIST. [ft]
ASTRO 035	4.5	5.4	11	55	96
ASTRO 05	6.5	6.24	13	80	31
ASTRO 15	7.5	17.5	25	120	17

After deciding on the ASTRO 05, it was then necessary to select the type and number of batteries needed for the mission. Again, since one of our main objectives was to minimize the weight of the propulsion system, we wanted to use as few batteries as possible while supplying the motor with the necessary current. Due to the internal layout considerations of our RPV, it was also necessary to select batteries small in size. Furthermore, rechargeable batteries were chosen so as to keep the cost of batteries minimal if the aircraft is repeatedly flown. Using these guidelines, we utilized a TKSolver program (a programming tool found in the Notre Dame Aerospace Lab) which allowed us to vary the total battery voltage (number of batteries) and battery capacity while holding all other parameters constant (see Appendix A-2 for program 'rules' and output). Doing so, we found that a battery system of eight 500 MAH ('AA') Nickel Cadmium batteries would satisfy each of the objectives earlier defined. These cells will provide constant thrust throughout the flight, allow a motor current draw of 9.31 Amps and keep battery weight at only 6.24 oz.

2.2.2 PROPELLER SELECTION

In order to achieve maximum efficiency at cruise velocity for the ASTRO 05 motor, a ten inch, two-bladed propeller with six inch pitch must be matched with the ASTRO motor. The final selection for the propeller resulted in the acquisition of the ZINGER 10-6.

In trying to chose a propeller, the diameter is the most important parameter to consider since it effects every aspect of the performance of the aircraft. When conducting the analysis of several propellers, the diameter was constantly changed while other parameters such as battery voltage (9.6V),battery capacity (.5 amp-hr),weight (2.656 lbs), AR (12), and wing area (6 ft^2) are all held constant. The maximum diameter considered was twelve inches because this is the maximum allowable length to fit properly on the fuselage. The aircraft must have sufficient ground clearance for the propeller, and some reasonable landing gear lengths were chosen, which gave the maximum prop length. The minimum diameter considered was the eight inch because below this value the aircraft can not receive the necessary thrust to lift-off.

A propeller-motor combination was needed that would achieve a short takeoff distance of approximately fifty feet with a large rate of climb, and have a flight time of over 120 seconds. A quick takeoff is desired in order to reach the cruise height of fifteen feet quickly and allow ample time for the pilot to prepare for the first turn. A large rate of climb will allow the pilot to climb quickly after each turn in case any altitude is lost while executing the turns.

The results of the Independent Trade Study, indicates that a ten inch propeller will deliver all of the needed abilities. The propeller-motor combination will takeoff in approximately 31 feet, climb at 3.8 ft/s, and have a flight time of around 193 seconds (3.2 min.).

Figure 2.2-1 shows the ZINGER 10-6 propeller efficiency vs advanced ratio curve. At cruise conditions the advanced ratio for the propeller is .277, which corresponds to a propeller efficiency of approximately .59. The curve was obtained from Dr. P. Dunn, who gave to his students during a design project in his class.

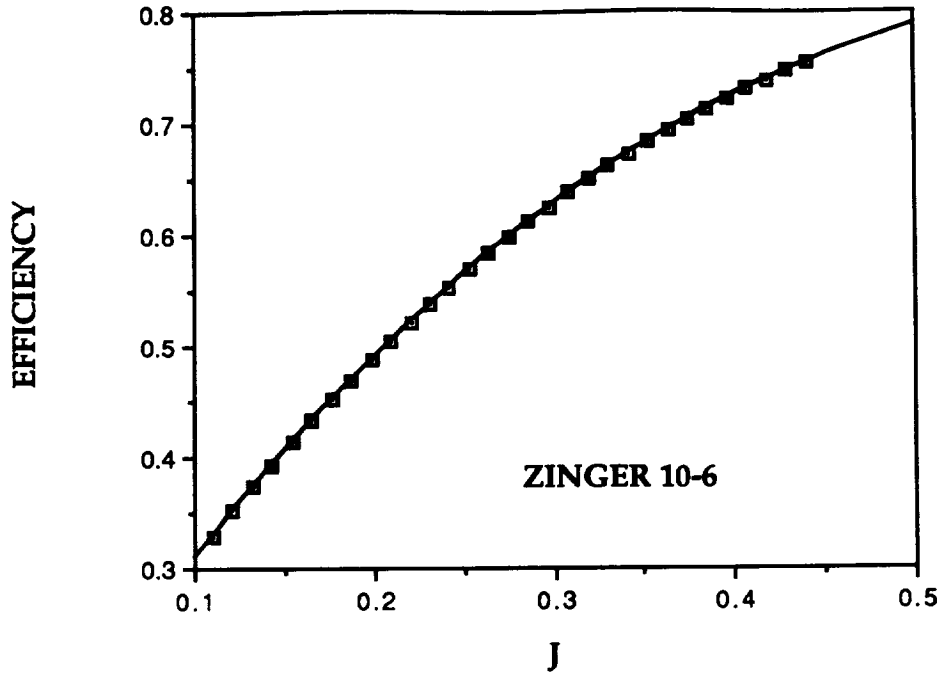

FIGURE 2.2-1 EFFICIENCY VS ADVANCED RATIO

2.2.3 ENGINE CONTROL

Once the aircraft has lifted off, the Drag-n-Fly will attempt to fly at a relatively constant altitude. During the straight portions of the course, we anticipate cruising at a gear RPM of 7200. However, during turning flight, if we continue at the same RPM setting and flight speed, the aircraft will lose altitude. This occurs because as the aircraft turns, the vehicle will bank through the turns, changing the angle at which lift is acting and causing the vertical force on the wings to be diminished and consequently, creating less lift. Therefore, since we would like to maintain a constant altitude throughout the flight, an electronic speed control must be utilized. This speed control will allow the pilot to increase the RPM to approximately 8000, thus increasing the velocity of the vehicle and creating more lift over the wings. This additional lift will be used to maintain altitude through the turn. Once the turn is completed, the pilot will be able to decrease the RPM setting back to 7200 and slow the plane to its proper cruising velocity of 25 ft/s.

2.3 STABILITY AND CONTROL

In the area of longitudinal stability and control the primary design parameter was the static margin. A target value was set at 15% and the design entailed sizing the aircraft to achieve this goal. The other primary concern was trimming the aircraft at the desired lift coefficient of 0.67. These areas will be presented in the next two sections, 2.3.1 and 2.3.2. In the area of lateral stability and control, the primary concerns were with achieving adequate roll control power with a combination of the rudder and the dihedral angle since the aircraft had no ailerons. The equations governing this control will be developed and used to size the vertical tail, dihedral angle, and rudder. With the resulting large dihedral angle, large vertical tail, and a high wing, the roll and yaw stability of the aircraft was assumed more than adequate for the mission. Section 2.3.3 will present the analysis.

2.3.1 STATIC MARGIN

The primary goal in setting the longitudinal stability was achieving the desired static margin. The analysis of the static margin was performed in two separate phases. In the first phase the target static margin and center of gravity were set and the analysis depended on sizing and locating the aircraft components to attain the proper neutral point. An equation representing the neutral point of this aircraft thus had to be derived and will be later in this section. In equation form the definition used for the static margin was as follows.

$$SM = Xnp/c - Xcg/c$$

The second phase, or more detailed phase, used the same equation but the center of gravity location and the neutral point were calculated and the resulting static margin determined using the equation above. This phase was used as the aircraft was in the production stage to check if the static margin was agreeing with the target value so changes could be made, if possible.

The static margin target value for this design was 15%. Typical aircraft have a static margin between 5 and 10% but the target value was set higher in this case to account for the different type of aircraft. The primary reason being the pilot is on the ground and needs extra stability for the RC aircraft to allow a longer response time for the control. The target of 15% was primarily used for sizing and placement of the tails. The target aircraft center of gravity that was initially used was 35% of the mean aerodynamic chord thus the target neutral point was 50% of the mean aerodynamic chord.

The detailed method used in determining the static margin was to estimate the neutral point and the center of gravity and take the difference between the two. The center of gravity was calculated from estimates of the sizes, weights, and locations of the internal layout and the components of the aircraft. This was discussed in the weights and structures portion of the proposal. The neutral point is defined as the furthest aft point where the center of gravity could be located without having a statically unstable aircraft. If the center of gravity was at the neutral point then the aircraft would be neutrally stable. The neutral point is found by setting the slope of the pitching moment equation equal to zero and solving for the center of gravity. The equation for the slope of the pitching moment curve is found by considering the contribution to the moment from each of the three major components of the aircraft; wing, tail, and fuselage. The following equation for Cm_α represents a typical aircraft. [1]

$$Cm_\alpha = Cm_{\alpha f} - \eta V_H C_{L\alpha t} (1-d\varepsilon/d\alpha) + C_{L\alpha w}(X_{cg}/c - X_{ac}/c)$$

For the RPV aircraft considered here this equation neglects one contribution. The contribution to Cm_α resulting from the moment created by the drag on the wing. This equation is valid for aircraft with the center of gravity a negligible vertical distance from the wing aerodynamic center. Since our wing was not at a negligible vertical distance from the center of gravity and the drag on the wing was high due to the low Reynolds number this contribution was considered. The equation for this contribution was approximated by considering moment as the drag times the vertical distance of the aerodynamic center minus the vertical location of the center of gravity. This equation then must be non-dimensionalized.

$$M_D = Drag\ (Z_{ac} - Z_{cg})$$

$$Cm_D = C_{Dw}\ (Z_{ac}/c - Z_{cg}/c)$$

From the definition of the coefficient drag

$$C_{Dw} = C_{Dow} + C_L^2/(\pi\ AR\ e)$$

and the definition of the coefficient of lift

$$C_L = C_{Low} + C_{L\alpha w}\ \alpha_w$$

At this point since we are only interested in the contribution to the slope of the pitching moment curve, the terms independent of angle of attack, intercept terms, are neglected. Combining the previous equations and ignoring the portion that does not depend on angle

---

[1] Nelson, R.C., Flight Stability and Automatic Control, p.64 McGraw-Hill, St. Louis, 1989.

of attack produces the following approximation for the contribution to the coefficient of the pitching moment slope due to the drag on the wing.

$$Cm_{\alpha D} = (1/(\pi\, AR\, e))(2C_{Low}\, C_{L\alpha w} + C_{L\alpha w}^2\, i_w)*(Z_{ac}/c - Z_{cg}/c)$$

A couple of approximations were made in calculations using this equation. First of all, the vertical distance of the aerodynamic center of the wing (Zac) from the tip of the nose was an approximation of the location. Since the wing is a three panel polyhedral wing a large dihedral angle, Zac varies along this span. To make the equations easier to work with the value was averaged across the span. Also, in the above equation one term was dependant on the square of the wing angle of attack. For simplification of the calculations, this was approximated as the wing angle of attack times the incidence angle of the wing. Adding the previous equation to the previous equation for Cm_α produces the approximation of the pitching moment slope for our RPV.

$$Cm_\alpha = Cm_{\alpha f} - \eta V_H C_{L\alpha t}(1-d\varepsilon/d\alpha) + C_{L\alpha w}(X_{cg}/c - X_{ac}/c) + Cm_{\alpha D}$$

Setting it equal to zero then solving for X_{cg} produces the following equation for the neutral point.

$$X_{NP} = X_{ac}/c + \eta\, V_H\, C_{L\alpha t}/\, C_{L\alpha w}(1 - d\varepsilon/d\alpha) - Cm_{\alpha f}/C_{L\alpha w} - Cm_{\alpha D}/C_{L\alpha w}$$

The wing drag contribution comprises about 8% of the total coefficient of moment due to a change in angle of attack. The primary reason being the difference between the aerodynamic center and the center of gravity is about 6.5 inches or 75% of the chord. The above equation was used to size the aircraft components and orientations and also to produce the final approximations for the static margin as will be detailed in the next section.

2.3.2 LONGITUDINAL STABILITY

The primary goal of longitudinal stability was to achieve the targeted static margin, 15%. The other goal of the longitudinal stability was to trim at the necessary cruise lift coefficient of 0.67. The primary design parameters affected by these two conditions were the horizontal tail area, horizontal tail incidence angle, horizontal tail aspect ratio, and the distance to the tail aerodynamic center from the aircraft center of gravity. The distance to the tail had limitations though. The aircraft total length was set at 41 inches to minimize weight which limits the distance from the center of gravity to the tail to about 30 inches. The horizontal tail incidence angle was not effected by the static margin so it was primary set to trim the aircraft at the desired angle of attack. The wing incidence angle was not considered a stability design parameter as it was set at 5 degrees to produce the desired

cruise lift coefficient of 0.67. With the wing angle set, the fuselage will not have to fly at a positive angle of attack during cruise and extra fuselage drag can be avoided.

The primary tool used in the analysis was the equation for the neutral point developed in the previous section. Since the target static margin was 15% and the target center of gravity location was 35% of the mean chord, the neutral point should be at 50%. Several of the parameters were varied and the design point that produced the static margin desired was used.

2.3.2.1 HORIZONTAL TAIL SIZING, LOCATION, AND ORIENTATION

Initially the horizontal tail area was set at 17% of the wing area of six square feet, or 1.02 ft^2, based on some RC aircraft rules of thumb.[2] Another area was used to note how the neutral point was affected by the different areas. This area was 20% of the wing area or 1.2 square feet. Figure 2.3-1 demonstrates how the neutral point varies with the tail moment arm for the two different areas.

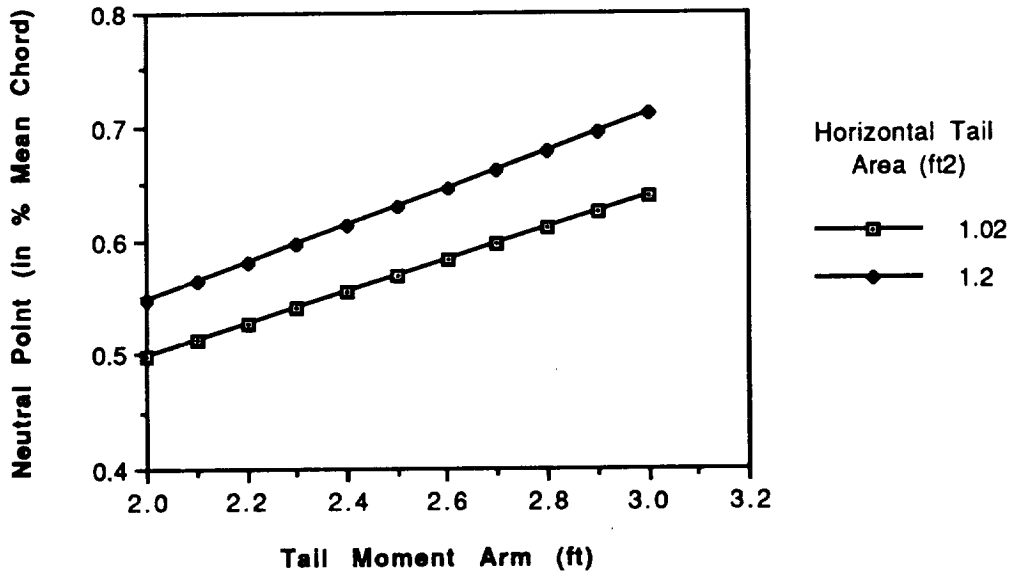

Figure 2.3-1

---

[2] Lab Handout on rules of thumb for "Stability and Control" ,p.9, 1990.

The tail moment arm is the distance from the aerodynamic center of the tail to the center of gravity of the aircraft. Note how the neutral point moves back for increases in the tail moment arm. The only point on this graph with a neutral point of 50% was for a tail moment arm of 2.0 feet and a tail area of 1.02 square feet as marked on the graph.

The next plot, Figure 2.3-2 shows the neutral point as a function of the horizontal tail area for the two different moment arms. To yield a neutral point at 0.5 times the mean aerodynamic chord of the wing, the 2.1 foot moment arm and a 0.97 square foot tail were required. When the tail area moment arm is increased to 20% the tail area necessary is only 0.83 ft^2.

Neutral Point Location as a Function of Horizontal Tail Area

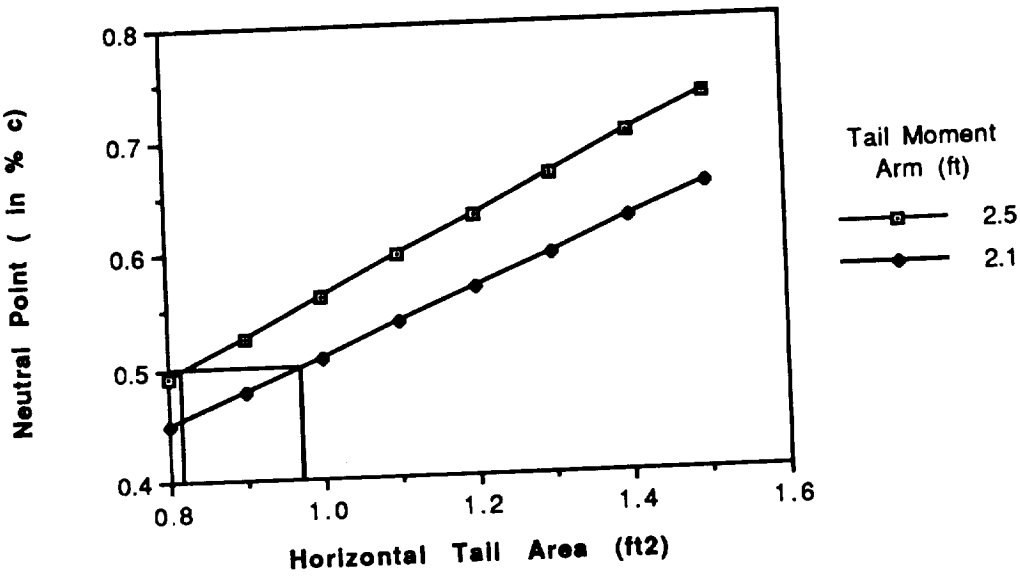

Figure 2.3-2

One further plot, Figure 2.3.3 shows the how the neutral point travels with respect to the aspect ratio of the horizontal tail. This was done for a tail area of 1.02 ft^2 and a tail moment arm of 2.3 feet. As the aspect ratio of the tail increased the neutral point traveled further back towards the rear of the aircraft. For the target of 50%, a tail aspect ratio of 3 was necessary. For a tail aspect ratio of 3 and a tail area of 1.02 the mean chord of the tail would be 0.6 feet which would make the local Reynolds number less than the mean aerodynamic chord Reynolds number. The flight Reynolds number is 1.2×10^5 and the

tail local Reynolds number is about 0.95 x 10^5. Despite this difference, no further problems associated with low Reynolds numbers were expected for this range.

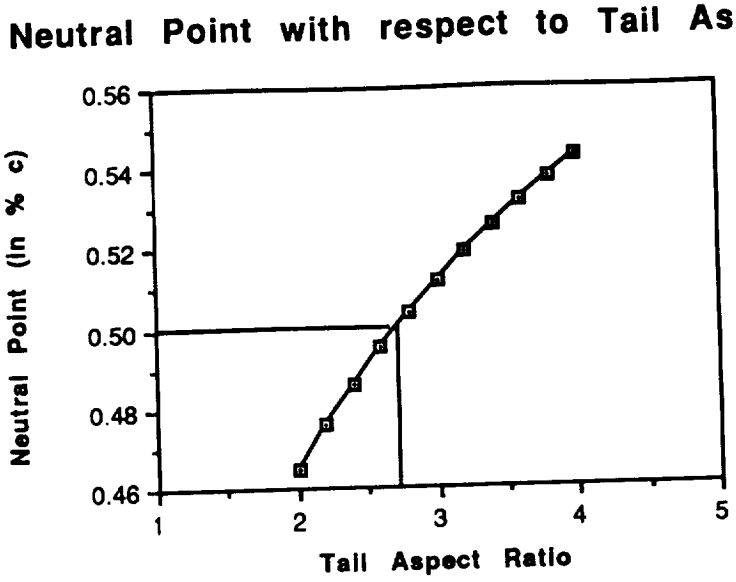

Figure 2.3-3

One further analysis that was done was to trim the aircraft at the desired lift coefficient of 0.67. This was done by primarily altering the intercept term of the coefficient of the pitching moment curve. Again this included contributions from the wing, tail, and fuselage but the primary controllable variable was the tail incidence angle. The results were produced by a simple computer program which used equations from the Stability and Control reference cited earlier. Oddly enough, the tail angle turned out to be about zero degrees (actually 0.6 degrees). This will make the construction of the tail easier as it will not have to be tilted at any angle and can be just mounted relatively straight. The following figure 2.3.4 displays the moment coefficient as a function of the wing angle of attack for each of the components of the aircraft. These contributions were added together and the resulting Cm versus alpha relationship is noted as "aircraft" on the graph. The trim wing angle of attack of 6.5 degrees corresponds to a lift coefficient of 0.67 which is the desired trim lift coefficient.

Pitching Moment Coeff. for Components of the Aircraft

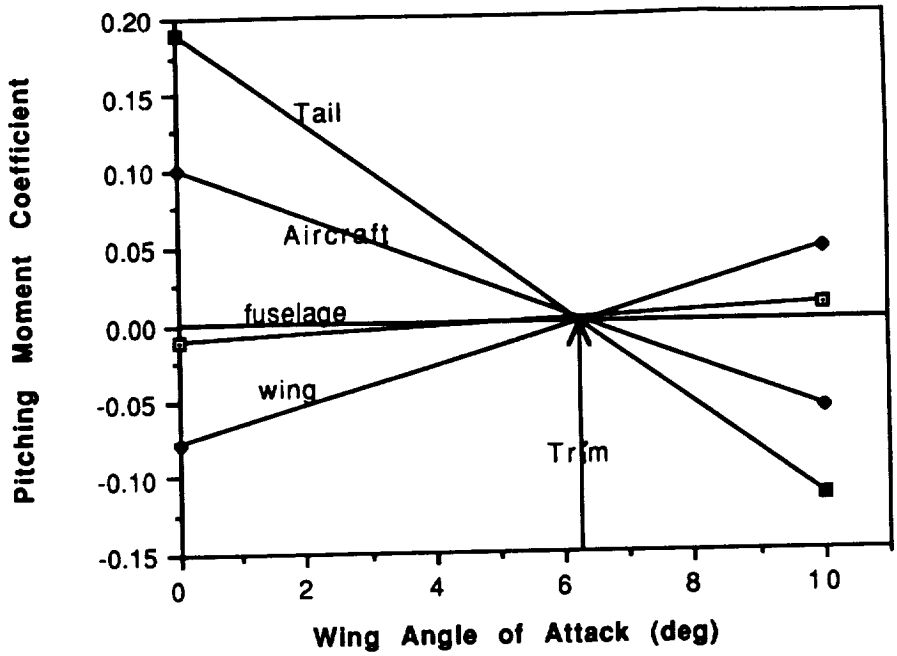

Figure 2.3-4

The final values of the horizontal tail size, location, and incidence angle are summed up in the following Table. They were all based on the longitudinal stability goals of a static margin of 15% and trim CL of 0.67 although some values have been slightly modified.

Longitudinal Stability Summary

Horizontal Tail Area	1.00 ft^2
Tail Moment Arm	2.3 ft
Tail Incidence Angle	0 degrees
Horizontal Tail Aspect Ratio	3.0

In the analysis it was assumed that the tail moment arm was constant. This was considered a fairly valid assumption for this type of aircraft since the center of gravity will move very little. The reason the center of gravity will move little is that no mass will be lost by the aircraft during the flight. No fuel will be burned and no mass dropped.

The elevator effectiveness was also examined by considering its contribution to the pitching moment curve. The analysis demonstrated that a 15 degree elevator deflection would be

plenty to trim the aircraft from -2 to 12 degrees wing angle of attack. There is thus plenty of control power and maybe even too much. The aircraft will also be able to rotate to and trim at the 10 degree climb angle. Figure 2.3-5 displays the results.

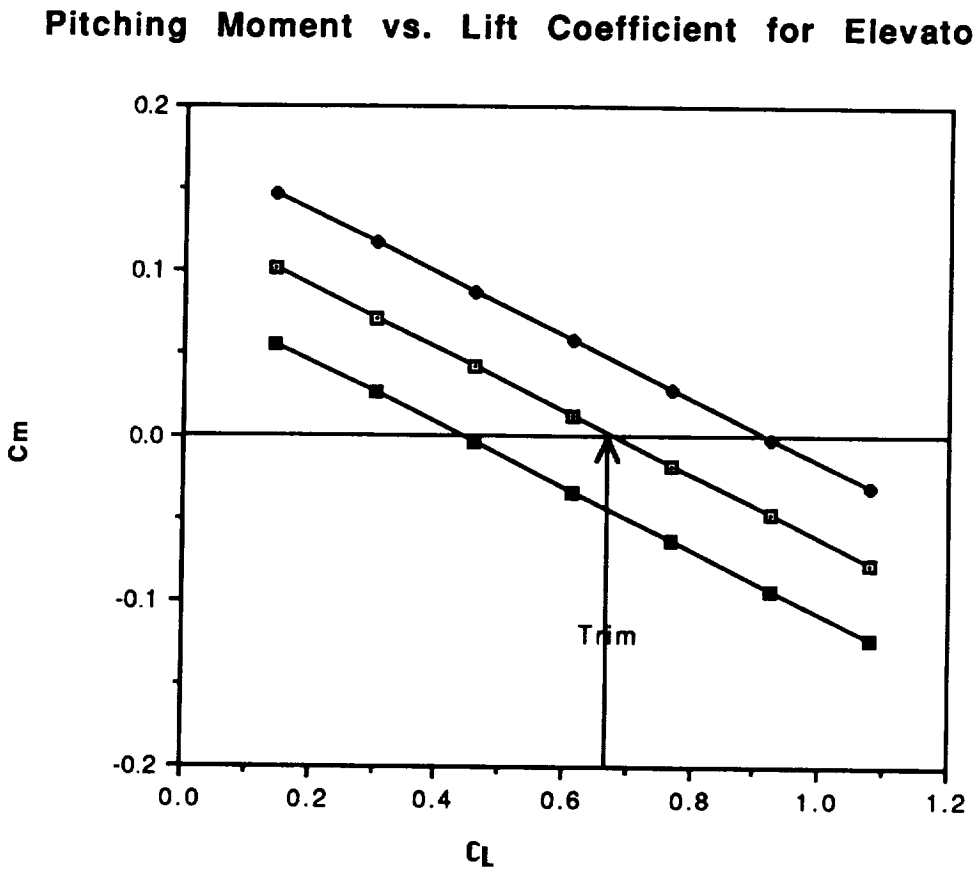

Figure 2.3-5

2.3.2.2 FINAL DESIGN

In the final analysis the neutral point, using the equation given previously, turned out at 55% of the mean aerodynamic chord. The center of gravity, estimated from simply balancing the plane, was at 45% of the mean aerodynamic chord. This meant a static margin of 10% as compared to the target of 15%. The reason the static margin was so small was because the center of gravity of the aircraft had slipped back during the construction of the aircraft. To alleviate the problem some of the internal layout of the aircraft were shifted forward and the wing shifted back to move the center of gravity forward. After some tests the center of gravity was moved forward even further by slightly weighting the front end of the aircraft. The final center of gravity location was at 30% of

the mean chord providing a static margin of 25%. This high static margin produced a very stable smooth flying aircraft.

2.3.3 ROLL AND DIRECTIONAL STABILITY AND CONTROL

The low Reynolds number RPV design that was proposed had to have a minimal weight in order to succeed. One step that was taken to reduce the weight was to discard the conventional ailerons. This eliminated the servos and control linkages for the two ailerons with the only penalty being a slightly larger tail and dihedral angle. The roll maneuvers then had to be performed with a rudder deflection. The main design parameters that affect this roll are the dihedral angle and the rudder area. Other less significant parameters are the lift coefficient, drag coefficient, and the vertical tail area. This section examines how the rudder induced roll can be approximated and how the design parameters effect this roll moment. In addition, the roll rate and how it was affected by the design parameters was studied. The process for the study was as follows. First, the governing equations were developed. Then, graphs were produced demonstrating the affect of the different variables. Next, the limits and constraints on the different variables were applied to produce a range of possible solutions. Finally, the most appropriate set of parameters was decided upon. In the analysis, it was assumed that the dihedral had the primary effect on the roll. All other affects such as the fuselage and the horizontal tail were considered negligible and were not quantified. In addition, as decided previously, the dihedral will be dispersed across the wing with a three-panel polyhedral. Thus this section includes the evaluation of the equivalent dihedral angle (EDA) and not its distribution across the wing.

2.3.3.1 ANALYSIS TOOLS

The theory behind the rudder controlled roll is that when the rudder is defected it creates a sideslip angle, β. As a result of the dihedral angle, the sideslip angle causes an effective change in the angle of attack of the wing. The leading half of the wing effectively sees an increase in the angle of attack and thus an increase in lift while the trailing wing sees a decreased angle of attack and decrease in lift. The derivation for the expression quantifying this change in angle of attack as well as a diagram are given in Appendix D in the back of this proposal. The result is listed below.

$$\Delta\alpha = \beta \sin\Gamma$$

In this equation, Γ is the dihedral angle and $\Delta\alpha$ is the change in angle of attack. Using equation 1, an expression for the roll moment coefficient was derived. This derivation

began by assuming that the roll moment is equal to the change in lift on the wing, which is proportional to the change in angle of attack, times the moment arm. Page 1 of Appendix D includes this derivation that results in the equation given below.

$$Cl = -0.25\, CL_{\alpha}\, \sin(\Gamma)\, \beta \qquad (1)$$

The quantity $C_{L\alpha}$ is the corrected lift curve slope of the wing. For a roll moment to be created a sideslip angle must be induced. A fixed rudder accomplishes this but does not produce a yaw moment as the RPV will trim at a non-zero sideslip angle. The equation for this relation is:

$$Cn = 0 = Cn_{\beta}\, \beta + Cn_{dr}\, dr \qquad (2)$$

where dr is the rudder deflection. Equations for Cn_{β} and Cn_{dr} were extracted from reference 1 and are listed below.

$$Cn_{\beta} = Cn_{\beta wf} + n_v\, V_v\, CL_{\alpha v}\, (1 + d\sigma/d\beta)$$

$$Cn_{dr} = -\, n_v\, V_v\, CL_{\alpha v}\, \tau$$

In equation 4, $Cn_{\beta wf}$ is an empirical factor representing the wing and fuselage contribution and was again estimated using a formula given in reference 1. Vv is defined as the vertical volume ratio (lt*Sv/(S*b)) and n_v is the ratio of the vertical tail dynamic pressure to the freestream dynamic pressure. The term $d\sigma/d\beta$ was approximated using an equation in reference 3 as cited below.[3] The parameter τ is a factor which is related to the ratio of the rudder surface area to the vertical tail surface area.

The only other tools used for the analysis were the LinAir program and the four part article "Dihedral" (reference 4).[4] LinAir was used to examine the affect of dihedral on the lift coefficient and the drag coefficient. The dihedral article was used to validate the data produced by the equations listed above and to produce a graph demonstrating the dihedral effect on roll rates.

2.3.3.2 OBJECTIVES AND CONSTRAINTS

The main objective of this study was to choose the dihedral angle and the rudder area. Merit was accredited to designs that produced an adequate roll moment which is defined in the next section. In deciding upon a dihedral angle, demerit was given to increased drag

---

[3] Nelson, R.C., Flight Stability and Automatic Control, p. 71, McGraw-Hill, Inc., St. Louis, 1989.

[4] Beron-Rawdon, B., " Dihedral ", 4 part article, Model Aviation, Aug. '88 - Nov. '88.

and decreased lift as a result of increased dihedral. Another goal included a roll rate of 25 degrees per second which is explained later on in the text. The lower limitation on the dihedral angle was a minimum of 5 degrees. From previous RC aircraft data, 5 degrees was the minimum amount needed to provide the necessary roll stability. The maximum dihedral was set at 13 degrees. This limit was set by structural and manufacturing considerations. An EDA of 13 degrees would mean approximately a 20 degree angle on the outer half of the span. Angles of this magnitude would cause considerable loss of lift, weakness in the joint and difficulties in construction. Constraints on the rudder included an area of less than 75% of the vertical tail corresponding to a rudder effectiveness parameter (τ) of about 0.81. This constraint was imposed because the rudder would have to have some part of the tail to pivot on. An all moveable tail would be unfeasible from an construction standpoint and make the aircraft too sensitive to rudder input. Furthermore, the rudder was limited to a +/- 20 degree deflection. This restriction was imposed because larger deflections would be difficult to apply with the avionics and because the drag becomes too large with large deflections. Limitations on the size of the vertical tail stemmed from Stability and Control rules of thumb for RC aircraft (See footnote 2). The applicable range is about 0.4 ft^2 to 0.6 ft^2 to provide sufficient directional stability.

2.3.3.3 DIHEDRAL, RUDDER AND VERTICAL TAIL SIZING

When all the tools needed were available, the analysis began. Initially, the rudder angle was varied and the corresponding sideslip angles were calculated using equation 2. Then the roll moment for these sideslip angles was calculated using equation 1 and different dihedral angles. The results present the magnitude of the roll moment that could be achieved with the rudder roll control. Figure 2.3-6 presents a graph of the results. This graph was done to get an idea of the type of roll moment coefficient that would result for rudder input. Thus the rudder was sized at an average value of 50% of the vertical tail and the vertical tail was sized at 0.5 ft^2 to produce this graph (later in this section the vertical tail and rudder areas are varied). The next graph was done for the purpose of demonstrating how the roll moment coefficient varied with the rudder to vertical tail area ratio. The ratio is used because the vertical tail area has only been estimated at a low level of decision and, when it is decided, the rudder area can be easily calculated. For the graph in Figure 2.3-7, the dihedral angle was set to a typical value of 8 degrees and the vertical tail area was set at 0.5 ft^2. As would be expected, when the rudder area was increased the roll moment becomes larger for each rudder input. Comparing Figures 2.3-6 and 2.3-7 it appears that

FIGURE 2.3-6

Roll Moment Coeff. vs. Rudder Input for Varying Dihedral

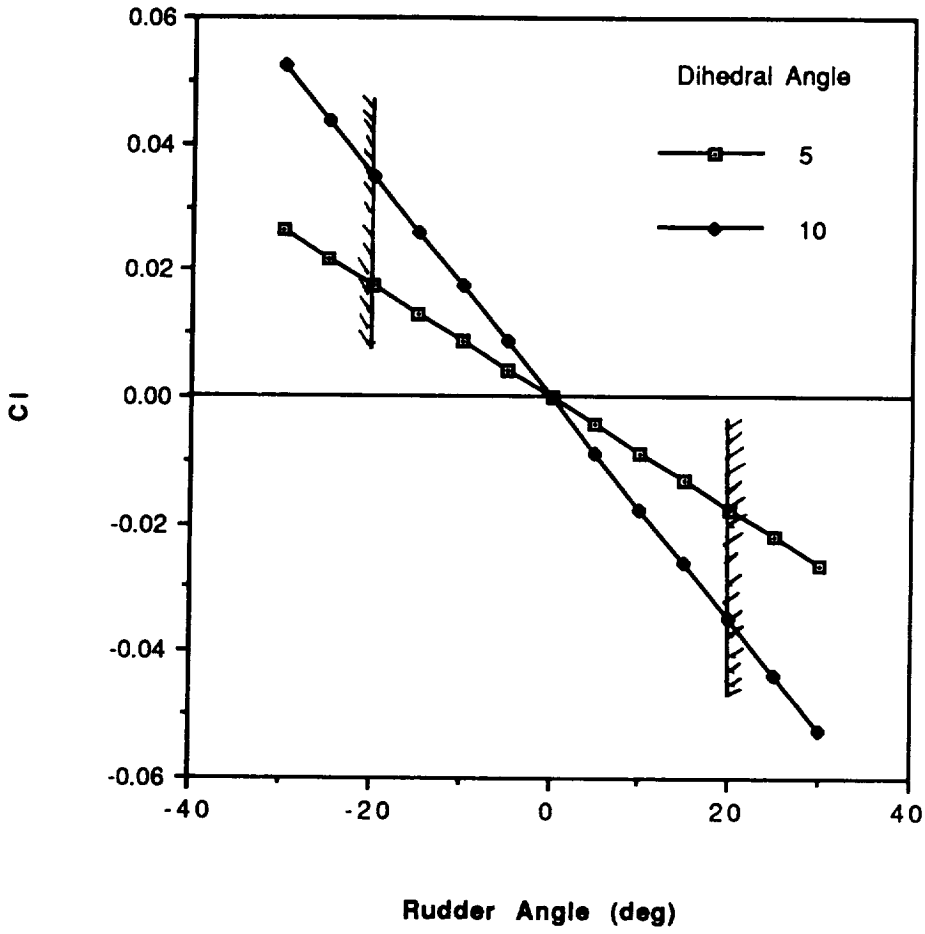

FIGURE 2.3-7

Roll Moment Coeff. vs. Rudder Input for Different Rudder Areas

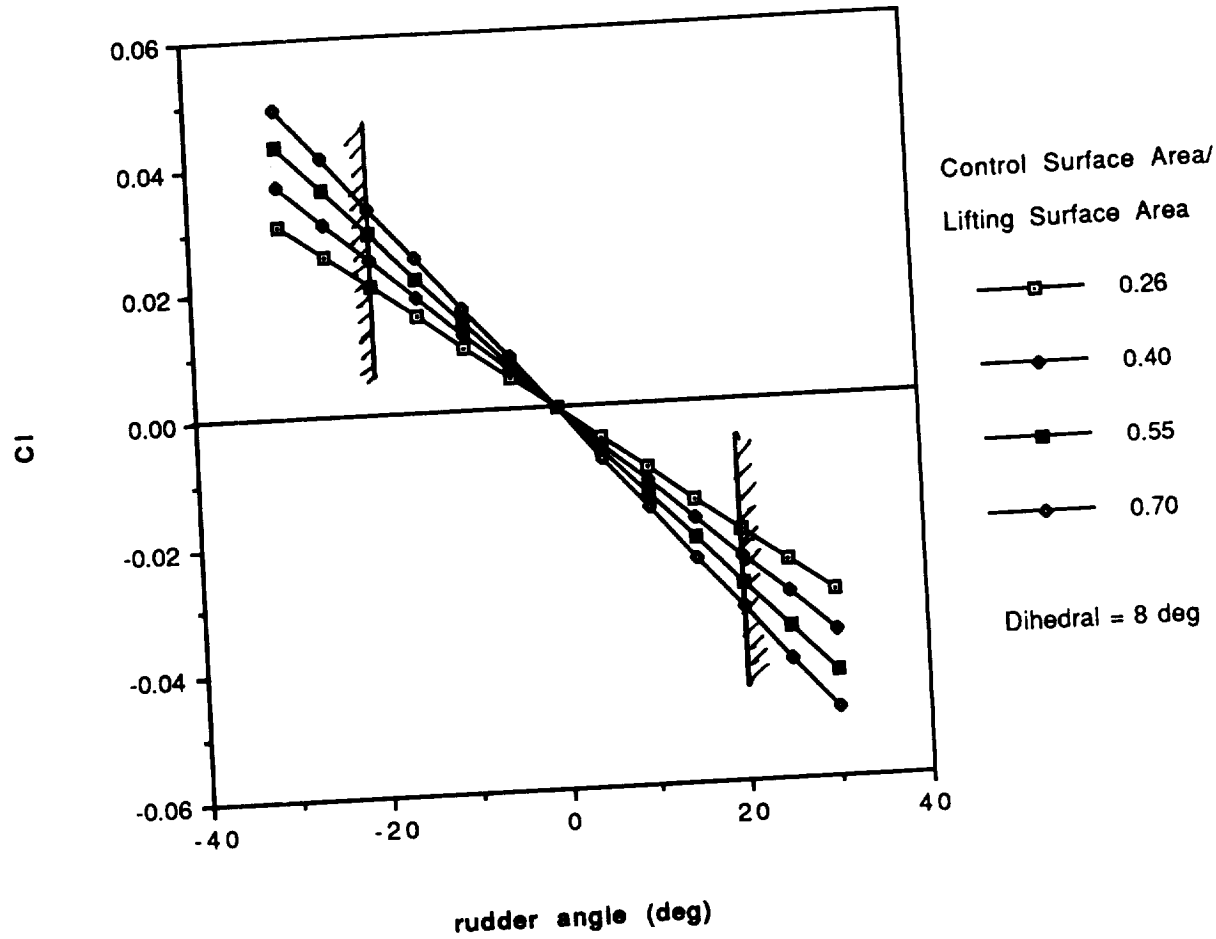

each degree increase in dihedral is equivalent to about a 9% increase in the area ratio. The question at this point in the study was "Was this enough Cl to roll the aircraft?".

To determine an adequate range of Cl it was imagined that the aircraft had ailerons. The ailerons were sized using typical RC airplane data with reference to our aircraft. Then, using Equation 2.97 in reference 1 (see footnote 1), Cl versus the aileron deflection was plotted for a maximum aileron deflection of +/-15 degrees. Figure 2.3-8 includes this plot. Based on this plot and the constraint for the aircraft that the rudder will not deflect more than 20 degrees, the necessary slope of the Cl versus rudder plot for our aircraft was determined to be 0.0024 per degree. Using this number the controlled variables could be varied so that the final design could be selected.

The next set of graphs were the main tools in deciding on the final design for the dihedral and rudder. The slope of the Cl versus rudder input graph was set to produce adequate roll. Now all the parameters could be included on one graph to determine trends. The equation for Cl was of the form Cl=(A)dr where A was the slope. The equation for A is the following.

$$A = 0.0024\ 1/deg = -1/4\ CL_{\alpha w} \sin\Gamma\ *(Cn_{dr}/Cn_{\beta})$$

All the parameters in this equation were defined previously. This equation could be solved for τ which is called the rudder effectiveness parameter. The data for the plot was produced using the software Excel. The roll moment model data with the imaginary ailerons was typical data for a fairly acrobatic aircraft. This aircraft, requiring less roll control would not have to meet those standards. To correct this, it was assumed that only 80% of the roll moment would be necessary (0.80*0.0024 1/deg). Figure 2.3-9 is the plot of the resulting data. Figure 2.3-9 indicates with the constraints that the dihedral angle would have to be something upwards of about 8 degrees and the rudder effectiveness parameter somewhere less than 0.81. As was noted previously, a one degree increase in the dihedral angle leads to a 9% decrease in the rudder effectiveness parameter. To find out which combination is the most feasible, more study had to be done.

LinAir was used to determine if an increase in the dihedral angle to something above 8 degrees would change the lift and drag significantly. Table 1 below gives the results for the modeled wing and horizontal tail at an angle of attack of 3 degrees.

FIGURE 2.3-8

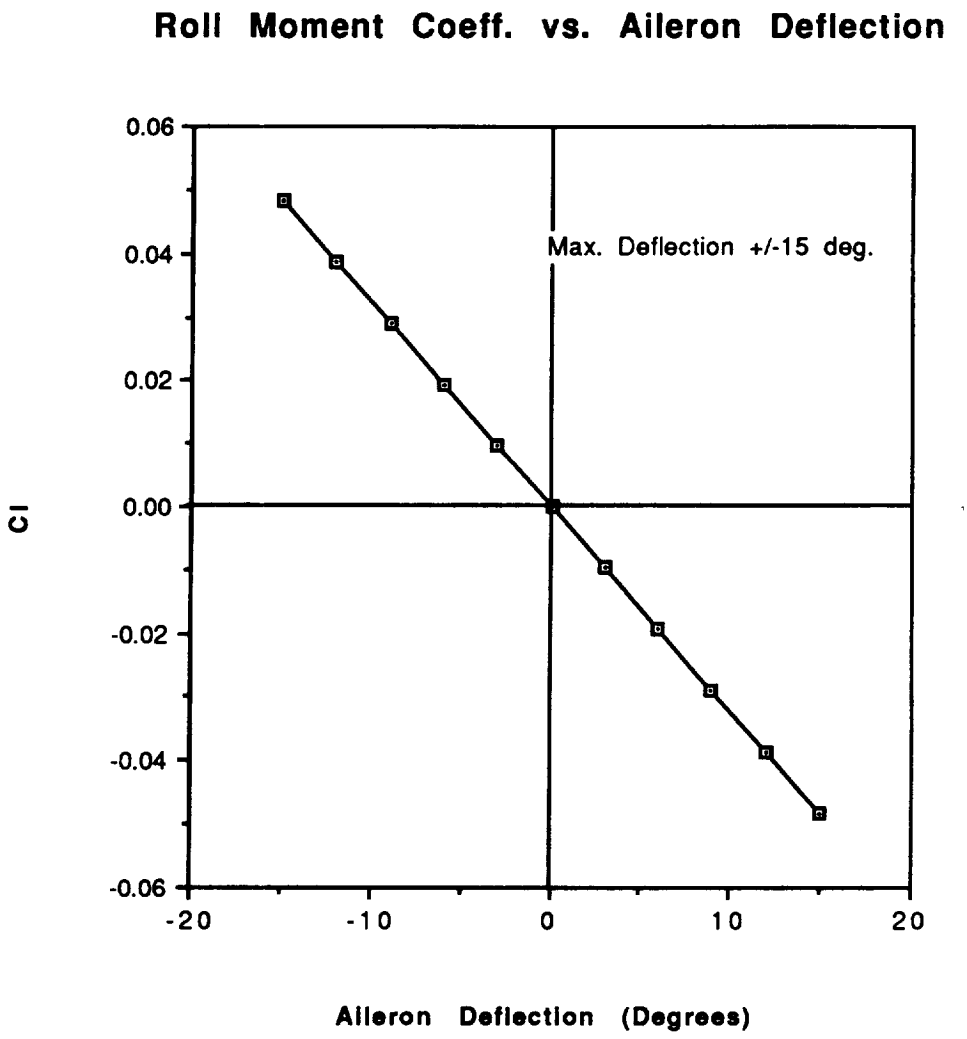
Roll Moment Coeff. vs. Aileron Deflection
Max. Deflection +/-15 deg.
0.06
0.04
0.02
0.00
-0.02
-0.04
-0.06
Cl
-20
-10
0
10
20
Aileron Deflection (Degrees)

FIGURE 2.3-9

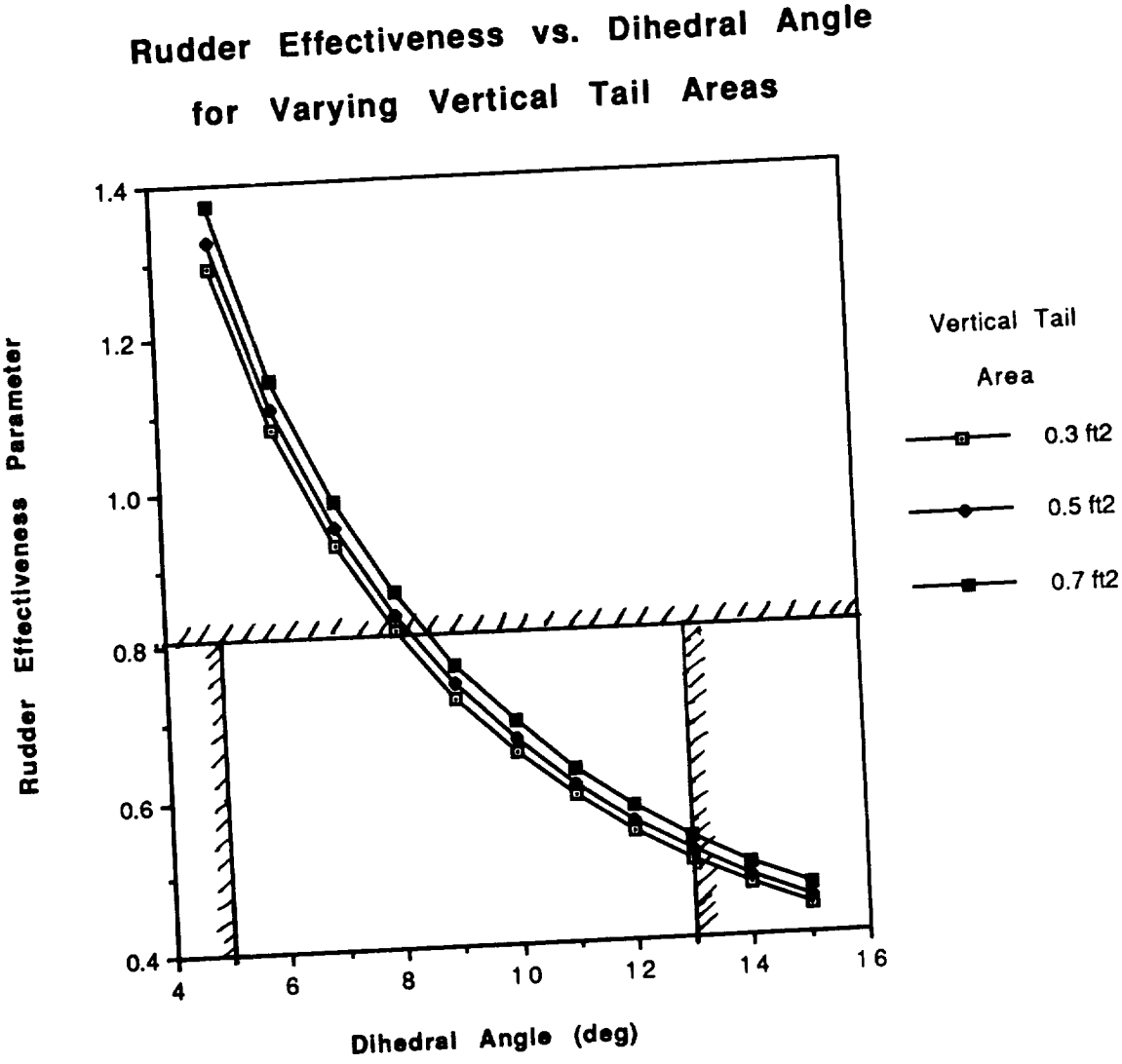
Rudder Effectiveness vs. Dihedral Angle
for Varying Vertical Tail Areas
Rudder Effectiveness Parameter
1.4
1.2
1.0
0.8
0.6
0.4
4
6
8
10
12
14
16
Dihedral Angle (deg)
Vertical Tail
Area
0.3 ft2
0.5 ft2
0.7 ft2

Table 1

Dihedral (deg)	C_L	C_D (wing and horiz. tail)
8	0.44521	0.01887
11	0.43990	0.01894
14	0.43295	0.01883

This data suggests that, for example, an increase in dihedral from 11 to 14 degrees would reduce the lift by 1.58% and increase the drag by 0.6%. This is not a significant amount if the dihedral amount needs to be increased.

One other parameter that was affected by the dihedral amount was the roll rate. Based on some typical data given in footnote 4, the roll rate as a function of the dihedral angle was plotted for different yaw angles. Figure 2.3-10 is the plot. The roll rate that was desired for this aircraft was 20 degrees per second. This was based on a necessary bank angle of 20 degrees, the cruise velocity of 25 ft/s, and a distance of 25 feet within which the bank angle is to be achieved. According to Figure 2.3-10, the only way the 20 degrees per second could be achieved for a yaw angle of 10 degrees is with a high dihedral angle (greater than 11 degrees). For a yaw angle of 12 degrees the desired roll rate could be achieved with a 9.5 degree dihedral. But a 12 degree yaw angle would need about a 24 degree rudder deflection and the maximum deflection was set at 20 degrees previously. One other option would be to keep the yaw angle at 10 degrees and increase the speed of the aircraft as the roll is entered and then, decrease the speed and the rudder deflection as the roll is achieved (only a 5 degree yaw angle is needed to hold the circular course).

All calculations using the equations given in section 2.3.3.1 were validated with graphs from the four part article "Dihedral". The article supported the data produced and was in agreement to within a few percent. The LinAir drag and lift calculations were easily validated by calculating the change in the lift vector as it is tilted by the dihedral angle.

Based on all the data and trends shown in the previous six graphs the following parameters were selected: a dihedral angle of 10.5 degrees: a rudder effectiveness of 0.68 which is equivalent to a rudder to tail area ratio of 50%: a vertical tail area of 0.50 ft^2: a roll rate of 18 degrees per second. The resulting rudder area will be 0.275 ft^2. Note that these parameters give a roll performance slightly better than the 80% of the fictitious aileron performance (Figure 2.3-9). Because the roll rate is smaller than the desired value, the aircraft will have to increase speed entering the turns to achieve the proper roll rate. The

FIGURE 2.3-10

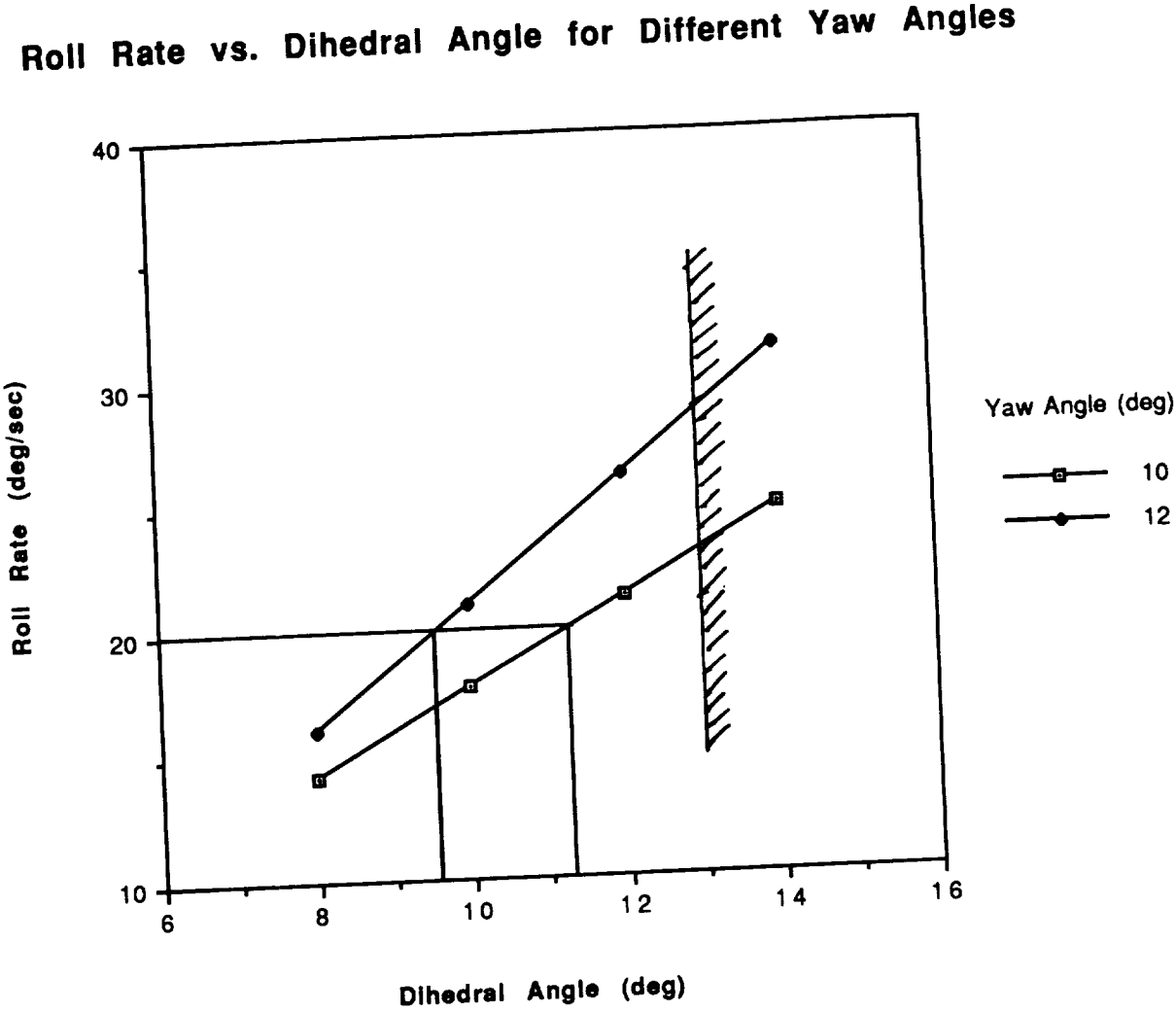
Roll Rate vs. Dihedral Angle for Different Yaw Angles
Roll Rate (deg/sec)
40
30
20
10
6
8
10
12
14
16
Dihedral Angle (deg)
Yaw Angle (deg)
10
12

dihedral was not increased above 10.5 degrees because of the losses in lift and possible difficulties in construction and durability. The aircraft needs all the lift it can get to fly at slow velocities. The EDA of 10.5 degrees will be spread over a three-panel polyhedral. The outer section of the span will be 3.1 feet long on each end and have a local dihedral of 12 degrees. The inner section will have an zero dihedral angle and be 1.2 feet on each side. With the large vertical tail and large rudder the directional stability and control was more than adequate for the mission. The large dihedral angle and high wing provided roll stability. A summary of the final design values for roll and directional stability and control are given in the Table below.

Roll, Directional Stability and Control Summary

Equivalent Dihedral Angle	10.5 degrees
Vertical Tail Area	0.50 ft^2
Rudder Area	0.25 ft^2
Vertical Tail Aspect Ratio	2.0

FINAL REMARKS

The stability and control design of the aircraft is now complete. The design shows a very stable aircraft with plenty of control power. Based on how the technology demonstrator performed, the stability and control was adequate for the aircraft. The only necessary changes for future reproductions of this RPV would be to ensure the center of gravity is at 30% of the mean aerodynamic chord.

2.4 STRUCTURAL ANALYSIS

2.4.1 V-n DIAGRAM

The velocity versus load factor (V-n diagram) is presented below as Figure 2.4-1. The vehicle has a maximum lift coefficient of 1.0, a weight of 3.0 lbs. and will be flying at an altitude of 15 ft. The limit load factor, which is representative of normal loads that the vehicle will endure during normal flight, is 1.5 and the ultimate load factor is 2.25; nl and nu respectively. The stall speed, which occurs at the point where the load factor is equal to one, is at 17.6 ft/s. The cruise speed is also indicated on the diagram at approximately 22.0 ft/s. No negative loads are indicated on the diagram due to the fact that in the operating regime for our RPV no maneuvers will be undertaken which will produce negative loads on the aircraft. Since the diagram deals with the flight envelope for this particular RPV, no negative loads are indicated. Gust loads have also been neglected in the diagram since the vehicle will perform its mission indoors where no significant gusts exist. The maximum speed for the RPV is indicated to be at 40 ft/s.

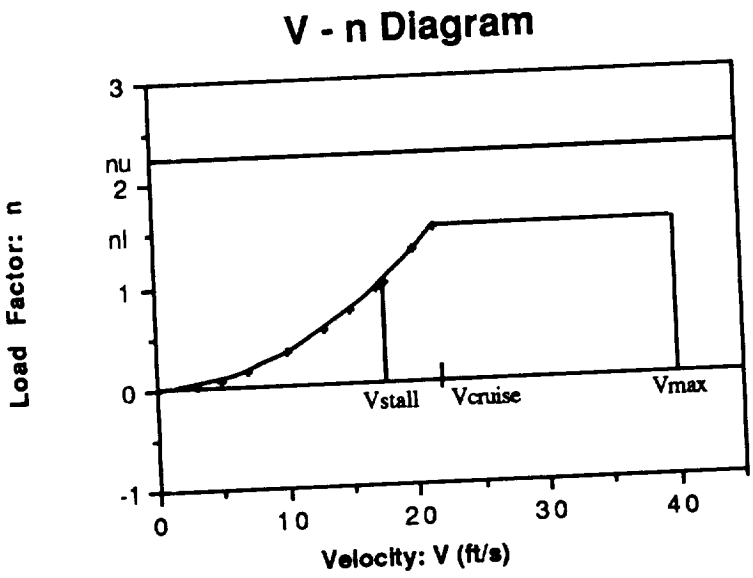

Figure 2.4-1

2.4.2 STRUCTURAL COMPONENTS .

2.4.2.1 WING

The objective of the wing design is to produce a wing of minimum weight which would not fail under the maximum loading conditions during flight. This load condition is a load factor of 1.5 in a turn (48.2 ° in bank angle). Failure criterion is based on the axial stress due to bending at the root of the main spar, causing a shear failure.

The design of the wing began with a Level 0 estimation. This estimation is based on prior database information for RPV's. This information allowed the preliminary weight calculation and the preliminary design of the layout of the wing. It was from this analysis that it was found that the wing weight should not exceed 12 ounces and that the wing would consist of a single spar or multiple spars supporting the load.

From the Level 0 estimation the Level 1 estimation takes a more in depth look at the wing design. This step involved the production of a short code on TKSolver! (a programming tool available in the Notre Dame Aerospace Laboratory). This code is used to calculate the bending moment at the root of the wing due to the lift on the wing. For this analysis, it was assumed that the spars of the wing carry all of the load on the wing as would a simple cantilevered beam. For this, half of the lift was placed at the midpoint of each side of the wing and the axial stress was found at the root based on the relation:

$$\text{Axial Stress} = \frac{-Mx*y}{I_x}$$

This equation is found in Beer and Johnston's Mechanics of Materials text p. 170. For greater detail on the analysis method and on the computer code used see Appendix B-1. The number of spars, rib spacing, t/c of the airfoil, leading edge and trailing edge size can be chosen and varied in this program. Some of these parameters do not enter the failure analysis of the program. For example the leading edge and trailing edge are assumed to not contribute to the strength of the wing, and hence are set to some reasonable size (based on database information, cross sectional area of leading edge = 0.0625 in^2 and trailing edge = 0.25 in^2), and used only in the calculation of the total wing weight. The same is true of rib spacing which was set to 4" to maintain a smooth wing (spacing was set based on database information also), but has no effect on wing strength. Design of the wing depends on the factors that contribute to the spars ability to withstand bending. These factors are the number of spars, spar cap dimensions, and t/c of the airfoil.

The purpose of the code is primarily to calculate the maximum axial stress in the spar to determine stress limits which must be met in order to avoid failure of the wing. Thus, a design figure of merit is the wing strength, as judged by a lower axial stress evident in the

spar. At this point the materials available and their stress allowable are important. Referring to Table 2.4-1, page 2.4-18, the possible range of allowable axial stresses can be seen. This gives an idea where failure will occur in order to make design judgements. A related result of the program is then to calculate the entire weight of the wing, providing another figure of merit upon which to judge any particular successful design. Wing weight is calculated in the TKSolver! code as described in Appendix B-1.

First it was desired to determine the number of spar caps necessary. From initial analyses, it was quickly seen that one main spar placed at the maximum thickness of the airfoil would be sufficient to withstand the loading on the wing. Therefore, for further analysis the number of spars was set to one. Second it was desired to determine the t/c of the wing. The t/c of the airfoil determines the height of the spar thereby greatly affecting the necessary spar cap dimensions to create a sufficiently strong wing. Based on aerodynamic conditions, as noted previously in the aerodynamics section, and weight conditions, the airfoil was chosen in the medium thickness range (t/c = 10% - 14%). It was then desired to find the effects of spar cap dimensions and wing size on axial stress.

It is at this point that it was desired to narrow down some the parameters still undetermined in the wing. This was done in an iterative type analysis which can be broken down into three main parts. In the first part, the surface area of the wing, aspect ratio, span, chord, and t/c ratio are all fixed and held constant. The effect of spar cap dimensions on axial stress can then be viewed (See Figure 2.4-2). It is important to note that the spar was assumed to have the basic geometry and configuration as given in Appendix B-1. From this figure it was determined that axial stress becomes relatively insensitive to changes in spar cap height above 0.25 in. (for any particular constant value of spar cap width). This reveals that there is no added benefit in increasing the spar cap height beyond 0.25 in., which will only result in added weight.

Axial Stress vs. Height of Spar Cap:
Lines of Constant Spar Cap Width

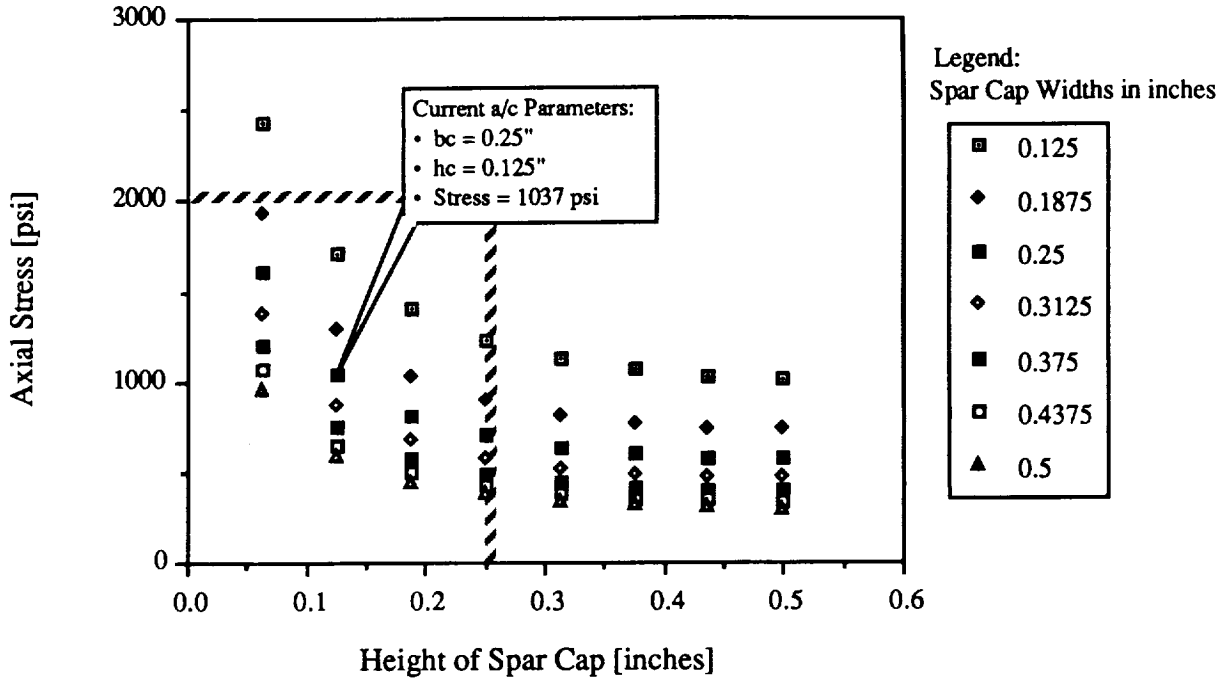

Analysis done with the following criterion set as constants:

- Surface area of wing = 5 sq. ft
- AR = 10
- Span = 85.5 in
- Chord = 8.5 in
- t/c = 12%

Figure 2.4-2

The second part of the analysis involves relating spar cap cross sectional area to the total weight of the wing (See Figure 2.4-3). In this analysis wing surface area and t/c ratio are held constant. Since spar cap cross sectional area is obviously spar cap width multiplied times spar cap height, this graph can be used in conjunction with Figure 2.4-2. As one examines Figure 2.4-2 to select appropriate spar cap dimensions based on wing strength (resultant maximum axial stress), it is necessary to keep in mind the effect on weight that this will have, hence Figure 2.4-3 is used to see the relative effects on total wing weight. Total wing weight is based on calculations which include two spar caps, ribs spaced every four inches, a 0.25 in^2 trailing edge, a 0.0625 in^2 leading edge, spar webs 1/64" in

thickness, and a coating of Monokote. For these calculations spar caps were asssumed to be spruce, and everything else (other than the coating) was assumed to be balsa.

Wing Weight vs. Spar Cap Area:
Lines of Constrant Span

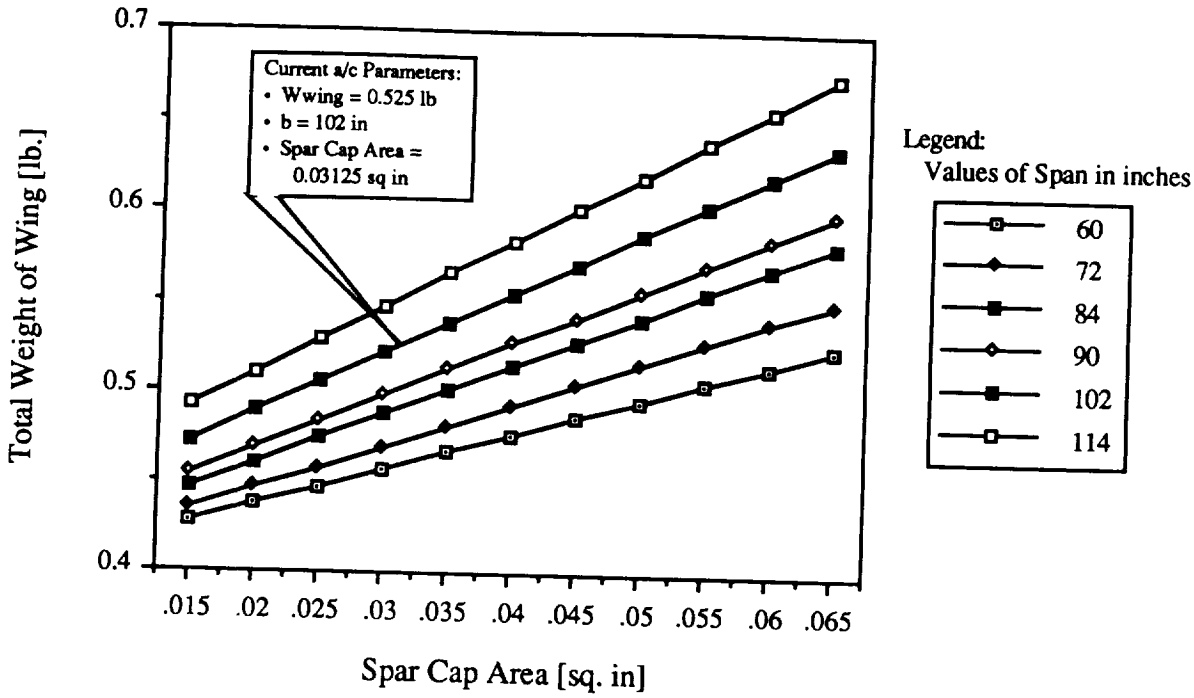

Analysis done with the following criterion set as constants:

- Surface area of wing = 6 sq. ft
- t/c = 12%

Figure 2.4-3

At this point the third part of the analysis becomes useful. In Figure 2.4-4 spar cap dimensions and t/c ratio are held constant, while the effect of wing surface area on axial stress is examined. Lines of constant weight are added to maintain a reference for judging any design. Wing design cannot be based solely upon strength and weight considerations. Performance considerations are the primary consideration in design of the wing. For propulsion reasons it would be desirable to have as large a wing area as possible in order to

minimize power requirements. This however, leads to structural considerations, necessitating a larger spar cap and often corresponding to a larger chord and/or aspect ratio. It is here where the constraints can best be seen. Constraints must be applied to this graph, based on the initial design requirements. In order to maintain steady level flight at an achievable flight velocity, the wing area cannot be less than 720 in^2 (5 ft^2). Also the wing chord cannot exceed 10 in. or the plane will not be able to fly within the required 100,000 to 200,000 Reynolds number regime. Then from this figure it is possible to pinpoint or select values such that they do not fall outside of the constraints. Now that each graph has been described it will be useful to describe the process followed to reach some reasonable design values. It is important to note that this analysis is used to determine primarily qualitative results rather than quantitative. This analysis was performed while the geometry of the wing and plane were being modified and therefore some of the constants change from one graph to the next. This doesn't mean that useful data and relationships cannot be drawn, since changing the constants would not change the same general trends that appear. Figure 2.4-4 is the most useful graph as it allows relations of chord, span , aspect ratio, surface area and gives the related stress and total wing weight. The initial configuration had a wing surface area of 5 ft^2. Propulsion considerations led to desire a wing of 6 ft^2 or larger. Looking at Figure 2.4-4 it was desired to keep stress below 2000 psi, maintaining a factor of safety of 3 for spruce (most likely material option at this point). The 2000 psi constraints stems from a desired factor of safety of 3, and the maximum allowable stress in spruce of 6200 psi as given in Table 2.4-1. It was also desired to keep chord as low as possible in order to stay as close to Reynolds number = 100,000 as possible. A compromise was reached and the point shown was chosen. Using Figure 2.4-2 spar cap dimensions were chosen that would minimize axial stress, but keep the weight as low as possible (check weight based on spar cap area in Figure 2.4-3). By using all three graphs the optimum combination was chosen. Finally, it was necessary to enter the chosen values in the TKSolver! code (which originally generated these graphs) and get a set of data for an exact set of points. At this point the following values have been chosen:

Wing Area = 864 in^2 (6 ft^2)
Aspect Ratio = 12
Chord = 8.5 in
Span = 101.8 in (8.49 ft)
t/c = 12%
t = 1.275 in
Height of Spar Cap = 0.125 in

Height of Spar Cap = 0.125 in

Width of spar Cap =0.25 in

Total Weight of Wing = 0.525 lb (8.4 oz.)

Axial Stress vs. Surface Area of Wing

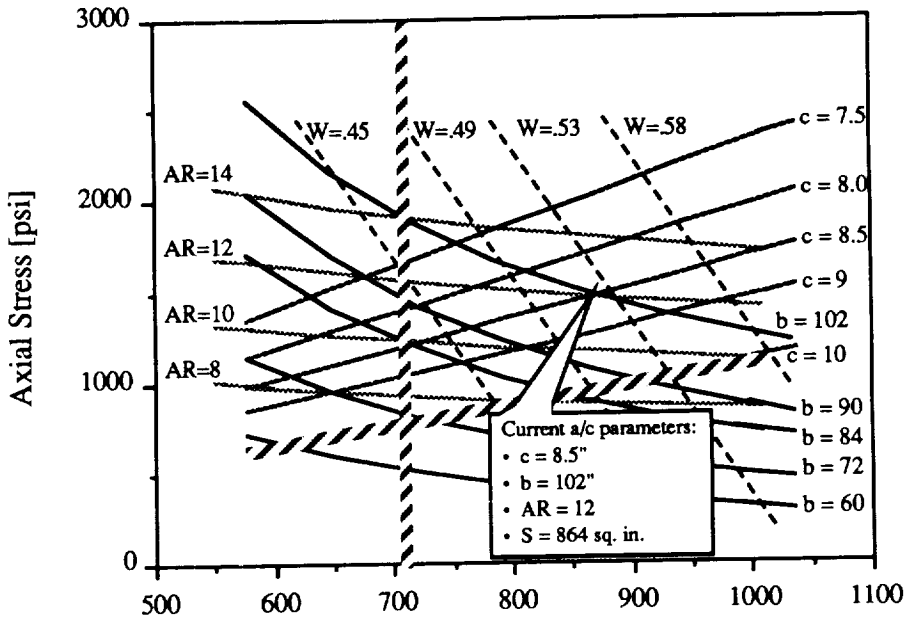

- Spans (b values) , and chords (c values) are in inches
- Weights (W values) are in pounds
- ////// = Constraints

Analysis done with the following criterion set as constants:

- Width of spar cap = 0.125 in
- Height of spar cap = 0.25 in
- t/c = 12%

Figure 2.4-4

After this Level 1 estimation was complete, the values determined for the wing were placed into Astros (a finite element analysis program) to verify their accuracy. This was used primarily as a check on what had been done previously, in order to ensure that the wing will not fail, and it was found that the wing was sufficiently strong to avoid failure.

2.4.2.2 FUSELAGE

The fuselage design was also based on strength and weight. The primary design factor is weight for the fuselage. For this reason the team decided to use a truss configuration in order to minimize the weight. Preliminary truss design began with selection of the optimum fuselage length. The length of the fuselage is governed by stability and control considerations. Differing fuselage lengths correspond to varying horizontal and vertical tail sizes. From work done in stability and control, a fuselage length of 2.5 ft was chosen to give a reasonable length fuselage and tails which were not inordinately large. Truss layout was based on a simple yet common layout (See Figure 2.4-5 a,b), and analysis was done by again using a simple beam bending analysis. For a free body diagram used in the analysis see Appendix B-2. The fuselage is subject to 0.4 lbs. vertically and 0.35 lbs. horizontally due to the max forces possible on the tail surfaces. In this analysis it was assumed that the four main beams would carry all of the load as cantilevered beams. For more detail on this analysis see Appendix B-2. Though a rather crude analysis, it gives a qualitative result on failure which will be accurate. Further analysis would involve the determination of truss coordinates and placement of loads in order to use a 3-D truss analysis program. Due to the 'rubber' nature of the fuselage this was not done. It was also felt that this higher level analysis would only yield better quantitative results but the same qualitative result, and was therefore neglected in order to save effort in a time constrained project, since initial analysis revealed that the present truss configuration would not fail under the flight load conditions.

2.4.2.3 EMPENNAGE

The horizontal and vertical tail layouts were also done based on a simple beam bending analysis. The external 'frame' of each tail is assumed to carry the load, while the internal ribbing is merely to maintain the shape of the tail. For a free body diagram see Appendix B-3. The tail is primarily locked into a supporting structure, with the movable surfaces connected through the middle by a thin rod. The vertical tail seat is somewhat more complicated as it cannot be placed all of the way through the fuselage. For this reason the seat is a solid piece of spruce with two square spruce pins running through it horizontally to attach to the sides of the fuselage. To analyze this tail the moment produced at the base of the vertical tail by loading is assumed to transfer directly through the horizontal pins.

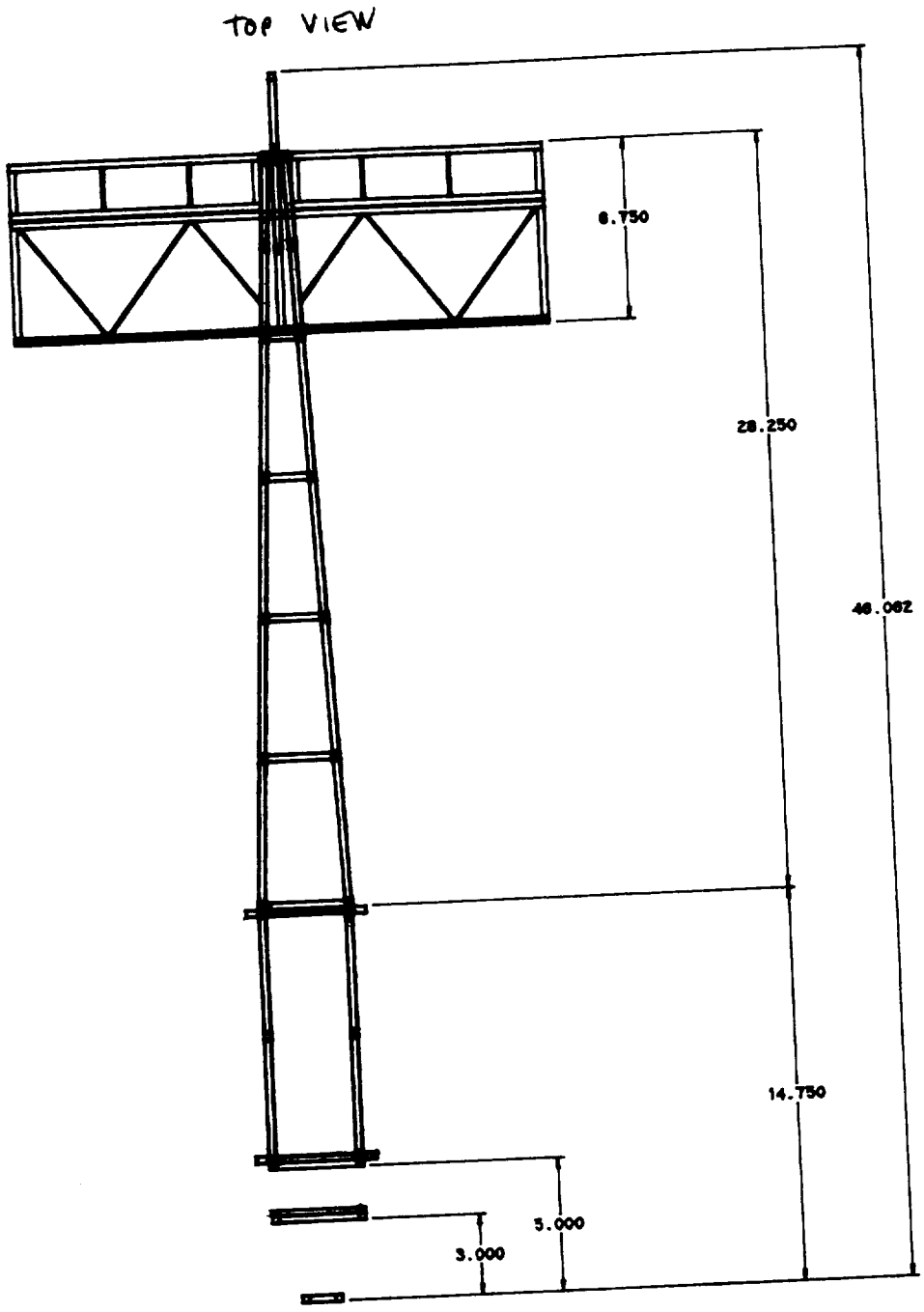

FIGURE 2.4-5 a

SIDE VIEW

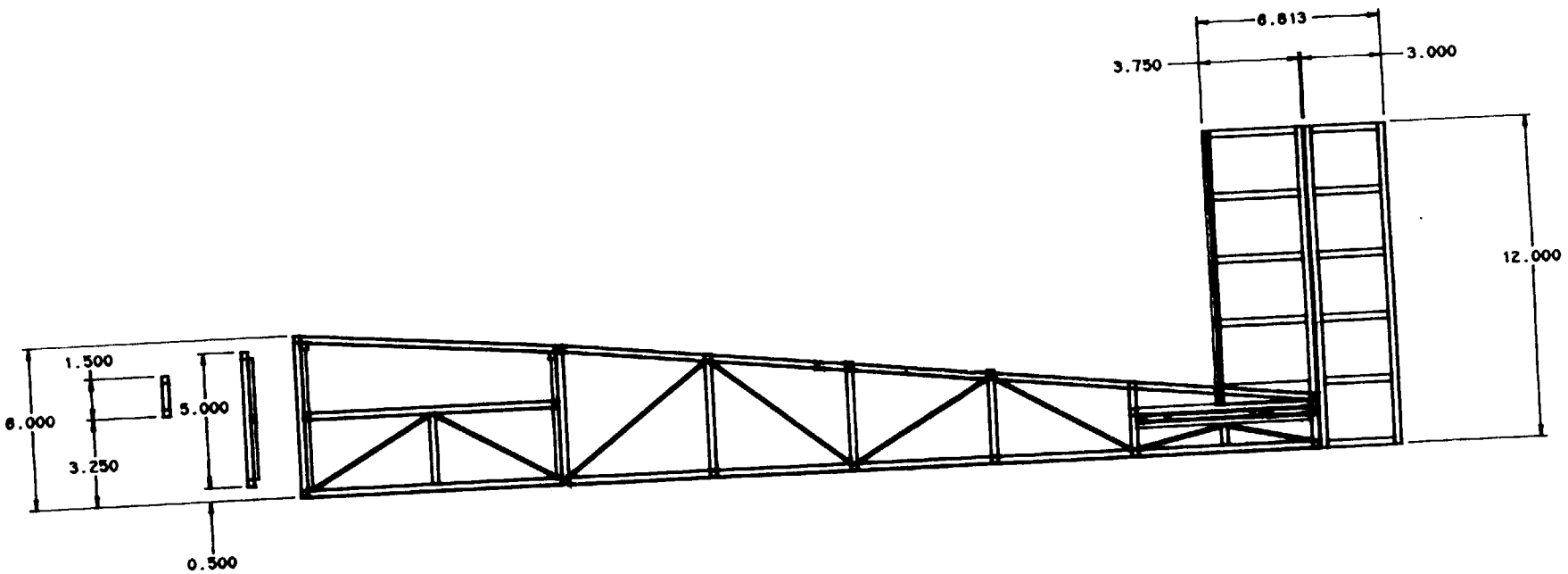

FIGURE 2.4-5 b

These pins are then analyzed as cantilevered beams. For more detail on the analysis of the empennage see Appendix B-3.

2.4.2.4 LANDING GEAR

The landing gear of the vehicle is an important consideration. It is desired to have gear that will be strong enough to endure the landing loads but also have the ability to deflect and absorb some of the energy that will be transferred to the vehicle during landing. In sizing the landing gear for the RPV many parameters must be considered. The parameters that will be controlled in this particular analysis are modulus of elasticity, the length and the radius for the struts. The tire size was chosen based on research of the existing data and articles in model airplane magazines. The tire size was selected to be 2 in in diameter. Once these parameters have been solidified, the deflection of the gear due to the landing loads will be determined.

In modeling the loads on the landing gear, the gear wire is assumed to be a circular cantilever beam with the load P acting at the end.(see Figure 2.4-6) The load is small enough that it may be assumed that the beam undergoes only elastic deformation due to the load. The give in the tire during the landing process has been assumed to be negligible compared to the deflection of the beam. The maximum deflection, x, due to this load occurs at the end of the beam and calculated by the following equation: $x=P*L^3/3*E*I$, where E is the modulus of elasticity, L is the length of the beam and I is the moment of inertia of the beam cross section. This equation is found in Beer and Johnston's Mechanics of Materials text.The stiffness of the beam, K, must be determined and then used in the following equality to determine the deflection of the beam due to the landing load, $1/2*m*v^2=1/2*K*x^2$. In this equation, the mass of the RPV, m, and the landing velocity, v, are set by the structure and design requirements of the RPV and can not be varied.

A) Landing Loads

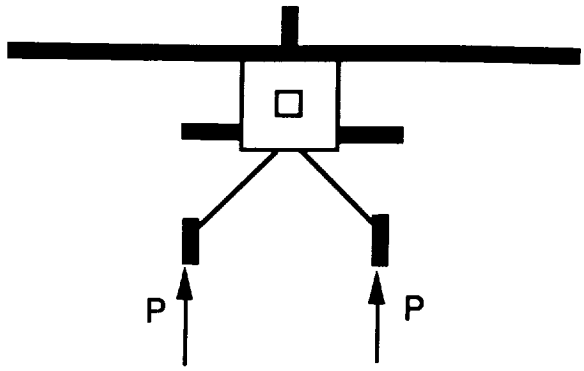

B) Cantilever Model

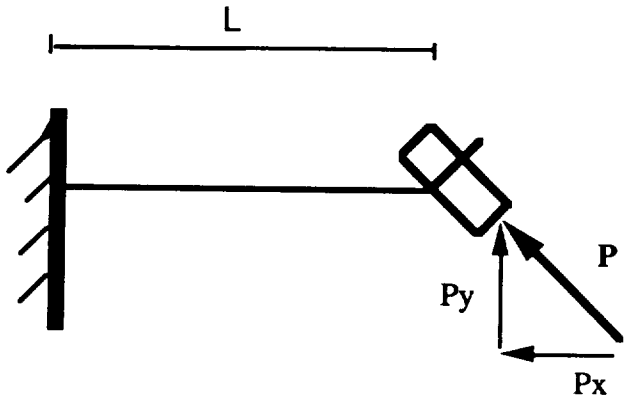

Figure 2.4-6

The stiffness of the beam varies with the radius, length and modulus of elasticity of the beam. A simple computer code was written to calculate the deflections due to loads varying from 10 to 100 pounds for varying radii of the beam with the length and modulus of elasticity as input. The code made use of the equations mentioned previously. (see Appendix B-4 for computer code and data) The data was then plotted and trends and restrictions were examined in order that a specific range of radii and lengths could be determined.

The material of the beam was selected by holding the radius and length of the beam constant and calculating the stiffness from the load vs deflection curve. It is desired that a low stiffness will be used in order that the beam will bend and not remain stiff and transfer the load to the main wall in the fuselage. Observing Figure 2.4-7, it is obvious that the

stiffness for aluminum is less than the other materials. However, steel is the material that will be used due to its availability.

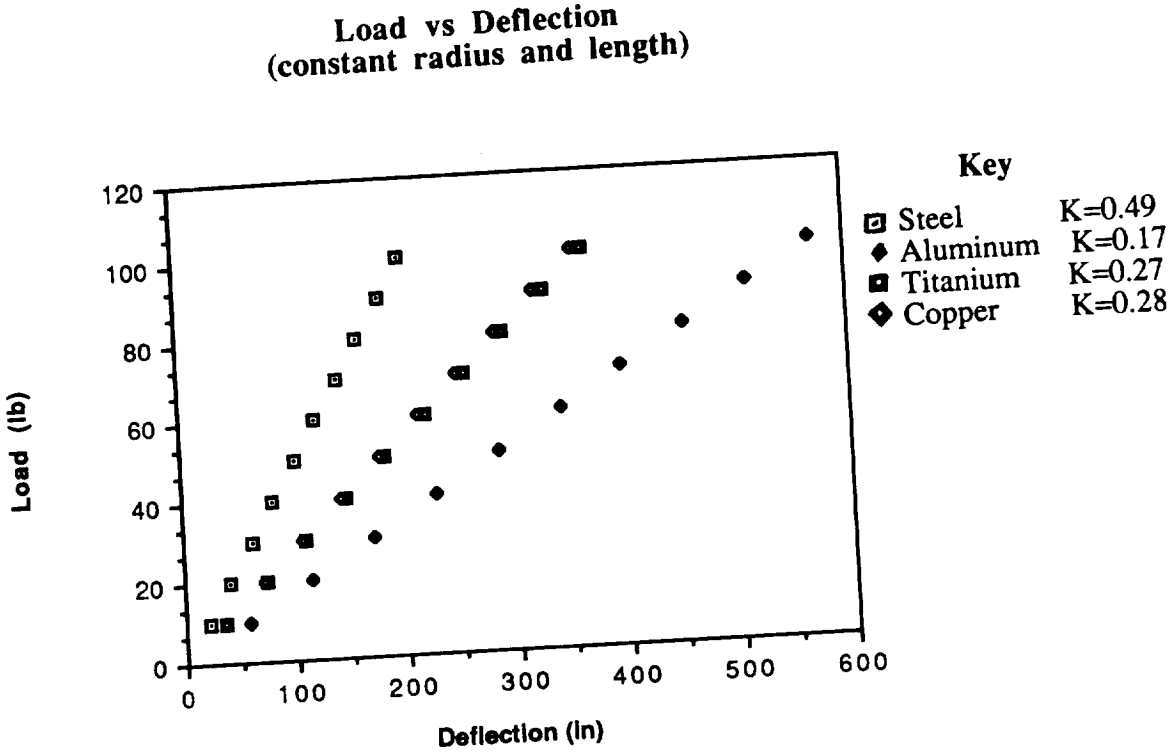

Figure 2.4-7

There are restrictions that exist on the amount of deflection that is acceptable in this design. The beam can not deflect such that the propeller will touch the ground. With the original design of the twelve inch propeller being mounted high on the six inch high fuselage, it was considered that the length would have a lower boundary of two inches. However, this design was updated and propeller is now being mounted at the center of the fuselage. Thus the gear lengths of two and three inches and the radii of 1/64 to 1/16 inches will not be acceptable here. The gear of length four inches can be used as long as it does not deflect more than one inch, the five inch gear may not deflect more than two inches, the six more than three and the seven more than four. This upper boundary of seven inches was set by examining a data base.

It can be seen in Figures 2.4-8 and 2.4-9 that the stiffness decreases with increasing length for a beam of constant radius. It can also be seen in Figures 2.4-10, 2.4-11, 2.4-12 and 2.4-13 that for a beam of constant length, the stiffness increases with increasing radius.

Therefore it is desirable to design a beam that will be long and slender but will still meet the constraints. This will also result in the beam being light weight which is a great concern in designing all parts of the RPV. From the Figures referenced previously, it is observed that for some of the lengths of the beam there are limited radii that may be used to meet the constraints. For example the beam of length seven inches can only have a radius of 7/64 inches of 1/4 inches to meet the constraints. From the data generated and studied, the radius of the beam was selected to be 3/32 inches and the length of the beam was selected to be five inches.

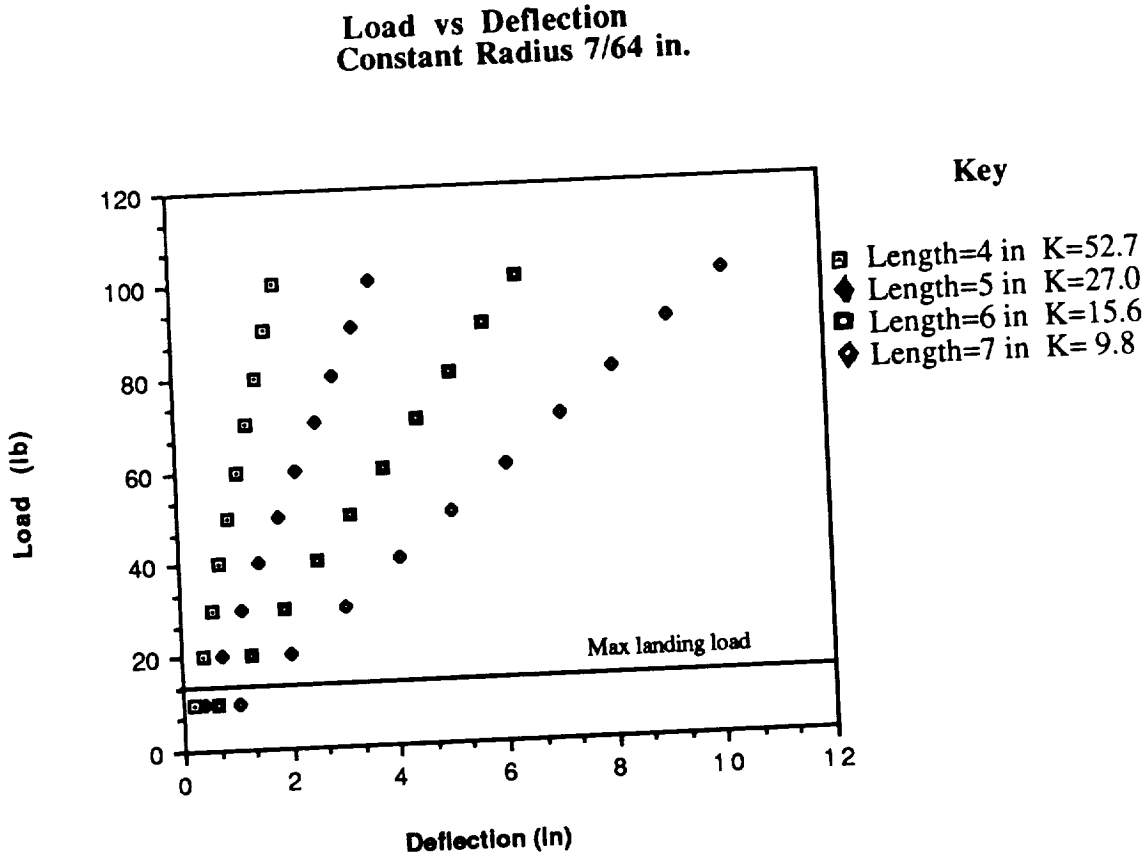

Figure 2.4-8

Load vs Deflection
Constant Radius of 1/4 in.

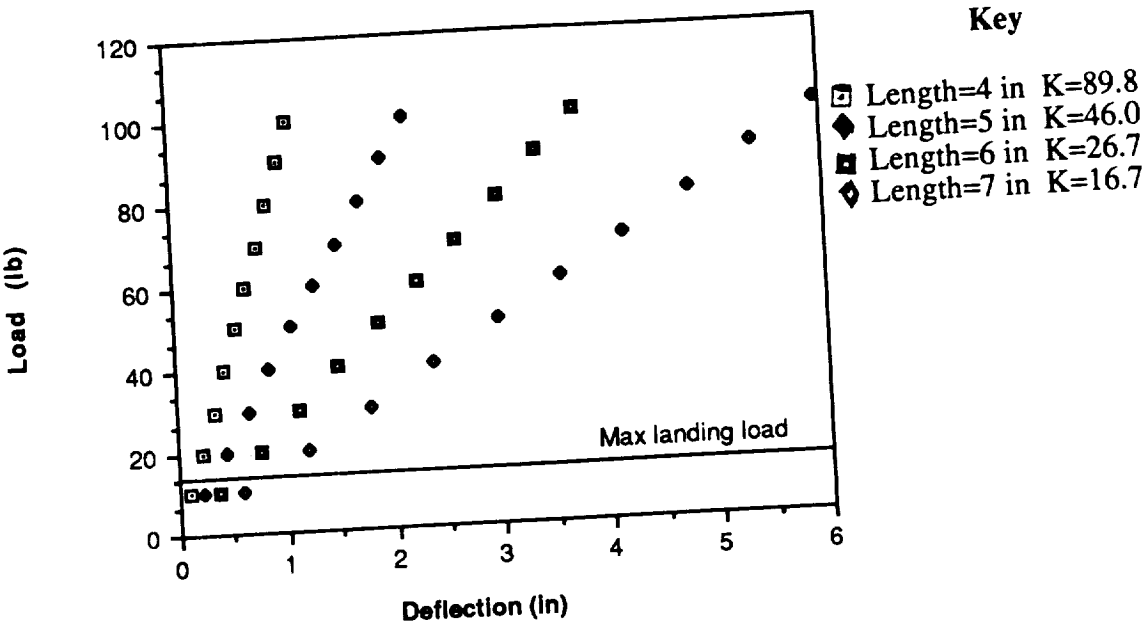

Figure 2.4-9

Load vs Deflection
Constant Length of 4 in.

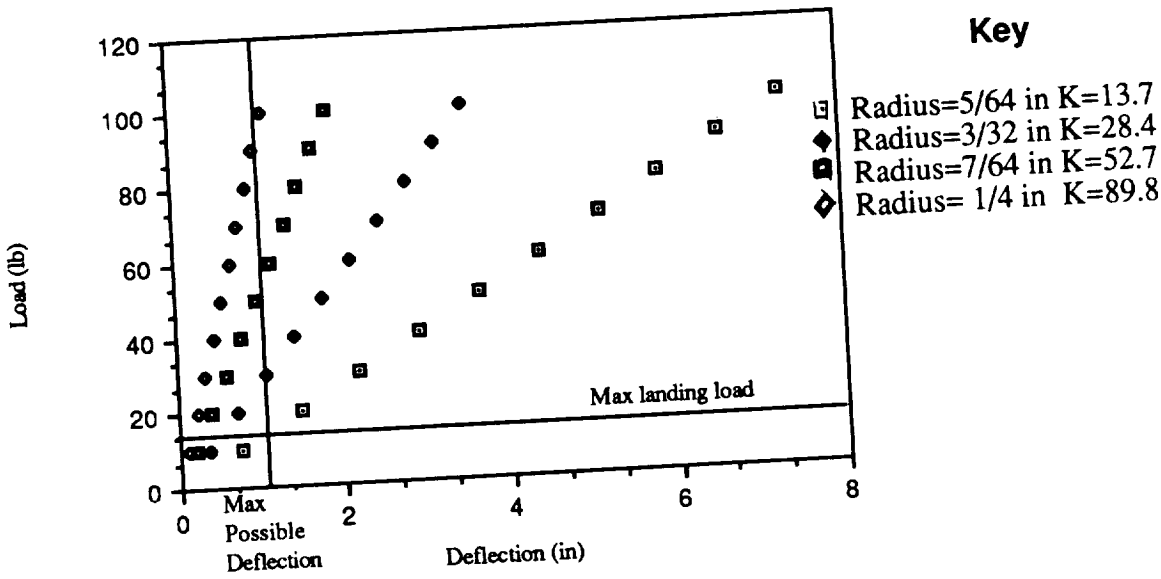

Figure 2.4-10

Load vs Deflection
Constant Length of 5 in.

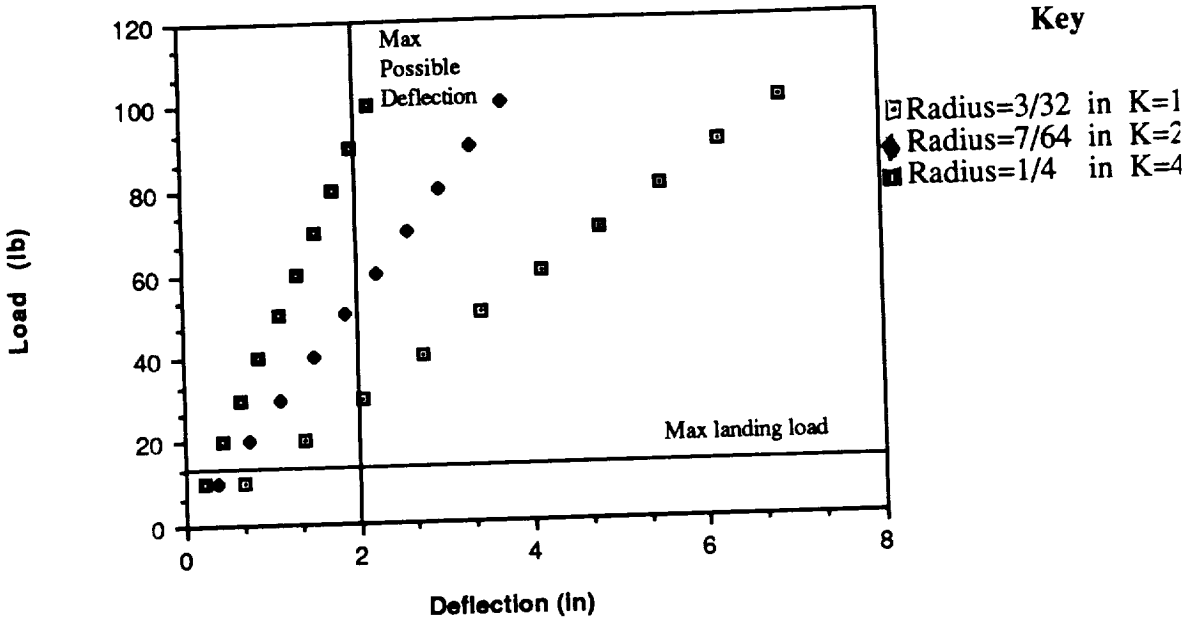

Figure 2.4-11

Load vs Deflection
Constant Length of 6 in.

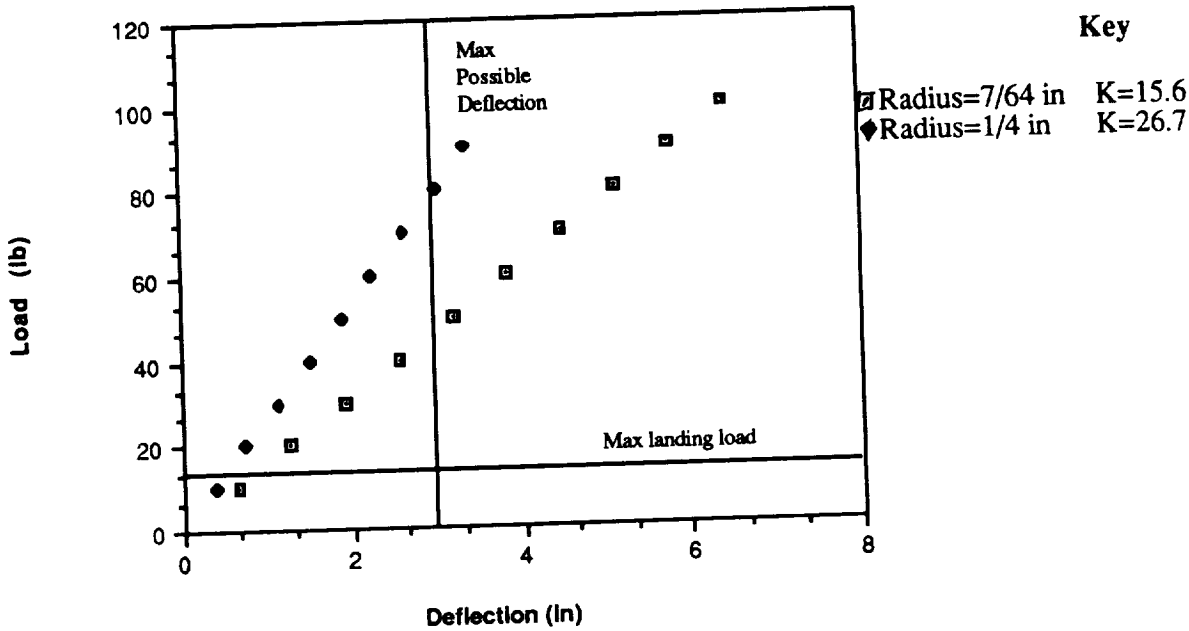

Figure 2.4-12

Load vs Deflection
Conatant Length of 7 in.

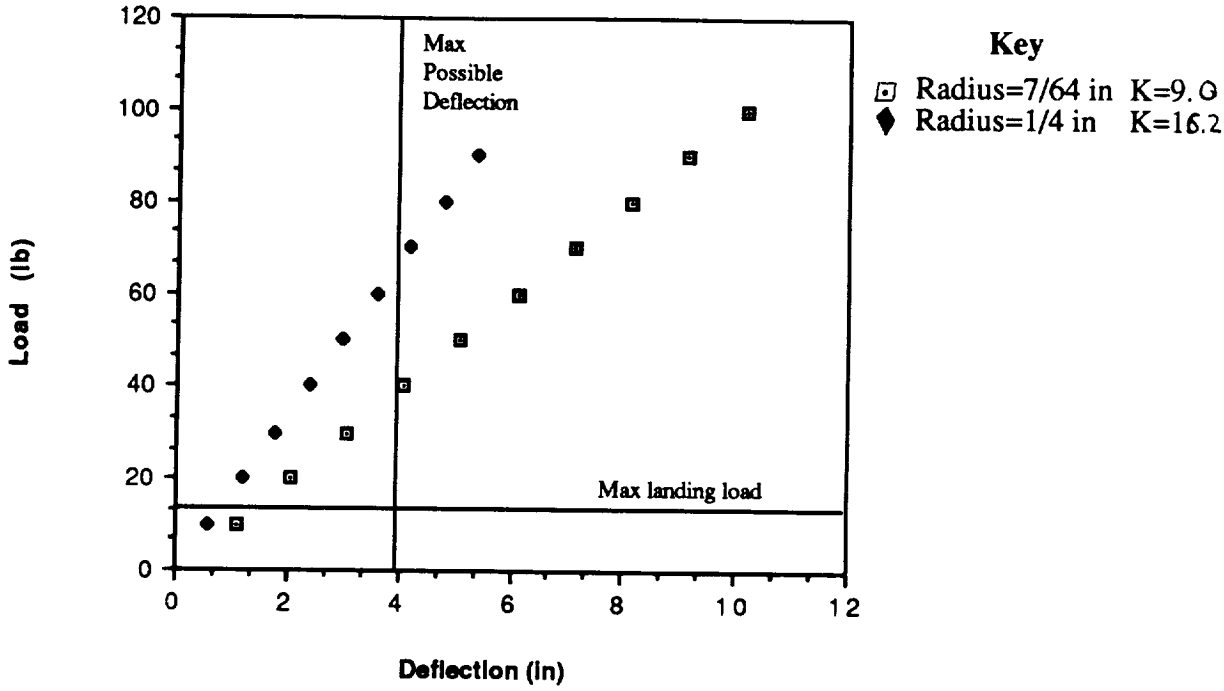

Figure 2.4-13

2.4.2.5 MATERIALS SELECTION

In the design of each component in the RPV some type of analysis was performed in order to find the maximum stress during flight. From available data provided by the aerodynamics laboratory on some materials (See Table 2.4-1), the maximum stress can be compared with the maximum allowable stress of the materials, and an appropriate material can be chosen. From this, the RPV will be primarily made from balsa, except for some key structural pieces. These are the two spar caps, the wing hold down rods, and the vertical tail seat and pins, which will all be constructed from spruce. The three panels in the forward section of the plane are made of plywood due to the high loads in the payload area.

Table 2.4-1

MATERIAL	DENSITY [lb/in^3]	ALLOWABLE STRESS [psi]
Balsa wood	0.0058	400
Spruce	0.016	6200
Birch Plywood	0.023	2500

2.4.2.6 GENERAL CONSTRUCTION

2.4.2.6.1 INTERNAL LAYOUT

The internal components of the RPV consists of a motor, motor batteries, speed controller, receiver, receiver batteries, two servos, and a payload (2" x 2" x 2" two ounce box). The design of the RPV requires that all of this weight be supported forward of the main truss section of the fuselage. It is also desired to tie these weights into the wing which will be supporting them during flight. For this design the motor is placed as far forward as possible, supported by a plywood fire wall on an end mount system. The motor area is then connected to the main wing box area through a small box which holds the motor batteries. The main wing box is connected to the wing by rubber band hold down pins. Two plywood panels at each end of the box add to its structural integrity. The wing box is also the area where most of the payload is contained. The 2 in cube is placed to the extreme front of the wing box, with the servos at the extreme rear. The servos are supported on two bars across the width of the fuselage, while just behind the servos are the speed controller and receiver stacked on top of one another, vertically. In between the box payload and the speed controller lays the system batteries, velcroed down to the shelf. (See Figure 2.4-14)

Top View of Fuselage - Internal Layout

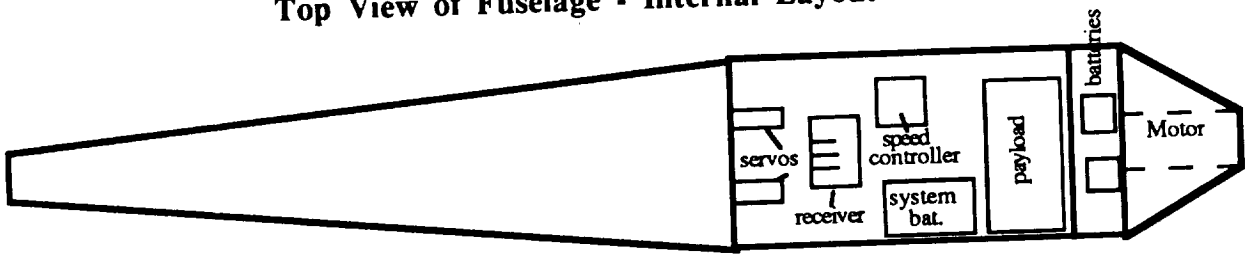

Figure 2.4-14

2.4.2.6.2 SCALE RPV DRAWING

Since the design team consists of amateur builders it was desired to keep the design of the RPV as simple as possible. As the design process developed and continued a 3-D computer picture of the airplane was produced. It was through the development of this picture that some construction difficulties were identified and resolved. The primary accomplishment of this task was to generate an accurate scale picture of the RPV which can be used as a guide during actual construction (See Figures 2.4-5 a,b for plots of this drawing). This exercise also allowed accurate placement of the shelf holding the servos, such that control rods will reach there respective control surfaces. It also allows for determination of necessary connections between components, such as the vertical tail seat.

2.5 WEIGHT AND CENTER OF GRAVITY ESTIMATION

Much of the initial work done by the weights and structures division was to estimate the weight and center of gravity for our RPV. Due to the fact that the weight of the RPV was a primary concern throughout the design process, it was necessary to spend the effort and time in keeping the RPV systems and structure to a minimal weight to increase the possibility of a successful mission. The initial step was to investigate the existing data base. Once this was done and a "preliminary" estimation of the weight of the RPV was completed, the center of gravity could be calculated. It was desired that this center of gravity fall within the range of 25% to 40% of the chord of the wing in order to obtain the desired stability and control for the RPV. Of course as the design progressed and different aspects of the vehicle changed, these values also changed. The design group set initial goals for each particular division, for example structures and weights, propulsion, and stability and control, to meet. Once the data base was reviewed, the design weight for the RPV was set at 3 lbs (48 oz). The structures and weights group felt that if this design goal was met, as well as the other design goals, the mission would be successful.

2.5.1 COMPONENT WEIGHTS

As stated previously, the first step that was necessary in this particular analysis was to examine the existing data base. Speaking to our 'resident expert' on RPV systems, Mr. Joe Mergen, a good estimation for the sizes, material and weights for RPV components was obtained. From this review of the data and making estimates based on this data and the desired size of our RPV, a "preliminary" estimation of the weight was made; level one of the weight estimation.

Level two of the weight estimation for the vehicle consisted of obtaining more concrete values for the weights of the components of the RPV, such as the motor, servos, radio receiver and batteries. Once these have been determined, the size and weight for the structure of the vehicle was estimated. Again the existing data base was consulted, but values were also obtained from the manufacturers of these components once these components were selected. The propulsion team selected a certain motor and the required batteries to operate this motor. The number of servos was determined by the stability and control division. The initial estimation for the weight of the propulsion system was 25.0 oz, which includes the battery pack and motor. The remaining avionics were initially estimated to weigh 18.5 oz.

Once the weights for the propulsion system, control system and remaining avionics were estimated, the weight for the RPV structure was estimated. From the design goals determined early in the design process, it was noted that the total weight for the RPV was a critical factor in completing the mission successfully. The weights and structures division of the group decided that in order to keep this weight a minimum, the avionics and propulsion system would be selected and a minimal structure would be constructed around it. In speaking with Mr. Mergen and examining RPVs built in previous years, the materials were tentatively selected and the general structure of the RPV determined. The initial estimation for the wing weight was 12.0 oz and the weight for the fuselage / empennage section was 12.0 oz. This brought our initial estimation to a value of 4.3 lb (68.8 oz) for the total weight of the RPV.

The wing section was then studied in greater detail and was designed to be a wing of minimal weight that could withstand normal flights loads. This design process was discussed previously and resulted in a second estimation of the wing weight of 8.0 oz. As the design of the vehicle proceeded this value changed. The final estimation for the weight of the wing is 8.4 oz. The fuselage / empennage section was then examined in greater detail. It was decided by the weights and structures division of the group that the fuselage would be of a truss configuration in order to keep the weight down by reducing the need for solid sections in the fuselage structure. Solid panels would be included in the main wing box section, where the propulsion system and avionics will be located, for strength reasons and the empennage was designed to be a minimal structure that could withstand the load incurred during the mission. The sizes and materials for the members of the truss and other portions of the fuselage were determined by examining model airplane magazines and consulting Mr. Mergen. Once this structure of minimal weight was designed it was analyzed to insure that failure would not occur during flight and a value for the weight of this fuselage / empennage section was estimated to be 7.2 oz. Again, as the design of the RPV proceeded the weight of the fuselage / empennage section changed. The final estimation for the weight of this section is 8.4 oz. The landing gear was also studied in greater detail and resulted in an estimation of a weight of 3.5 oz. As was stated previously, the structure would be changing as the design progressed and thus the weights of these components would be changing. The following table, Table 2.5-1, shows the final values for the weight and weight percents for the components of the RPV.

TABLE 2.5-1

COMPONENT	WEIGHT (oz)	WEIGHT PERCENT
Avionics	8.0	18.3
Payload	2.0	4.5
Motor	12.7	29.1
Propeller	0.7	1.6
Wing	8.4	19.2
Fuselage/Emp	8.4	19.2
Landing Gear	3.5	8.1
TOTAL WEIGHT	**43.7 oz**	
DESIGN WEIGHT	**48.0 oz**	

2.5.2 CENTER OF GRAVITY ESTIMATION

Once the component weights were estimated, the center of gravity could be located. This calculation was done several times throughout the design process, due to the fact that it was a necessary piece of information for the stability and control division. The weight and location for the individual components must be known in order to calculate the center of gravity. Therefore it is essential to study the internal layout for the systems and avionics in order to position them correctly. The systems were positioned and mounted in such a manner that they would be easily accessible and push the center of gravity as far forward as possible. This was desired due to the short nose of the vehicle. Due to this short nose, it was a concern of the weights and structures division that the center of gravity would be too far rearward.

After the initial estimates of weights were refined through the design process, the center of gravity was found using locations and weight figures for each component of the RPV. These component weight figures are more accurate than the initial weight figures, since the initial figures were based largely on preliminary estimates. A table summarizing the majority of the RPV's component weights and locations is given below, Table 2.5-2. The component center of gravity location is referenced from the nose of the RPV. (See Figure 2.5-1)

TABLE 2.5-2

COMPONENTS	WEIGHT (oz)	CENTER OF GRAVITY LOCATION (in)
Motor	6.5	2.125
Motor Batteries	6.24	6.5
Payload	2.0	9.0
Receiver Batteries	2.0	12.5
Receiver	0.95	14.0
Speed Control	3.23	14.0
Servos	1.2	16.0
Wing	8.4	6.75
Fuselage (main truss)	1.0	24.0
Landing Gear	3.5	5.5
Horizontal Tail	0.67	38.8
Vertical Tail	1.5	41.5
Wing Box	3.686	9.0
Nose (motor casing)	0.142	1.5
Nose (batteries)	1.37	3.75

Xcg from nose = 9.4 in.

The following equation was used to calculate the center of gravity in the X direction:

$$\text{Xcg from nose} = \Sigma (\text{Xcg comp} * \text{W comp}) / \text{W total}$$

The center of gravity was not calculated in the Y direction. Due to the symmetry of the RPV it is expected to fall near the X axis.

Side View Fuselage - Component Location

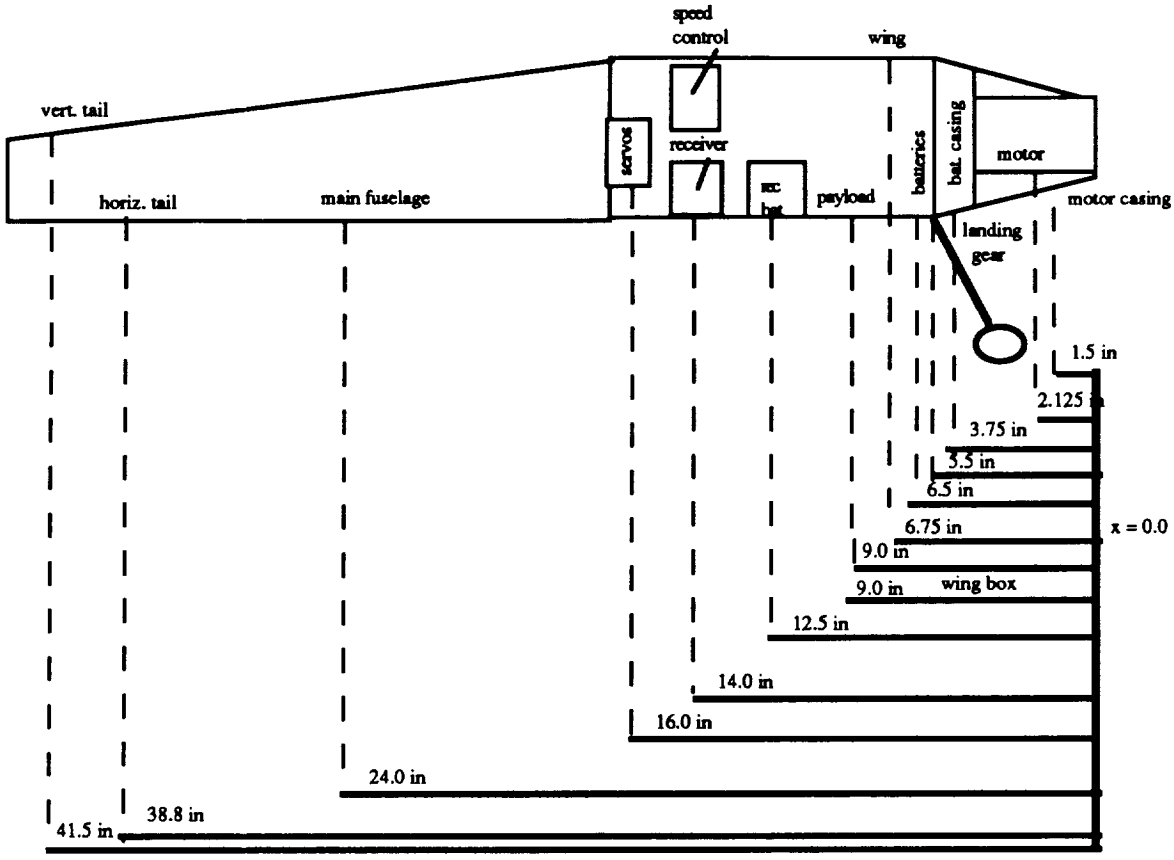

Figure 2.5-1

3 PERFORMANCE ESTIMATION

3.1 TAKE-OFF AND LANDING ESTIMATES

Take-off distance for the aircraft is constrained to only 150 feet. This is due to the fact that the flight will occur inside the LOFTUS Sports Complex (Notre Dame, IN) and space is limited. With the proposed propeller-motor combination, a take-off distance of 31 feet is achieved. This value is based on equations found in Introduction To Flight (p. 309-311) by Anderson.

$$\text{take-off distance} \qquad \frac{1.44 * W^2}{g * \rho * S * C_{l,max} * T[D + \mu_r (W - L)]}$$

When using the equations, ground effect was neglected because the effects are beneficial and a worse case scenario was used to insure that the aircraft would lift-off. Also, a ground friction coefficient of .04 was assumed for the astro turf found in the LOFTUS center.

Once the aircraft completes the required three laps is must prepare itself to approach the runway and land. Upon the wheels touching the ground, the aircraft will rely strictly upon ground friction as a means to slow the aircraft to a halt. Using the equations found in Anderson's Introduction To Flight (p. 313-315), the total ground landing distance is 133 feet.

$$\text{landing distance} \qquad \frac{1.69 * W^2}{g * \rho * S * C_{l,max} * (D * \mu_r * W)}$$

This distance is the actual distance it will take the aircraft to stop once the wheels touch the ground. A ground friction coefficient of .04 was once again assumed for the astro turf.

3.2 RANGE AND ENDURANCE

In evaluating the range and endurance of our RPV, it must be noted that these parameters are of importance because the vehicle must be able to complete the full three laps as slowly as possible and return to the landing area. However, excess range and endurance capabilities are of no extra benefit and, in fact, could be detrimental to the goals of the mission if these "benefits" caused an increase in the RPV's weight. Thus, it was necessary to try maximizing endurance and range by using the aerodynamic relationships and conditions in R. C. Nelson's Flight Mechanics text (pp. 4.16-4.17). However, since it is impossible to simultaneously maximize range and endurance, it was decided that endurance would be maximized since this was one of the design objectives specified in section 1.1. This was accomplished by trying to minimize power (thus maximizing $C_L^{3/2}/C_D$).

To actually estimate the range and endurance, a TKSolver program was again utilized to determine the sensitivities inherent to these performance characteristics. As flight speed and propeller diameter were varied, it was found that the endurance proved to be very sensitive to a decrease in propeller diameter. This is evidenced by the fact that a three inch decrease in diameter increases endurance by nearly 110 seconds (see figure 3.2-1).

Endurance vs. Prop. Diameter For Varying Flight Velocities

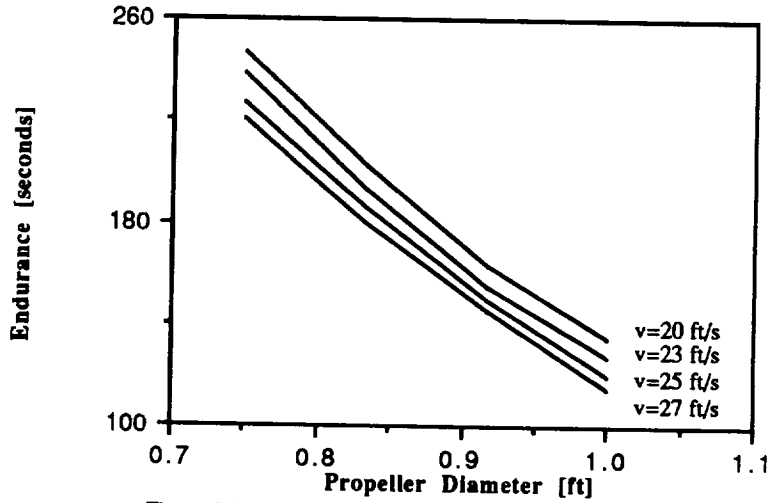

Figure 3.2-1: Endurance at 25 ft/s and dia. of 10" is 193 seconds

This corresponds to the fact that as the propeller diameter decreases, the motor does not have to work as hard to drive the propeller. Thus, motor current draw decreases and endurance increases. As a result, it is estimated that the Drag-n-Fly can stay in the air for

up to 193 seconds on a single charge (full battery capacity) at an airspeed of 25 ft/s and a propeller diameter of 10 inches.

A similar analysis was done to determine the sensitivities of range. Once again, it was seen that the general trend is for range to increase with decreasing propeller diameter (see figure 3.2-2). Furthermore, in analyzing the course over which the RPV will fly, we determined that the RPV must travel approximately 2800 feet from the time it starts moving to the time it stops after landing. Consequently, our aircraft must be able to safely fly this distance in order to complete the mission. Thus, it is estimated that our RPV can fly up to 4831 feet at an airspeed of 25 ft/s and with a propeller diameter of 10 inches. Although the range is substantially greater than that required, it was determined that the excess range did not adversely effect the weight of the RPV (as discussed earlier) and provides a comfortable margin of safety.

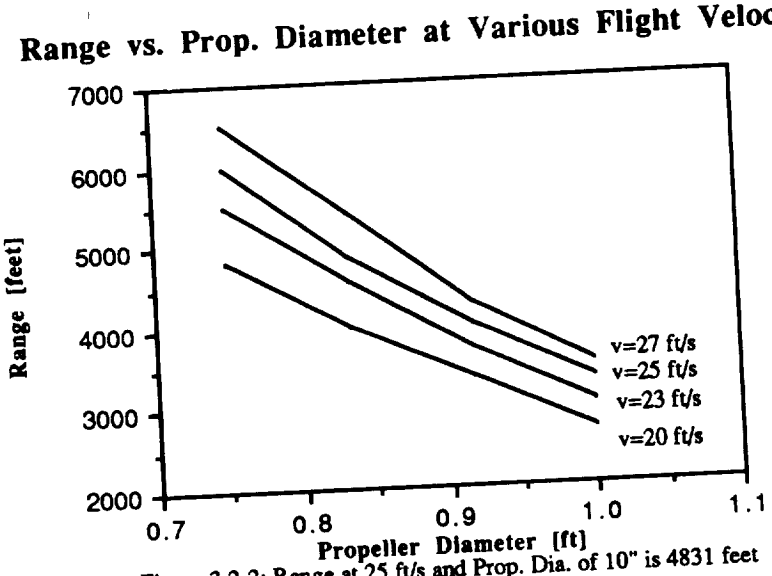

Figure 3.2-2: Range at 25 ft/s and Prop. Dia. of 10" is 4831 feet

3.3 POWER REQUIRED AND POWER AVAILABLE

In analyzing the power required for the RPV, a number of parameters had to be considered. Parameters such as aspect ratio, planform area, Oswald efficiency, total vehicle weight and parasite drag all had to be estimated and refined to come up with an actual power required curve. Once these parameters were set, a computer program was written which accepted these values as input and then varied airspeed over a specified range (see Appendix A-3 for

listing and output). Using this program it can be seen from figure 3.3-1 that at our cruise velocity of 25 ft/s, 7.83 Watts of power are required to power the RPV. Furthermore, at 25 ft/s we are a safe distance from the minimum power required, thus eliminating any concerns about "bottoming out" the power required curve, but also maximizing endurance as much as possible. Bottoming out the power required curve is a problem because at minimum power required, the vehicle's speed is not very stable and has a tendency to vary. Therefore, for effective speed stability, we did not want to fly at precisely the minimum power required. At take-off, our calculations determined that 46.2 Watts of power are required for a worse case situation (no ground effects contribution to lift). Thus, it was necessary to ensure that we had at least 46.2 Watts at all times. Figure 3.3-2 demonstrates that at our setting of 7200 RPM, our power available is safely more than our power required.

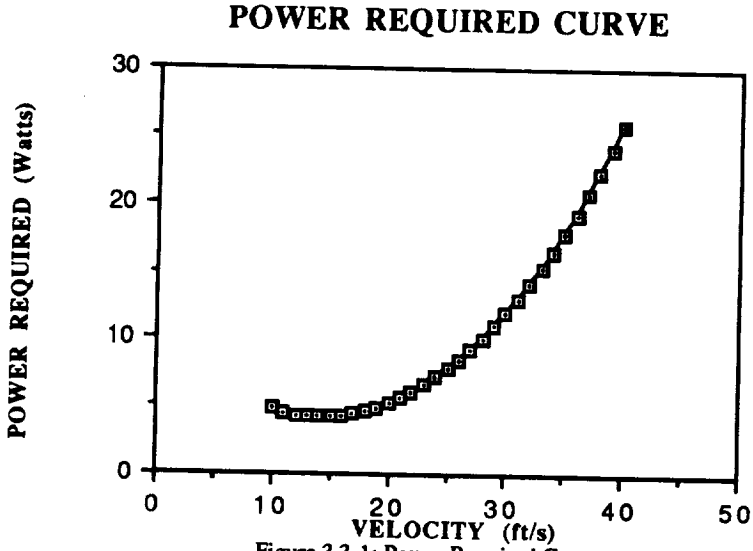

Figure 3.3-1: Power Required Curve

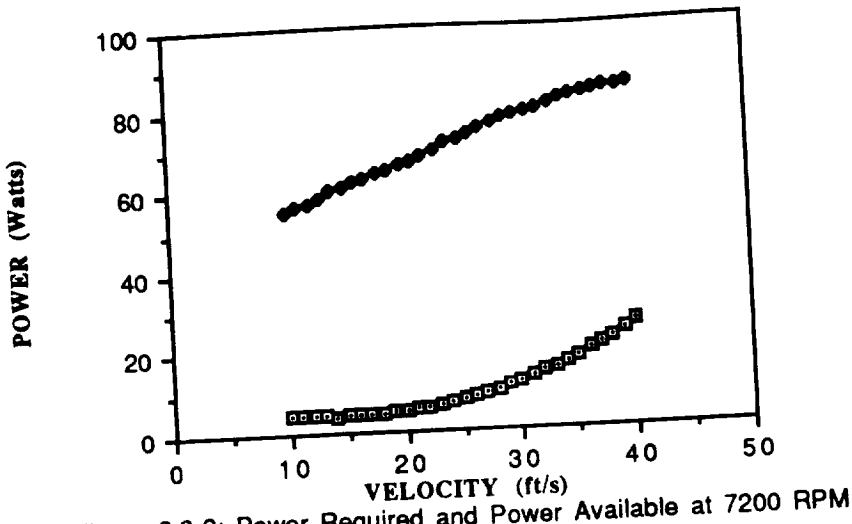

Figure 3.3-2: Power Required and Power Available at 7200 RPM

3.4 CLIMB AND GLIDE PERFORMANCE

The aircraft must complete and extra lap and turn in order to align itself up with the runway for landing at the end of the mission. The glide angle for the aircraft will be approximately sixteen degrees and at a height of fifteen feet the distance covered in the air to finally reach the ground is 52 feet (dist = h / tan γ). If the descent is begun immediately after the final turn, the aircraft will have enough distance to touch down on the runway and come to a complete stop. This is possible because of the 55 foot radius turn and 150 feet of runway distance is ample distance for the aircraft.The distance to stop the aircraft once on the ground is 133 feet and the distance in the air is 52 feet, which adds up to enough room for the aircraft to glide and stop completely.

The aircraft's sea level climb and glide performance as a function of flight velocity is shown in figure 3.4-1. The rate of climb at take-off is approximately 3.5 ft/s and the maximum rate of climb is 4.1 ft/s at a flight velocity of 23 ft/s.

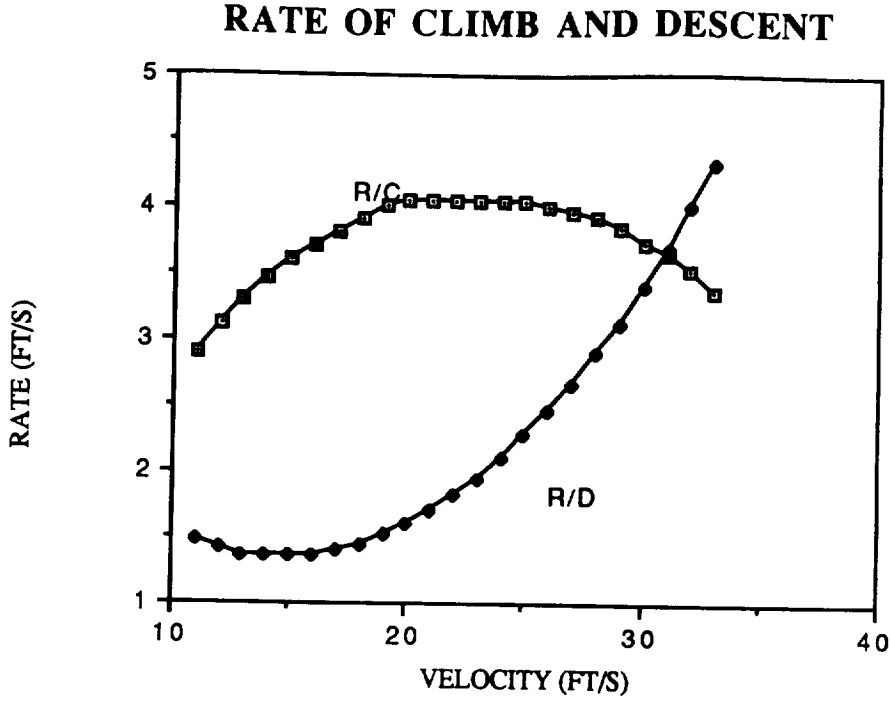

FIGURE 3.4-1 RATE OF CLIMB AND DESCENT

4 TECHNOLOGY DEMONSTRATOR

4.1 FINAL CONFIGURATION

The final flight aircraft rolled out with a number of changes to the original plans. It must be noted that computer aided drawings were very important to building accurately to the original design. Changes were made as construction showed their necessity. Holes were cut in the rear spar of the main wing to reduce weight, on the order of an ounce for each of the three sections. Flat pieces of balsa were added to the main spar for torsional strength. Rounded tips were added to the ends for smoother flow around the tips. Clear monocote was chosen to allow viewing of the model's insides. Holes were cut in the rear spar of the main wing to reduce weight, on the order of an ounce for each of the three sections.

Weights of components were taken as fabrication progressed. These are summarized in Table 4.1-1

Table 4.1-1 Measured Demonstrator weights

COMPONENT	WEIGHT (grams)	WEIGHT (oz)
Fuselage (Avionics-Motor included)	800.0	28.22
Full Wing	210.0	7.41
Horizontal Tail	49.5	1.75
Vertical Tail	25.2	0.89
Landing Gear	57.0	2.0
Total (by component)	40.27 oz (2.52 lb)	
Total (final)	48.8 oz (3.05 lb)	

The sum of the component weights does not equal the final weight. There are several reasons for this. The components were weighed before the monocote was applied. Lead weight weighing 4.0 oz was added to balance out the center of gravity. Also, a brass spinner (weight unknown) was put on to place the propeller even farther .

4.2 TECHNICAL DEMONSTRATOR FLIGHT TEST

With fabrication complete, the Flight Test program had as the primary goal, validation of the functional airworthiness of the Demonstrator in all phases of flight. Tests were conducted on May 1, 3, 4 at the Loftus Sports Center indoor football field at Notre Dame. Each test had specific objectives to accomplish and a flight plan to meet these objectives.

Due to the unpredictability of the aircraft performance, only the design team members, and the pilot were allowed on the field. All spectators watched from behind the track, or from the bleachers.

Tuesday, May 1: Taxi tests

Objectives:

1. Validate ability of aircraft to perform takeoff roll.
2. Determine the basic handling characteristics of the aircraft on the ground.

Flight Plan:

1. Run aircraft up field.
2. Quick take-off and short glide if possible.

Attempt 1

Center of Gravity placement:

- Check shows C.G. at approx. 40 % chord.
- C.G. Placement should be at main spar.
- Conclusion: Placed too far rearward.
- Solution: ballast the nose with coins and keys and move engine forward approximately one inch.

System checkout:

- Propulsion okay.
- Controls range check okay.
- Landing gear check:
    - gear bowed outward.
    - questionable stiffness.
    - provisional okay.

Performance:

- Attempt to taxi unsuccessful.
- Propulsion could not overcome roughness of Astroturf due to bowing of landing gear.
- Solution: Attach two more pieces of wire to the fuselage to make landing gear more rigid.

Attempt 2

- C.G. placement : still too far forward, though improved.
- Systems check okay.
- Landing gear okay.

Performance:

- TO distance of 20 yards.
- Climb to 8-12 feet.
- Power cut.
- Glide to landing.

Conclusions:

1. Objectives met.
2. Demonstrated capability to taxi, takeoff, and glide.

Wednesday, May 2 : modifications

- Lead ballast bringing C.G. to correct position painted and taped to nose.
- Wing moved as far back as possible.
- Additional wire strung to landing gear.

Thursday, May 3 : flight test

Attempt

Objective:

Repeat successful test of Tuesday.

Systems Checkout:

- C.G. and all systems check out. Some concern over slight wing lean.

Performance:

- Takeoff Distance of 20 yards.
- Reached altitude of 10 ft.
- Engine cut after flying in straight line.

Conclusions:

1. Demonstrated:
   - Repeated taxi capability.
   - Repeated takeoff capability.
   - Extended glide 10 yards.
   - Flight in straight line.
   - Dynamic stability.
2. An unqualified success!

Friday, May 4: Final Flight Test

Objectives:

1. Validate turning capability (right and left turns).
2. Perform 3 figure eights as required.

Attempt 1

- No further changes to aircraft from Thursday.
- Successfully completed the proposed flight path. A total of six figure eight laps were made. However, this flight was run at a velocity much faster than desired.
- All systems checked out okay.

Performance:

- Total flight time: 0:01:53 hours.
- Pilot started plane slowly for approx 10 yards.
- Takeoff distance was approximately 20-25 yards (total 35 yards).
- Flew six full figure eights.
- Maintained level, controlled flight; no imbalance in wings.

- Full turn approximately 60-75% of field width (40 yards).
- After the final figure eight lap, the plane performed a turn to return to level flight and landed before batteries emptied.

Conclusions:

1. Both goals accomplished.
2. Full flight requirements accomplished.
3. Established:
    - Turning capability.
    - Dynamic stability.
    - Endurance to complete mission without power failure.

Attempt 2

Objectives:

1. Quantify flight speed and altitude.
2. Fly again to establish repeatability.

Plan:

1. Takeoff.
2. Fly oval around field.
3. Fly figure eight.

Performance :

- Total flight time 0:01:35 hours.
- Cruise velocity : 24 ft/s.
- Re = 99,000.
- Take-off distance of 75 ft.
- Flew to level with nets approx 30-35 ft.while flying in an oval path.
- Reduced altitude to 20 feet to prepare for landing approach.

Conclusions:

1. Both goals accomplished.
2. Established repeat performance.

5 FEASIBILITY OF HIGH ALTITUDE MISSION

The basic objective of this low altitude design study was to determine some of the problems and requirements involved in low Reynolds number flight. Low Re flight has implications for the design of aircraft and estimation of the loads and drag forces it will encounter. Over the course of the study, many of these implications were discovered; they came out when normal techniques of estimation of parameters were applied to situations that are out of the scope of the ordinary. These implications are also valid for low Reynolds flight at high altitudes.

A high altitude mission could encounter low Reynolds flight, both because of lower speed and drops in air density. For example, the density of air at 10,000 feet is 74% that of sea level. Assuming the viscosity is constant, this would drop the Reynolds number by 25%. At 75,000 feet, the density is 5% of sea level. The station keeping nature of the mission would require low speeds, as it is difficult to fly in a tight area at high speed.

One of the problems of low Reynolds flight comes at the level of data sources. Commonly, the experimental data coming out of wind tunnel research does not extend into the range of Re=100,000 unless that level or lower is the target of the study. For example, much NACA data are taken at an Re ten times greater than this, Re=1 x 10^6 and above.

In aerodynamics, the implications come with estimation of the aircraft lift characteristics. Infinite wing airfoils can deliver coefficients of lift in excess of 1.0. However, in reality, the true wing lift coefficient can be much smaller, in the ranger of 0.5 - 0.8. Aircraft designed for higher speeds (higher Reynolds number) can overcome this loss by flying at a faster velocity. At low Re, the lifting area of the aircraft must be larger to offset the corresponding loss of lift associated with low speeds or low density.

Drag is another area affected by low Re flight. The data base is one of the problems here. The key problem can be seen from looking at the drag polar. As the aircraft goes to lower coefficients of lift, to the left of bottom of the drag bucket, the drag actually goes up. Increased drag can then be a problem.

Propulsion is affected also by lower velocities and densities. At low Re, the required

power, a direct function of drag, also goes up. Power required is also inversely proportional to the square root of the density. As density decreases, the power rises. Therefore, low Reynolds flight increases the demands on the propulsion system.

Stability and control is particularly sensitive to low Re flight. Control surfaces must be enlarged to account for the loss in effectiveness due to the decrease in air flowing by the surfaces. The surfaces cannot effect as much influence as at higher speeds or lower densities.

The design study has been useful for exploring the difficulties of design and analysis of a low Reynolds flight vehicle. The successful flight of the Technology Demonstrator shows that these difficulties can be overcome.

Appendix A-1

Power Available Analysis and Computer Code

To determine the power available for each particular motor, it first was necessary to vary velocity and RPM using a DO loop in the code. After a velocity was chosen, an RPM setting was then selected. Knowing these parameters, the advance ratio could be determined by assuming a propeller diameter:

$$\text{Advance ratio} = V/nD$$

where D is 10 inches because for this program, the Zinger 10-6 was arbitrarily selected. Next, since the velocity vs. advance ratio data was available for the Zinger 10-6,the efficiency was determined for the propeller at this velocity and RPM setting. The gear power was then determined by using the data provided by ASTRO for each motor, creating a plot of engine RPM vs. gear power and then determining the equation of that curve. In this manner, it was then possible to approximate gear power solely as a function of RPM. Finally, the actual power available for this velocity and RPM was found by multiplying the gear power and propeller efficiency. The program then selected new values of velocity and RPM and the process was repeated.

```
SALFORD UNIVERSITY FTN77 VER. 2285     <USER2>S424049795>STUDENT>PR.F77
COMPILER OPTIONS:  LISTING INTL DCLVAR NOMAP CHECK NOBIG LOGL DYNM NOOFFSET LG
                   NOFRN FPN NOLUNFREC NOSILENT NO_OPTIMISE NOIMPURE

0001                REAL X(31), Y(31,1)
0002                WRITE (1,*) 'ENTER IWR'
0003                READ(1,*) IWR
0004                WRITE (1,*) 'ENTER ASPECT RATIO,S (FT**2),E,W (LBS),CDO'
0005                READ(1,*) AR,S,E,W,CDO
0006                WRITE (1,*)'ENTER DIAMETER OF PROP IN FT'
0007                READ(1,*) DI
0008
0009                WRITE(IWR,*)
0010                WRITE(IWR,*)'ASPECT RATIO=',AR
0011                WRITE(IWR,*)'PLANFORM AREA (ft**2)=',S
0012                WRITE(IWR,*)'EFFICIENCY=',E
0013                WRITE(IWR,*)'WEIGHT (lbs)=',W
0014                WRITE(IWR,*)'CDO=',CDO
0015
0016                WRITE(IWR,*)
0017                WRITE (IWR,*) '      V(ft/s)              PR(W)                  CL
0018                   CD                D(lb)'
0019                I=1
0020                DO 10 V=10,40
0021.01                X(I)=V
0022.01                CL=W/(.00119*(V**2.)*S)
0023.01                CD=CDO+(CL**2)/(3.14159*E*AR)
0024.01                D=0.00119*CD*V**2.*S
0025.01                PRI=D*V
0026.01                Y(I,1)=PRI*1.356
0027.01                PR=PRI*1.356
0028.01                I=I+1
0029.01             WRITE (IWR,*) V,PR,CL,CD,D
0030.01          10 CONTINUE
0031.01   C
0032.01   C        IOPT=-011
0033.01   C        ND=31
0034.01   C        NF=1
0035.01   C        CALL TPLOT(IOPT,X,Y,31,ND,NF)
0036.01   C        CALL TLABEL('RELATIVE VELOCITY (ft/s)','POWER REQUIRED (watts)'
0037.01   C        CALL TITLE('PRELIMINARY POWER REQUIRED CURVE')
0038.01
0039                WRITE (IWR,*)
0040                WRITE (IWR,*)'      V(ft/s)                    RPM          EP
0041                EAL(W)              PG'
0042                DO 98 V=10,40
0043.01             DO 99 N=4700,9000,500
0044.02                AN=N/60
0045.02                AJ=V/(AN*DI)
0046.02                EP=+.07807+2.5764*AJ-2.7452*AJ**2.+.86713*AJ**3.
0047.02   C            PG=-80.062+.11418*N-1.1731E-5*N**2.
0048.02                PG=-88.153+.08739*N-8.5894E-6*N**2.
0049.02                PA=PG*EP
0050.02                PAREAL=PA*1.356
0051.02             WRITE(IWR,*)V,N,EP,PAREAL,PG
0052.02          99 CONTINUE
0053.01          98 CONTINUE
0054             77 CONTINUE
0055                STOP
0056                END
WARNING - Label 77 has not been referenced



END OF COMPILATION CLOCKED       .457 SECONDS
```

ASPECT RATIO= 12.0000
PLANFORM AREA (ft**2)= 6.00000
EFFICIENCY= 0.800000
WEIGHT (lbs)= 2.65600
CDO= 4.000000E-02

V(ft/s)	PR(W)	CL	CD	D(lb)
10.0000	4.82946	3.71989	0.498817	0.356155
11.0000	4.55381	3.07429	0.353378	0.305297
12.0000	4.37103	2.58326	0.261266	0.268623
13.0000	4.26791	2.20112	0.200644	0.242110
14.0000	4.23567	1.89790	0.159434	0.223118
15.0000	4.26851	1.65328	0.130630	0.209858
16.0000	4.36264	1.45308	0.110010	0.201080
17.0000	4.51573	1.28716	9.493427E-02	0.195893
18.0000	4.72646	1.14811	8.370678E-02	0.193644
19.0000	4.99430	1.03044	7.520662E-02	0.193848
20.0000	5.31928	0.929972	6.867602E-02	0.196139
21.0000	5.70187	0.843512	6.359184E-02	0.200234
22.0000	6.14286	0.768572	5.958611E-02	0.205915
23.0000	6.64334	0.703192	5.639561E-02	0.213010
24.0000	7.20458	0.645814	5.382910E-02	0.221380
25.0000	7.82802	0.595182	5.174570E-02	0.230915
26.0000	8.51525	0.550279	5.004027E-02	0.241526
27.0000	9.26796	0.510273	4.863344E-02	0.253140
28.0000	10.0879	0.474476	4.746460E-02	0.265695
29.0000	10.9770	0.442317	4.648704E-02	0.279143
30.0000	11.9371	0.413321	4.566440E-02	0.293439
31.0000	12.9702	0.387085	4.496812E-02	0.308551
32.0000	14.0784	0.363270	4.437561E-02	0.324446
33.0000	15.2636	0.341587	4.386885E-02	0.341101
34.0000	16.5279	0.321790	4.343339E-02	0.358492
35.0000	17.8736	0.303664	4.305749E-02	0.376602
36.0000	19.3026	0.287028	4.273167E-02	0.395415
37.0000	20.8172	0.271723	4.244811E-02	0.414916
38.0000	22.4195	0.257610	4.220041E-02	0.435093
39.0000	24.1117	0.244569	4.198326E-02	0.455936
40.0000	25.8961	0.232493	4.179225E-02	0.477435

V(ft/s)	RPM	EP	PAREAL(W)	PG
10.0000	4700	0.412732	74.3459	132.840
10.0000	5200	0.386578	70.2521	134.018
10.0000	5700	0.361553	64.1760	130.900
10.0000	6200	0.342435	57.3408	123.488
10.0000	6700	0.325698	49.3681	111.782
10.0000	7200	0.309207	40.1593	95.7805
10.0000	7700	0.296272	30.3255	75.4845
10.0000	8200	0.284697	19.6474	50.8937
10.0000	8700	0.273050	8.14866	22.0082
11.0000	4700	0.439775	79.2173	132.840
11.0000	5200	0.412090	74.8882	134.018
11.0000	5700	0.385484	68.4237	130.900
11.0000	6200	0.365086	61.1338	123.488
11.0000	6700	0.347182	52.6246	111.782
11.0000	7200	0.329499	42.7948	95.7805
11.0000	7700	0.315602	32.3040	75.4845
11.0000	8200	0.303145	20.9205	50.8937
11.0000	8700	0.290592	8.67216	22.0082
12.0000	4700	0.465727	83.8920	132 840
12.0000	5200	0.436687	79.3583	134.018
12.0000	5700	0.408653	72.5363	130.900
12.0000	6200	0.387082	64.8170	123.488
12.0000	6700	0.368097	55.7947	111.782
12.0000	7200	0.349299	45.3664	95.7805
12.0000	7700	0.334495	34.2379	75.4845
12.0000	8200	0.321204	22.1668	50.8937
12.0000	8700	0.307790	9.18540	22.0082
13.0000	4700	0.490606	88.3734	132.840
13.0000	5200	0.460385	83.6647	134.018
13.0000	5700	0.431072	76.5156	130.900
13.0000	6200	0.408432	68.3920	123.488
13.0000	6700	0.388448	58.8795	111.782
13.0000	7200	0.368612	47.8748	95.7805
13.0000	7700	0.352957	36.1276	75.4845
13.0000	8200	0.338878	23.3866	50.8937
13.0000	8700	0.324647	9.68847	22.0082
14.0000	4700	0.514430	92.6649	132.840
14.0000	5200	0.483196	87.8102	134.018
14.0000	5700	0.452750	80.3635	130.900

14.0000	6200	0.429142	71.8600	123.488
14.0000	6700	0.408242	61.8798	111.782
14.0000	7200	0.387444	50.3205	95.7805
14.0000	7700	0.370992	37.9736	75.4845
14.0000	8200	0.356171	24.5800	50.8937
14.0000	8700	0.341166	10.1814	22.0082
15.0000	4700	0.537220	96.7701	132.840
15.0000	5200	0.505136	91.7973	134.018
15.0000	5700	0.473698	84.0819	130.900
15.0000	6200	0.449223	75.2224	123.488
15.0000	6700	0.427487	64.7968	111.782
15.0000	7200	0.405798	52.7044	95.7805
15.0000	7700	0.388605	39.7764	75.4845
15.0000	8200	0.373086	25.7474	50.8937
15.0000	8700	0.357350	10.6644	22.0082
16.0000	4700	0.558994	100.692	132.840
16.0000	5200	0.526218	95.6285	134.018
16.0000	5700	0.493928	87.6726	130.900
16.0000	6200	0.468680	78.4806	123.488
16.0000	6700	0.446188	67.6315	111.782
16.0000	7200	0.423681	55.0271	95.7805
16.0000	7700	0.405798	41.5363	75.4845
16.0000	8200	0.389628	26.8889	50.8937
16.0000	8700	0.373202	11.1375	22.0082
17.0000	4700	0.579770	104.435	132.840
17.0000	5200	0.546457	99.3065	134.018
17.0000	5700	0.513448	91.1375	130.900
17.0000	6200	0.487524	81.6360	123.488
17.0000	6700	0.464352	70.3847	111.782
17.0000	7200	0.441099	57.2892	95.7805
17.0000	7700	0.422578	43.2537	75.4845
17.0000	8200	0.405798	28.0049	50.8937
17.0000	8700	0.388725	11.6008	22.0082
18.0000	4700	0.599569	108.001	132.840
18.0000	5200	0.565867	102.834	134.018
18.0000	5700	0.532270	94.4785	130.900
18.0000	6200	0.505762	84.6900	123.488
18.0000	6700	0.481986	73.0576	111.782
18.0000	7200	0.458055	59.4914	95.7805
18.0000	7700	0.438947	44.9293	75.4845
18.0000	8200	0.421602	29.0955	50.8937
18.0000	8700	0.403921	12.0543	22.0082
19.0000	4700	0.618408	111.395	132.840
19.0000	5200	0.584461	106.213	134.018
19.0000	5700	0.550405	97.6974	130.900
19.0000	6200	0.523403	87.6439	123.488
19.0000	6700	0.499096	75.6510	111.782
19.0000	7200	0.474556	61.6345	95.7805
19.0000	7700	0.454911	46.5633	75.4845
19.0000	8200	0.437042	30.1611	50.8937
19.0000	8700	0.418795	12.4982	22.0082
20.0000	4700	0.636307	114.619	132.840
20.0000	5200	0.602255	109.446	134.018
20.0000	5700	0.567862	100.796	130.900
20.0000	6200	0.540454	90.4991	123.488
20.0000	6700	0.515688	78.1661	111.782
20.0000	7200	0.490606	63.7190	95.7805
20.0000	7700	0.470473	48.1562	75.4845
20.0000	8200	0.452123	31.2018	50.8937
20.0000	8700	0.433348	12.9325	22.0082
21.0000	4700	0.653285	117.677	132.840
21.0000	5200	0.619261	112.537	134.018
21.0000	5700	0.584653	103.776	130.900
21.0000	6200	0.556924	93.2570	123.488
21.0000	6700	0.531771	80.6038	111.782
21.0000	7200	0.506210	65.7458	95.7805
21.0000	7700	0.485638	49.7084	75.4845
21.0000	8200	0.466847	32.2179	50.8937
21.0000	8700	0.447584	13.3573	22.0082
22.0000	4700	0.669361	120.573	132.840
22.0000	5200	0.635495	115.487	134.018
22.0000	5700	0.600787	106.640	130.900
22.0000	6200	0.572821	95.9190	123.488
22.0000	6700	0.547349	82.9651	111.782
22.0000	7200	0.521375	67.7153	95.7805
22.0000	7700	0.500410	51.2205	75.4845
22.0000	8200	0.481219	33.2098	50.8937
22.0000	8700	0.461506	13.7728	22.0082
23.0000	4700	0.684554	123.309	132.840
23.0000	5200	0.650971	118.300	134.018

23.0000	5700	0.616275	109.389	130.900
23.0000	6200	0.588153	98.4865	123.488
23.0000	6700	0.562430	85.2510	111.782
23.0000	7200	0.536105	69.6284	95.7805
23.0000	7700	0.514794	52.6928	75.4845
23.0000	8200	0.495241	34.1775	50.8937
23.0000	8700	0.475116	14.1790	22.0082
24.0000	4700	0.698882	125.890	132.840
24.0000	5200	0.665702	120.977	134.018
24.0000	5700	0.631128	112.026	130.900
24.0000	6200	0.602930	100.961	123.488
24.0000	6700	0.577020	87.4626	111.782
24.0000	7200	0.550405	71.4857	95.7805
24.0000	7700	0.528794	54.1257	75.4845
24.0000	8200	0.508918	35.1214	50.8937
24.0000	8700	0.488418	14.5759	22.0082
25.0000	4700	0.712365	128.319	132.840
25.0000	5200	0.679703	123.521	134.018
25.0000	5700	0.645357	114.551	130.900
25.0000	6200	0.617158	103.343	123.488
25.0000	6700	0.591126	89.6007	111.782
25.0000	7200	0.564280	73.2878	95.7805
25.0000	7700	0.542414	55.5198	75.4845
25.0000	8200	0.522254	36.0416	50.8937
25.0000	8700	0.501415	14.9638	22.0082
26.0000	4700	0.725022	130.599	132.840
26.0000	5200	0.692988	125.935	134.018
26.0000	5700	0.658971	116.968	130.900
26.0000	6200	0.630846	105.635	123.488
26.0000	6700	0.604754	91.6664	111.782
26.0000	7200	0.577737	75.0355	95.7805
26.0000	7700	0.555658	56.8754	75.4845
26.0000	8200	0.535250	36.9386	50.8937
26.0000	8700	0.514109	15.3426	22.0082
27.0000	4700	0.736871	132.733	132.840
27.0000	5200	0.705571	128.222	134.018
27.0000	5700	0.671981	119.277	130.900
27.0000	6200	0.644003	107.838	123.488
27.0000	6700	0.617911	93.6607	111.782
27.0000	7200	0.590779	76.7294	95.7805
27.0000	7700	0.568530	58.1930	75.4845
27.0000	8200	0.547912	37.8124	50.8937
27.0000	8700	0.526503	15.7125	22.0082
28.0000	4700	0.747932	134.726	132.840
28.0000	5200	0.717467	130.384	134.018
28.0000	5700	0.684398	121.481	130.900
28.0000	6200	0.656636	109.954	123.488
28.0000	6700	0.630604	95.5846	111.782
28.0000	7200	0.603413	78.3702	95.7805
28.0000	7700	0.581036	59.4731	75.4845
28.0000	8200	0.560243	38.6634	50.8937
28.0000	8700	0.538601	16.0735	22.0082
29.0000	4700	0.758223	136.580	132.840
29.0000	5200	0.728688	132.423	134.018
29.0000	5700	0.696233	123.582	130.900
29.0000	6200	0.668754	111.983	123.488
29.0000	6700	0.642839	97.4391	111.782
29.0000	7200	0.615642	79.9586	95.7805
29.0000	7700	0.593179	60.7160	75.4845
29.0000	8200	0.572246	39.4917	50.8937
29.0000	8700	0.550405	16.4258	22.0082
30.0000	4700	0.767764	138.298	132.840
30.0000	5200	0.739251	134.342	134.018
30.0000	5700	0.707495	125.581	130.900
30.0000	6200	0.680364	113.927	123.488
30.0000	6700	0.654622	99.2252	111.782
30.0000	7200	0.627474	81.4953	95.7805
30.0000	7700	0.604963	61.9222	75.4845
30.0000	8200	0.583926	40.2978	50.8937
30.0000	8700	0.561918	16.7694	22.0082
31.0000	4700	0.776573	139.885	132.840
31.0000	5200	0.749168	136.145	134.018
31.0000	5700	0.718195	127.480	130.900
31.0000	6200	0.691477	115.788	123.488
31.0000	6700	0.665961	100.944	111.782
31.0000	7200	0.638912	82.9809	95.7805
31.0000	7700	0.616394	63.0922	75.4845
31.0000	8200	0.595284	41.0816	50.8937
31.0000	8700	0.573144	17.1044	22.0082
32.0000	4700	0.784670	141.344	132.840

32.0000	5200	0.758453	137.832	134.018
32.0000	5700	0.728344	129.282	130.900
32.0000	6200	0.702099	117.567	123.488
32.0000	6700	0.676861	102.596	111.782
32.0000	7200	0.649963	84.4161	95.7805
32.0000	7700	0.627474	64.2263	75.4845
32.0000	8200	0.606326	41.8437	50.8937
32.0000	8700	0.584084	17.4309	22.0082
33.0000	4700	0.792073	142.677	132.840
33.0000	5200	0.767122	139.408	134.018
33.0000	5700	0.737952	130.987	130.900
33.0000	6200	0.712238	119.264	123.488
33.0000	6700	0.687330	104.183	111.782
33.0000	7200	0.660630	85.8015	95.7805
33.0000	7700	0.638209	65.3251	75.4845
33.0000	8200	0.617055	42.5841	50.8937
33.0000	8700	0.594743	17.7490	22.0082
34.0000	4700	0.798802	143.889	132.840
34.0000	5200	0.775188	140.873	134.018
34.0000	5700	0.747030	132.599	130.900
34.0000	6200	0.721904	120.883	123.488
34.0000	6700	0.697374	105.705	111.782
34.0000	7200	0.670920	87.1380	95.7805
34.0000	7700	0.648602	66.3889	75.4845
34.0000	8200	0.627474	43.3031	50.8937
34.0000	8700	0.605123	18.0588	22.0082
35.0000	4700	0.804875	144.983	132.840
35.0000	5200	0.782666	142.232	134.018
35.0000	5700	0.755588	134.118	130.900
35.0000	6200	0.731104	122.423	123.488
35.0000	6700	0.707000	107.164	111.782
35.0000	7200	0.680837	88.4260	95.7805
35.0000	7700	0.658659	67.4183	75.4845
35.0000	8200	0.637587	44.0010	50.8937
35.0000	8700	0.615227	18.3603	22.0082
36.0000	4700	0.810311	145.962	132.840
36.0000	5200	0.789569	143.487	134.018
36.0000	5700	0.763637	135.546	130.900
36.0000	6200	0.739846	123.887	123.488
36.0000	6700	0.716213	108.561	111.782
36.0000	7200	0.690388	89.6664	95.7805
36.0000	7700	0.668383	68.4136	75.4845
36.0000	8200	0.647397	44.6780	50.8937
36.0000	8700	0.625059	18.6537	22.0082
37.0000	4700	0.815130	146.830	132.840
37.0000	5200	0.795911	144.639	134.018
37.0000	5700	0.771187	136.886	130.900
37.0000	6200	0.748139	125.276	123.488
37.0000	6700	0.725022	109.896	111.782
37.0000	7200	0.699576	90.8598	95.7805
37.0000	7700	0.677778	69.3753	75.4845
37.0000	8200	0.656908	45.3344	50.8937
37.0000	8700	0.634620	18.9390	22.0082
38.0000	4700	0.819350	147.590	132.840
38.0000	5200	0.801707	145.693	134.018
38.0000	5700	0.778249	138.140	130.900
38.0000	6200	0.755991	126.591	123.488
38.0000	6700	0.733431	111.171	111.782
38.0000	7200	0.708408	92.0068	95.7805
38.0000	7700	0.686849	70.3038	75.4845
38.0000	8200	0.666124	45.9704	50.8937
38.0000	8700	0.643914	19.2164	22.0082
39.0000	4700	0.822990	148.246	132.840
39.0000	5200	0.806971	146.649	134.018
39.0000	5700	0.784833	139.309	130.900
39.0000	6200	0.763410	127.833	123.488
39.0000	6700	0.741449	112.386	111.782
39.0000	7200	0.716888	93.1082	95.7805
39.0000	7700	0.695600	71.1995	75.4845
39.0000	8200	0.675048	46.5863	50.8937
39.0000	8700	0.652943	19.4859	22.0082
40.0000	4700	0.826070	148.801	132.840
40.0000	5200	0.811718	147.512	134.018
40.0000	5700	0.790950	140.394	130.900
40.0000	6200	0.770405	129.004	123.488
40.0000	6700	0.749081	113.543	111.782
40.0000	7200	0.725022	94.1646	95.7805
40.0000	7700	0.704036	72.0630	75.4845
40.0000	8200	0.683684	47.1823	50.8937
40.0000	8700	0.661712	19.7476	22.0082

Appendix A-2

Battery Voltage/Current Analysis and TKSolver Code

In deciding upon the desired battery voltage and motor current draw, a TKSolver computer code was implemented which was provided by the Notre Dame Aerospace Department. This code allowed for quantities such as velocity, weight, aspect ratio, wing area and other pertinent parameters to be set. Once done, the battery voltage and battery capacity could be varied while keeping all other parameters constant and the effects of these variations could be studied. While varying the battery voltage (essentially, the number of batteries) and battery capacity, the motor current draw had to be monitored carefully, because a motor current draw in excess of 20 Amps would exceed the maximum limit for the fuses in the speed control. Furthermore, range and endurance also had to be monitored so as to ensure the vehicle could meet the objectives of the mission. It was these two parameters (range and endurance) that were the driving factors in selecting the number and type of batteries for the Drag-n-fly.

```
S Rule
* Q= .5*rho*vel^2
* Cd=Cdo+Cl^2/(PI()*eff*AR)
* Cl=(n*W)/(Q*S)
*  preq=Q*S*Cd*vel
* ROC=(Pavail-Preq)/W
* v=vset-Kb*i
* motrpm=(v-i*Ra)/Kv
* proprps=motrpm/(60*gr)
* J=vel/(proprps*propd)
* CT=Ct(J)
* CP=Cp(J)
* eta=Ct(J)*J/Cp(J)
* Pavail=eta*Cp(J)*rho*proprps^3*propd^5
* Cp(J)*rho*proprps^3*propd^5=((Kt/Kv)*(v*i-i*i*Ra)*.0005454-floss(mo
* fltime=batcap/i
* range=vel*fltime*3600
```

St	Input	Name	Output	Unit	Comment
		Q	.743125	psf	dynamic pressur
	.002378	rho		slug/ft3	air density
	25	vel		ft/sec	air speed
		Cd	.05176546		a/c drag coefficient
	.04	Cdo			zero lift drag coefficient
		Cl	.59568265		a/c lift coefficient
	.8	eff			efficiency factor
	12	AR			aspect ratio
	1	n			load factor
	2.656	W		lb	a/c weight
	6	S		ft-ft	wing area
		Preq	7.822981	W	a/c power required - level f
		ROC	3.7636246	ft/s	rate of climb
		Pavail	21.375295	W	power available from propell
		v	8.6146064	volt	armature voltage
	9.6	vset		volt	battery voltage
	.1058	Kb			battery constant
		i	9.3137391	amp	motor current draw
		motrpm	16111.564	rpm	motor speed (rpm)
	.06	Ra		ohm	armature resistance
	.0005	Kv		volt/rpm	motor speed constant
		proprps	7290.3005	rpm	propeller speed (rps)
	2.21	gr			gear ratio
		J	.2470022		propeller advance ratio
	.833	propd		ft	propeller diameter
		eta	.58833081		propeller efficiency
	.62	Kt		in-oz/amp	motor torque constant
	.95	greff			gear efficiency
		fltime	193.26288	sec	flight time
	.5	batcap		amp-hr	battery capacity
		range	4831.5719	ft	range
		CT	.03730893		
		CP	.01566362		

Appendix A-3
Power Required Analysis and Code

To determine the power required curve for the Drag-n-Fly, a computer code was written that allowed for the Aspect ratio, planform area, Oswald Efficiency factor, weight and $C_{d,o}$ to be input into the program by the user. A DO loop was written to vary velocity from 10 ft/s to 40 ft/s and for each run through this loop, the lift coefficient was determined by assuming steady level flight (L=W):

$$C_L = W / (Q*S)$$

The drag coefficient was then determined by adding $C_{d,o}$ and the induced drag:

$$C_D = C_{d,o} + C_L^2 / \pi eAR$$

Next, the total drag was calculated from the drag coefficient above:

$$D = C_D*Q*S$$

Finally, the power required is simply the product of the drag and velocity:

$$P_{req} = D*V$$

Using this process for each run through the code, the power required curve seen in Section 3.3 was produced.

```
SALFORD UNIVERSITY FTN77 VER. 228S     <USER2>S424049795>STUDENT>PR.F77          15:
COMPILER OPTIONS:   LISTING INTL DCLVAR NOMAP CHECK NOBIG LOGL DYNM NOOFFSET LGO NO
                    NOFRN FPN NOLUNFREC NOSILENT NO_OPTIMISE NOIMPURE
    0001              REAL X(31), Y(31,1)
    0002              WRITE (1,*) 'ENTER IWR'
    0003              READ(1,*) IWR
    0004              WRITE (1,*) 'ENTER ASPECT RATIO,S (FT**2),E,W (LBS),CDO'
    0005              READ(1,*) AR,S,E,W,CDO
    0006              WRITE (1,*)'ENTER DIAMETER OF PROP IN FT'
    0007              READ(1,*) DI
    0008
    0009              WRITE(IWR,*)
    0010              WRITE(IWR,*)'ASPECT RATIO=',AR
    0011              WRITE(IWR,*)'PLANFORM AREA (ft**2)=',S
    0012              WRITE(IWR,*)'EFFICIENCY=',E
    0013              WRITE(IWR,*)'WEIGHT (lbs)=',W
    0014              WRITE(IWR,*)'CDO=',CDO
    0015
    0016              WRITE(IWR,*)
    0017              WRITE (IWR,*) '      V(ft/s)            PR(W)                CL
    0018                 CD                 D(lb)'
    0019              I=1
    0020              DO 10 V=10,40
    0021.01              X(I)=V
    0022.01              CL=W/(.00119*(V**2.)*S)
    0023.01              CD=CDO+(CL**2)/(3.14159*E*AR)
    0024.01              D=0.00119*CD*V**2.*S
    0025.01              PRI=D*V
    0026.01              Y(I,1)=PRI*1.356
    0027.01              PR=PRI*1.356
    0028.01              I=I+1
    0029.01           WRITE (IWR,*) V,PR,CL,CD,D
    0030.01        10 CONTINUE
    0031              GO TO 72
    0032        C
    0033        C     IOPT=-011
    0034        C     ND=31
    0035        C     NF=1
    0036        C     CALL TPLOT(IOPT,X,Y,31,ND,NF)
    0037        C     CALL TLABEL('RELATIVE VELOCITY (ft/s)','POWER REQUIRED (watts)'
    0038        C     CALL TITLE('PRELIMINARY POWER REQUIRED CURVE')
    0039
    0040              WRITE (IWR,*)
WARNING - This statement will never be executed
    0041              WRITE (IWR,*)'     V(ft/s)                    RPM          EP              F
    0042             .EAL(W)          PG'
    0043              DO 98 V=10,40
    0044.01           DO 99 N=4700,9000,500
    0045.02              AN=N/60
    0046.02              AJ=V/(AN*DI)
    0047.02              EP=+.07807+2.5764*AJ-2.7452*AJ**2.+.86713*AJ**3.
    0048.02  C           PG=-80.062+.11418*N-1.1731E-5*N**2.
    0049.02              PG=-88.153+.08739*N-8.5894E-6*N**2.
    0050.02              PA=PG*EP
    0051.02              PAREAL=PA*1.356
    0052.02           WRITE(IWR,*)V,N,EP,PAREAL,PG
    0053.02        99 CONTINUE
    0054.01        98 CONTINUE
    0055           77 CONTINUE
    0056           72 CONTINUE
    0057              STOP
    0058              END
WARNING - Label 77 has not been referenced



END OF COMPILATION CLOCKED      .448 SECONDS
```

ASPECT RATIO= 12.0000
PLANFORM AREA (ft**2)= 6.00000
EFFICIENCY= 0.800000
WEIGHT (lbs)= 2.65600
CDO= 4.000000E-02

V(ft/s)	PR(W)	CL	CD	D(lb)
10.0000	4.82946	3.71989	0.498817	0.356155
11.0000	4.55381	3.07429	0.353378	0.305297
12.0000	4.37103	2.58326	0.261266	0.268623
13.0000	4.26791	2.20112	0.200644	0.242110
14.0000	4.23567	1.89790	0.159434	0.223118
15.0000	4.26851	1.65328	0.130630	0.209858
16.0000	4.36264	1.45308	0.110010	0.201080
17.0000	4.51573	1.28716	9.493427E-02	0.195893
18.0000	4.72646	1.14811	8.370678E-02	0.193644
19.0000	4.99430	1.03044	7.520662E-02	0.193848
20.0000	5.31928	0.929972	6.867602E-02	0.196139
21.0000	5.70187	0.843512	6.359184E-02	0.200234
22.0000	6.14286	0.768572	5.958611E-02	0.205915
23.0000	6.64334	0.703192	5.639561E-02	0.213010
24.0000	7.20458	0.645814	5.382910E-02	0.221380
25.0000	7.82802	0.595182	5.174570E-02	0.230915
26.0000	8.51525	0.550279	5.004027E-02	0.241526
27.0000	9.26796	0.510273	4.863344E-02	0.253140
28.0000	10.0879	0.474476	4.746460E-02	0.265695
29.0000	10.9770	0.442317	4.648704E-02	0.279143
30.0000	11.9371	0.413321	4.566440E-02	0.293439
31.0000	12.9702	0.387085	4.496812E-02	0.308551
32.0000	14.0784	0.363270	4.437561E-02	0.324446
33.0000	15.2636	0.341587	4.386885E-02	0.341101
34.0000	16.5279	0.321790	4.343339E-02	0.358492
35.0000	17.8736	0.303664	4.305749E-02	0.376602
36.0000	19.3026	0.287028	4.273167E-02	0.395415
37.0000	20.8172	0.271723	4.244811E-02	0.414916
38.0000	22.4195	0.257610	4.220041E-02	0.435093
39.0000	24.1117	0.244569	4.198326E-02	0.455936
40.0000	25.8961	0.232493	4.179225E-02	0.477435

Appendix B-1
Wing Analysis and TKSolver! Code

The wing is assumed to structurally consist of only a main spar as configured in the figures below.

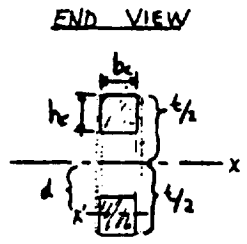

$$I_x' = \frac{1}{12} b_2 h_2^3$$

$$I_x = 2(I_x' + Ad^2)$$

$$I_x = 2(I_x' + (b_2 h_2)(\tfrac{h_1}{2} - \tfrac{h_2}{2})^2)$$

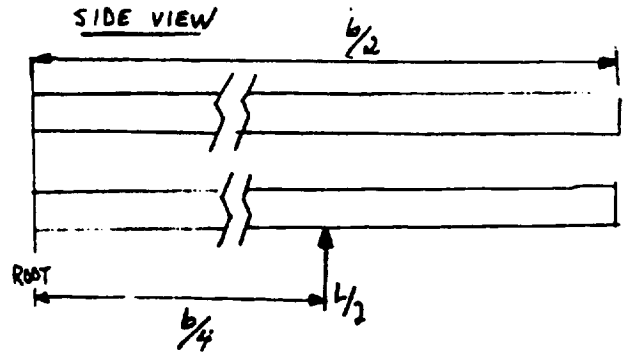

$$M_x = F \cdot d = L/2 \cdot b/4$$

For this analysis the maximum flight load factor is used to determine the loading condition. This is n=1.5. Lift force then equals n * W, where W is the estimated weight of 2.65 lbs. This force is distributed equally on both wings with a resultant at the midpoint of each side of the wing. This force creates a moment at the root of the wing given by $M_X = F * d = L/2 * b/4$. The other force acting on the wing is due to drag. Drag force is neglected because (1) it is small compared to the lift force and (2) the moment of inertia about a y axis for the entire wing would actually take into account the effects of the leading and trailing edges. These edges, spread 8.5" apart greatly increase the I_y of the wing giving a small axial stress due to the drag force. The effect of the leading and trailing edges are neglected in analysis of the axial stress due to lift force because the contribution to I_X of the leading and trailing edges is insignificant compared to that of the main spar. After moments have been calculated at the root the moment of inertia is calculated knowing that I_X' for a rectangle = 1/12 b * h3 (Reference 1). Using parallel axis theorem ($I_X = I_X' + Ad^2$, also Reference 1) the moment of inertia can be calculated for the entire spar. The above analysis has been coded and placed into TKSolver as can be seen on the following page. Weight of the wing is calculated as well in this code, by accepting inputs of the densities of the various components as well as their cross sectional areas. Weight is

then calculated by multiplying the length of the spar, leading edge, etc by their cross sectional area to get a volume and then multiplying by density to get a mass.

S Rule

* Ip=(1/12*bp*t^3)*2
* M=L/2*(b/4)
* t=c*tc
* Ac=bc*hc
* Io=1/12*(bc*hc^3)
* d=t/2-hc/2
* Ix=(Io+Ac*d^2)*2+Ip
* y=t/2
* Sig=(M*y)/Ix
* Sigfs= Sig*1.2
* Qual= Sig-Sigmax
* Wspar=Ac*b*2*Rhospar
* Q1=Ac*d
* Tau1=(L*Q1)/(Ix*tweb)
* H2=((t/2-hc)*tweb)
* Atot=A2+Ac
* d2=(Ac*d+A2*((t/2-hc)/2))/Atot
* Q2=Atot*d2
* Tau2=(L*Q2)/(Ix*tweb)
* Srib=(t*c)/2
* Numrib=b/4
* Wrib=Srib*trib*Rhorib*Numrib
* Wle=Sle*b*Rhole
* Wte=Ste*b*Rhote
* Wcover=b*c*2*Rhocover
* TotWw=Wspar+Wrib+Wle+Wte+Wcover+Wpanels
* Swing=b*c
* AR=b^2/Swing
* Wpanels=bp*t*b*2*rhopanel
* FS=Sigmax/Sig

Appendix B-2
Fuselage Analysis

The fuselage is configured as seen below.

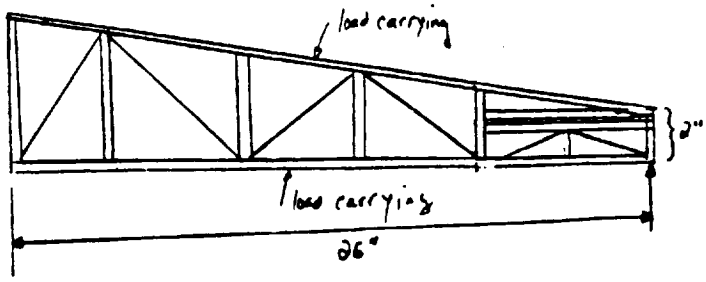

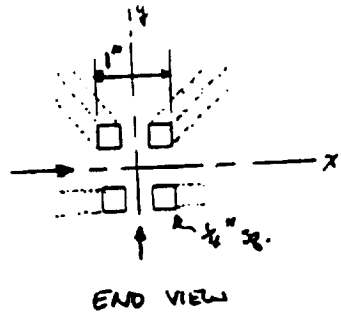

$M_y = 9.1$ lb $M_x = 10.4$

$y = 1$ in $x = 0.5$

$I_y = 0.0365$ in^4 $I_x = 0.1927$ in^4

The load on the fuselage is the load of the horizontal and vertical tails placed at the extreme end of the fuselage. The load carrying beams are assumed to be cantilevered at the main wing box. The fuselage supports 0.35 lbs from the vertical tail and 0.4 lbs from the horizontal tail. This gives bending moments of $M_y = 9.1$ in lb and $M_x = 10.4$ in lb. Using the same formulas cited in Appendix B-1 $I_x = 0.1927$ in^4, and $I_y = 0.0365$ in^4. Since there are two components to the load the stress calculation becomes:

$$\text{Axial Stress} = \frac{M_y * x}{I_y} + \frac{M_x * y}{I_x}$$

This equation is found from Allen and Haisler's Introduction to Aerospace Structural Analysis text. This yields a resultant axial stress of 178.63 psi.

HORIZONTAL TAIL:

The horizontal tail is analyzed in much the same way. Lift force on the tail is 0.4 lbs, found in stability and control analysis. This force is split between the two sides of the wing and placed at the midpoint of each side. It will be assumed that the leading and trailing edge of the non-movable area of the tail carry all of the load. Internal structure is non-load carrying and meant only to maintain the wing shape. Analysis follows as below. The stress in the members is found to be 365.4 psi.

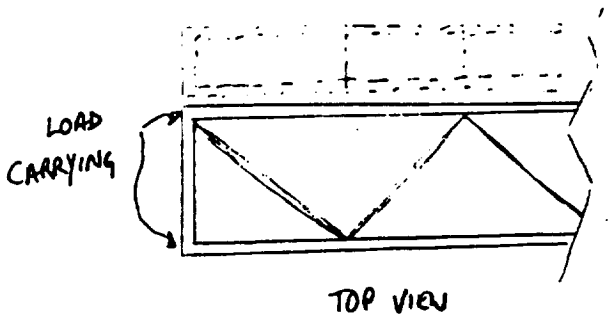

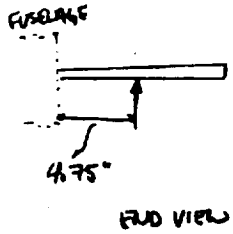

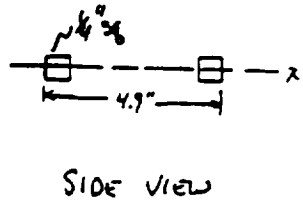

$M_X = 1.9$ in lb $\qquad I_X = 0.00065$ in^4

$A = 0.0625$ in^2 $\qquad y = 0.125$ in

Appendix B-3

Empennage Analysis

VERTICAL TAIL:

Again a simple cantilever beam analysis is used. The maximum load on the vertical tail is 0.35 lbs as determined by the stability and control group. The vertical tail is configured as follows:

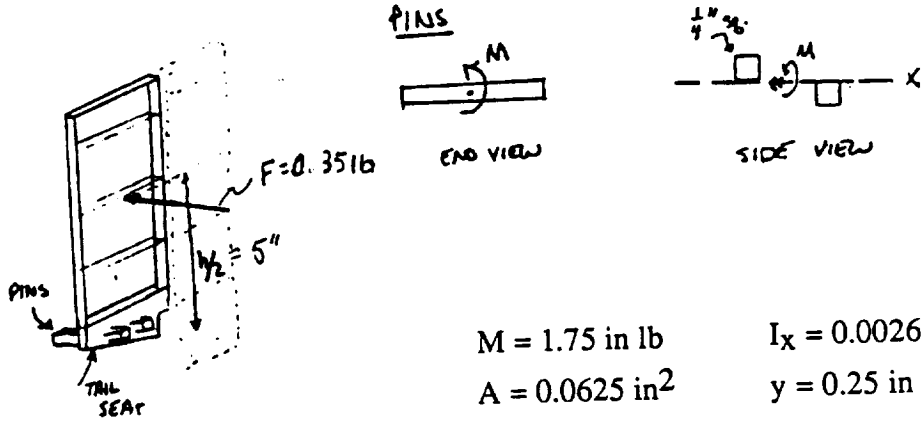

$M = 1.75$ in lb $\quad I_x = 0.0026$ in^4

$A = 0.0625$ in^2 $\quad y = 0.25$ in

It is assumed that the load acts halfway up the tail giving a bending moment of $M = L * h/2 = 1.75$ in lb. This moment will transfer directly in to the pins which can be analyzed as cantilevered beams. See above diagrams. Calculating as in Appendix B-1 axial stress is found to be 168 psi. It must also be ensured that the main area of the tail will not break away from the seat. Assume that the leading and trailing edge will carry all of the load. By the below analysis axial stress is 336 psi.

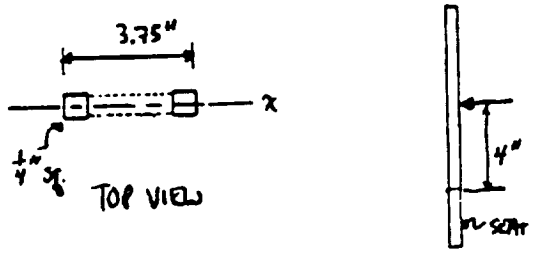

$M_x = 1.75$ in lb $\quad I_x = 0.00065$ in^4

$A = 0.0625$ in^2 $\quad y = 0.125$ in

Appendix B-4
Landing Gear Computer Code and Data

This computer code makes use of the cantilever beam analysis of the strut of the landing gear. The code varies the loading on the beam, the material of the beam and the radius and length of the beam. This simple code provided data, the corresponding deflection for the particular load, radius and length, to be analyzed for the sizing of the gear. The code and samples of the data provided are presented here in the code.

PROGRAM TRADE

```
      PROGRAM  TRADE
C        WRITTEN BY JERRY ZUROVCHAK
C           AE441 DESIGN
C
      REAL P,DELTA,I,R,L
      WRITE(1,*) 'ENTER THE WRITE CODE'
      READ(1,*)IWR
    5 WRITE(1,*)  'ENTER A LENGTH (in) '
      READ(1,*)L
      WRITE(1,*) 'ENTER A MODULUS OF ELASTICITY (psi)'
      READ(1,*)E
      PI=4.0*ATAN(1.0)
      WRITE(IWR,*) '  Modulus of Elasticity =',E
      WRITE(IWR,*) '  Load(lb)  Deflection(in)'
        DO 10 J=1,8
      R=J/64.0
        DO 20 J=10,100,10
      P=J
      I=(PI*R**4)/4.0
      DELTA=-P*L**3/(3*E*I)
      WRITE(IWR,99) P,DELTA
   20 CONTINUE
   10 CONTINUE
        WRITE(1,*)  'IF YOU WISH TO CONTINUE, ENTER 1.  IF NOT ENTER
        READ(1,*) IX
        IF(IX .EQ. 1) GOTO 5
   99 FORMAT(1X,F7.1,3X,E7.2,3X,F11.3)
          STOP
            END
```

Length = 2.00000 Modulus of Elasticity = 1.000000E+07

Radius(in)	Load(lb)	Deflection(in)
0.0156	10.00	-56.964
0.0156	20.00	-113.928
0.0156	30.00	-170.891
0.0156	40.00	-227.855
0.0156	50.00	-284.819
0.0156	60.00	-341.783
0.0156	70.00	-398.747
0.0156	80.00	-455.710
0.0156	90.00	-512.674
0.0156	100.00	-569.638
0.0312	10.00	-3.560
0.0312	20.00	-7.120
0.0312	30.00	-10.681
0.0312	40.00	-14.241
0.0312	50.00	-17.801
0.0312	60.00	-21.361
0.0312	70.00	-24.922
0.0312	80.00	-28.482
0.0312	90.00	-32.042
0.0312	100.00	-35.602
0.0469	10.00	-0.703
0.0469	20.00	-1.407
0.0469	30.00	-2.110
0.0469	40.00	-2.813
0.0469	50.00	-3.516
0.0469	60.00	-4.220
0.0469	70.00	-4.923
0.0469	80.00	-5.626
0.0469	90.00	-6.329
0.0469	100.00	-7.033
0.0625	10.00	-0.223
0.0625	20.00	-0.445
0.0625	30.00	-0.668
0.0625	40.00	-0.890
0.0625	50.00	-1.113
0.0625	60.00	-1.335
0.0625	70.00	-1.558
0.0625	80.00	-1.780
0.0625	90.00	-2.003
0.0625	100.00	-2.225
0.0781	10.00	-0.091
0.0781	20.00	-0.182
0.0781	30.00	-0.273
0.0781	40.00	-0.365
0.0781	50.00	-0.456
0.0781	60.00	-0.547
0.0781	70.00	-0.638
0.0781	80.00	-0.729
0.0781	90.00	-0.820
0.0781	100.00	-0.911
0.0937	10.00	-0.044
0.0937	20.00	-0.088
0.0937	30.00	-0.132
0.0937	40.00	-0.176
0.0937	50.00	-0.220
0.0937	60.00	-0.264
0.0937	70.00	-0.308
0.0937	80.00	-0.352
0.0937	90.00	-0.396
0.0937	100.00	-0.440
0.1094	10.00	-0.024
0.1094	20.00	-0.047
0.1094	30.00	-0.071
0.1094	40.00	-0.095
0.1094	50.00	-0.119
0.1094	60.00	-0.142
0.1094	70.00	-0.166
0.1094	80.00	-0.190
0.1094	90.00	-0.214
0.1094	100.00	-0.237
0.1250	10.00	-0.014
0.1250	20.00	-0.028
0.1250	30.00	-0.042
0.1250	40.00	-0.056
0.1250	50.00	-0.070
0.1250	60.00	-0.083
0.1250	70.00	-0.097
0.1250	80.00	-0.111

0.1250	90.00	-0.125
0.1250	100.00	-0.139

Modulus of Elasticity = 1.000000E+07

Length = 3.00000

Radius(in)	Load(lb)	Deflection(in)
0.0156	10.00	-192.253
0.0156	20.00	-384.506
0.0156	30.00	-576.758
0.0156	40.00	-769.011
0.0156	50.00	-961.264
0.0156	60.00	-1153.517
0.0156	70.00	-1345.770
0.0156	80.00	-1538.022
0.0156	90.00	-1730.275
0.0156	100.00	-1922.528
0.0312	10.00	-12.016
0.0312	20.00	-24.032
0.0312	30.00	-36.047
0.0312	40.00	-48.063
0.0312	50.00	-60.079
0.0312	60.00	-72.095
0.0312	70.00	-84.111
0.0312	80.00	-96.126
0.0312	90.00	-108.142
0.0312	100.00	-120.158
0.0469	10.00	-2.373
0.0469	20.00	-4.747
0.0469	30.00	-7.120
0.0469	40.00	-9.494
0.0469	50.00	-11.867
0.0469	60.00	-14.241
0.0469	70.00	-16.614
0.0469	80.00	-18.988
0.0469	90.00	-21.361
0.0469	100.00	-23.735
0.0625	10.00	-0.751
0.0625	20.00	-1.502
0.0625	30.00	-2.253
0.0625	40.00	-3.004
0.0625	50.00	-3.755
0.0625	60.00	-4.506
0.0625	70.00	-5.257
0.0625	80.00	-6.008
0.0625	90.00	-6.759
0.0625	100.00	-7.510
0.0781	10.00	-0.308
0.0781	20.00	-0.615
0.0781	30.00	-0.923
0.0781	40.00	-1.230
0.0781	50.00	-1.538
0.0781	60.00	-1.846
0.0781	70.00	-2.153
0.0781	80.00	-2.461
0.0781	90.00	-2.768
0.0781	100.00	-3.076
0.0937	10.00	-0.148
0.0937	20.00	-0.297
0.0937	30.00	-0.445
0.0937	40.00	-0.593
0.0937	50.00	-0.742
0.0937	60.00	-0.890
0.0937	70.00	-1.038
0.0937	80.00	-1.187
0.0937	90.00	-1.335
0.0937	100.00	-1.483
0.1094	10.00	-0.080
0.1094	20.00	-0.160
0.1094	30.00	-0.240
0.1094	40.00	-0.320
0.1094	50.00	-0.400
0.1094	60.00	-0.480
0.1094	70.00	-0.561
0.1094	80.00	-0.641
0.1094	90.00	-0.721
0.1094	100.00	-0.801
0.1250	10.00	-0.047
0.1250	20.00	-0.094
0.1250	30.00	-0.141
0.1250	40.00	-0.188
0.1250	50.00	-0.235
0.1250	60.00	-0.282

0.1250	70.00	-0.329
0.1250	80.00	-0.375
0.1250	90.00	-0.422
0.1250	100.00	-0.469

Length = 4.00000 Modulus of Elasticity = 1.000000E+07

Radius(in)	Load(lb)	Deflection(in)
0.0156	10.00	-455.710
0.0156	20.00	-911.421
0.0156	30.00	-1367.131
0.0156	40.00	-1822.841
0.0156	50.00	-2278.552
0.0156	60.00	-2734.262
0.0156	70.00	-3189.972
0.0156	80.00	-3645.683
0.0156	90.00	-4101.393
0.0156	100.00	-4557.104
0.0312	10.00	-28.482
0.0312	20.00	-56.964
0.0312	30.00	-85.446
0.0312	40.00	-113.928
0.0312	50.00	-142.409
0.0312	60.00	-170.891
0.0312	70.00	-199.373
0.0312	80.00	-227.855
0.0312	90.00	-256.337
0.0312	100.00	-284.819
0.0469	10.00	-5.626
0.0469	20.00	-11.252
0.0469	30.00	-16.878
0.0469	40.00	-22.504
0.0469	50.00	-28.130
0.0469	60.00	-33.756
0.0469	70.00	-39.382
0.0469	80.00	-45.008
0.0469	90.00	-50.634
0.0469	100.00	-56.261
0.0625	10.00	-1.780
0.0625	20.00	-3.560
0.0625	30.00	-5.340
0.0625	40.00	-7.120
0.0625	50.00	-8.901
0.0625	60.00	-10.681
0.0625	70.00	-12.461
0.0625	80.00	-14.241
0.0625	90.00	-16.021
0.0625	100.00	-17.801
0.0781	10.00	-0.729
0.0781	20.00	-1.458
0.0781	30.00	-2.187
0.0781	40.00	-2.917
0.0781	50.00	-3.646
0.0781	60.00	-4.375
0.0781	70.00	-5.104
0.0781	80.00	-5.833
0.0781	90.00	-6.562
0.0781	100.00	-7.291
0.0937	10.00	-0.352
0.0937	20.00	-0.703
0.0937	30.00	-1.055
0.0937	40.00	-1.407
0.0937	50.00	-1.758
0.0937	60.00	-2.110
0.0937	70.00	-2.461
0.0937	80.00	-2.813
0.0937	90.00	-3.165
0.0937	100.00	-3.516
0.1094	10.00	-0.190
0.1094	20.00	-0.380
0.1094	30.00	-0.569
0.1094	40.00	-0.759
0.1094	50.00	-0.949
0.1094	60.00	-1.139
0.1094	70.00	-1.329
0.1094	80.00	-1.518
0.1094	90.00	-1.708
0.1094	100.00	-1.898
0.1250	10.00	-0.111
0.1250	20.00	-0.223
0.1250	30.00	-0.334
0.1250	40.00	-0.445

0.1250	50.00	-0.556
0.1250	60.00	-0.668
0.1250	70.00	-0.779
0.1250	80.00	-0.890
0.1250	90.00	-1.001
0.1250	100.00	-1.113

Length = 5.00000 Modulus of Elasticity = 1.000000E+07

Radius(in)	Load(lb)	Deflection(in)
0.0156	10.00	-890.059
0.0156	20.00	-1780.118
0.0156	30.00	-2670.178
0.0156	40.00	-3560.237
0.0156	50.00	-4450.296
0.0156	60.00	-5340.355
0.0156	70.00	-6230.414
0.0156	80.00	-7120.474
0.0156	90.00	-8010.533
0.0156	100.00	-8900.592
0.0312	10.00	-55.629
0.0312	20.00	-111.257
0.0312	30.00	-166.886
0.0312	40.00	-222.515
0.0312	50.00	-278.143
0.0312	60.00	-333.772
0.0312	70.00	-389.401
0.0312	80.00	-445.030
0.0312	90.00	-500.658
0.0312	100.00	-556.287
0.0469	10.00	-10.988
0.0469	20.00	-21.977
0.0469	30.00	-32.965
0.0469	40.00	-43.954
0.0469	50.00	-54.942
0.0469	60.00	-65.930
0.0469	70.00	-76.919
0.0469	80.00	-87.907
0.0469	90.00	-98.895
0.0469	100.00	-109.884
0.0625	10.00	-3.477
0.0625	20.00	-6.954
0.0625	30.00	-10.430
0.0625	40.00	-13.907
0.0625	50.00	-17.384
0.0625	60.00	-20.861
0.0625	70.00	-24.338
0.0625	80.00	-27.814
0.0625	90.00	-31.291
0.0625	100.00	-34.768
0.0781	10.00	-1.424
0.0781	20.00	-2.848
0.0781	30.00	-4.272
0.0781	40.00	-5.696
0.0781	50.00	-7.120
0.0781	60.00	-8.545
0.0781	70.00	-9.969
0.0781	80.00	-11.393
0.0781	90.00	-12.817
0.0781	100.00	-14.241
0.0937	10.00	-0.687
0.0937	20.00	-1.374
0.0937	30.00	-2.060
0.0937	40.00	-2.747
0.0937	50.00	-3.434
0.0937	60.00	-4.121
0.0937	70.00	-4.807
0.0937	80.00	-5.494
0.0937	90.00	-6.181
0.0937	100.00	-6.868
0.1094	10.00	-0.371
0.1094	20.00	-0.741
0.1094	30.00	-1.112
0.1094	40.00	-1.483
0.1094	50.00	-1.854
0.1094	60.00	-2.224
0.1094	70.00	-2.595
0.1094	80.00	-2.966
0.1094	90.00	-3.336
0.1094	100.00	-3.707
0.1250	10.00	-0.217
0.1250	20.00	-0.435

0.1250	30.00	-0.652
0.1250	40.00	-0.869
0.1250	50.00	-1.086
0.1250	60.00	-1.304
0.1250	70.00	-1.521
0.1250	80.00	-1.738
0.1250	90.00	-1.956
0.1250	100.00	-2.173

Length = 6.00000 Modulus of Elasticity = 1.000000E+07

Radius(in)	Load(lb)	Deflection(in)
0.0156	10.00	-1538.022
0.0156	20.00	-3076.044
0.0156	30.00	-4614.067
0.0156	40.00	-6152.089
0.0156	50.00	-7690.111
0.0156	60.00	-9228.135
0.0156	70.00	-10766.156
0.0156	80.00	-12304.178
0.0156	90.00	-13842.201
0.0156	100.00	-15380.223
0.0312	10.00	-96.126
0.0312	20.00	-192.253
0.0312	30.00	-288.379
0.0312	40.00	-384.506
0.0312	50.00	-480.632
0.0312	60.00	-576.758
0.0312	70.00	-672.885
0.0312	80.00	-769.011
0.0312	90.00	-865.138
0.0312	100.00	-961.264
0.0469	10.00	-18.988
0.0469	20.00	-37.976
0.0469	30.00	-56.964
0.0469	40.00	-75.952
0.0469	50.00	-94.940
0.0469	60.00	-113.928
0.0469	70.00	-132.915
0.0469	80.00	-151.903
0.0469	90.00	-170.891
0.0469	100.00	-189.879
0.0625	10.00	-6.008
0.0625	20.00	-12.016
0.0625	30.00	-18.024
0.0625	40.00	-24.032
0.0625	50.00	-30.039
0.0625	60.00	-36.047
0.0625	70.00	-42.055
0.0625	80.00	-48.063
0.0625	90.00	-54.071
0.0625	100.00	-60.079
0.0781	10.00	-2.461
0.0781	20.00	-4.922
0.0781	30.00	-7.383
0.0781	40.00	-9.843
0.0781	50.00	-12.304
0.0781	60.00	-14.765
0.0781	70.00	-17.226
0.0781	80.00	-19.687
0.0781	90.00	-22.148
0.0781	100.00	-24.608
0.0937	10.00	-1.187
0.0937	20.00	-2.373
0.0937	30.00	-3.560
0.0937	40.00	-4.747
0.0937	50.00	-5.934
0.0937	60.00	-7.120
0.0937	70.00	-8.307
0.0937	80.00	-9.494
0.0937	90.00	-10.681
0.0937	100.00	-11.867
0.1094	10.00	-0.641
0.1094	20.00	-1.281
0.1094	30.00	-1.922
0.1094	40.00	-2.562
0.1094	50.00	-3.203
0.1094	60.00	-3.843
0.1094	70.00	-4.484
0.1094	80.00	-5.125
0.1094	90.00	-5.765
0.1094	100.00	-6.406

0.1250	10.00	-0.375
0.1250	20.00	-0.751
0.1250	30.00	-1.126
0.1250	40.00	-1.502
0.1250	50.00	-1.877
0.1250	60.00	-2.253
0.1250	70.00	-2.628
0.1250	80.00	-3.004
0.1250	90.00	-3.379
0.1250	100.00	-3.755

Length = 7.00000 Modulus of Elasticity = 1.000000E+07

Radius(in)	Load(lb)	Deflection(in)
0.0156	10.00	-2442.323
0.0156	20.00	-4884.646
0.0156	30.00	-7326.968
0.0156	40.00	-9769.291
0.0156	50.00	-12211.613
0.0156	60.00	-14653.936
0.0156	70.00	-17096.258
0.0156	80.00	-19538.582
0.0156	90.00	-21980.902
0.0156	100.00	-24423.227
0.0312	10.00	-152.645
0.0312	20.00	-305.290
0.0312	30.00	-457.935
0.0312	40.00	-610.581
0.0312	50.00	-763.226
0.0312	60.00	-915.871
0.0312	70.00	-1068.516
0.0312	80.00	-1221.161
0.0312	90.00	-1373.806
0.0312	100.00	-1526.452
0.0469	10.00	-30.152
0.0469	20.00	-60.304
0.0469	30.00	-90.456
0.0469	40.00	-120.609
0.0469	50.00	-150.761
0.0469	60.00	-180.913
0.0469	70.00	-211.065
0.0469	80.00	-241.217
0.0469	90.00	-271.369
0.0469	100.00	-301.521
0.0625	10.00	-9.540
0.0625	20.00	-19.081
0.0625	30.00	-28.621
0.0625	40.00	-38.161
0.0625	50.00	-47.702
0.0625	60.00	-57.242
0.0625	70.00	-66.782
0.0625	80.00	-76.323
0.0625	90.00	-85.863
0.0625	100.00	-95.403
0.0781	10.00	-3.908
0.0781	20.00	-7.815
0.0781	30.00	-11.723
0.0781	40.00	-15.631
0.0781	50.00	-19.539
0.0781	60.00	-23.446
0.0781	70.00	-27.354
0.0781	80.00	-31.262
0.0781	90.00	-35.169
0.0781	100.00	-39.077
0.0937	10.00	-1.885
0.0937	20.00	-3.769
0.0937	30.00	-5.654
0.0937	40.00	-7.538
0.0937	50.00	-9.423
0.0937	60.00	-11.307
0.0937	70.00	-13.192
0.0937	80.00	-15.076
0.0937	90.00	-16.961
0.0937	100.00	-18.845
0.1094	10.00	-1.017
0.1094	20.00	-2.034
0.1094	30.00	-3.052
0.1094	40.00	-4.069
0.1094	50.00	-5.086
0.1094	60.00	-6.103
0.1094	70.00	-7.120
0.1094	80.00	-8.138

0.1094	90.00	-9.155
0.1094	100.00	-10.172
0.1250	10.00	-0.596
0.1250	20.00	-1.193
0.1250	30.00	-1.789
0.1250	40.00	-2.385
0.1250	50.00	-2.981
0.1250	60.00	-3.578
0.1250	70.00	-4.174
0.1250	80.00	-4.770
0.1250	90.00	-5.366
0.1250	100.00	-5.963

Appendix C

The information found in this Appendix is the program code and output, used to find the three dimensional lift generated by a wing. Based upon the lifting line theory, this program utilizes a finite element method to solve for the wing lift. The lifting line theory is valid for high aspect ratio wings that have very little sweep. It allows for an accurate computation of the aerodynamic characteristics of finite wings for variation in wing planform parameters such as taper, apect ratio, and wing twist.

```
ALFORD UNIVERSITY FTN77 VER. 228S     <USER2>S474988736>STUDENT>FMECH.F77
OMPILER OPTIONS:  LISTING INTL DCLVAR NOMAP CHECK NOBIG LOGL DYNM NOOFFSET LG(
                  NOFRN FPN NOLUNFREC NOSILENT NO_OPTIMISE NOIMPURE
 0001                 PROGRAM FMECH
 0002           C     WRITTEN BY JENNIFER L. NEUMANN
 0003           C     13 FEBRUARY 1989
 0004           C
 0005           C     THIS PROGRAM WILL FIND THE FOURIER COEFFICIENTS FOR AN
 0006           C     AIRFOIL.
 0007           C
 0008                 INTEGER I,J,N,Q,K,L,M,H,JJ,KK
 0009                 REAL ALO,CLA, R,S,ALFAR,ALFAT,TR(4),B,CR,CT,C(4),MU(4),LCS
 0010                 REAL CL,GAMMA(4),VEL,TAU,SIGMA(4),BETA,SUM,CDi,RATIO(4),AZL
 0011                 REAL GANG(4),ALFA(4),A(4,4),THETA(4),Z(4),ANS(4),IT,IR
 0012                 REAL CLS(8),DEG,X,P
 0013                 INTEGER F(4),Y(4)
 0014           C
 0015                 WRITE(1,*) 'ENTER VARIABLE VALUES IN DEGREES.'
 0016                 WRITE(1,*) ' '
 0017                 WRITE(1,*) 'WHERE DO YOU WANT THE PROGRAM TO RUN?'
 0018                 WRITE(1,*) 'ENTER 1 FOR THE SCREEN AND 6 FOR THE PRINTER.'
 0019                 READ(1,*) Q
 0020                 VEL=25.0
 0021                 WRITE(Q,*) 'THE VELOCITY=',VEL,' ft/s'
 0022                 AZL=-2.0
 0023                 WRITE(Q,*) 'THE ANGLE OF ZERO LIFT=',AZL,' deg.'
 0024                 ALO=AZL/57.3
 0025                 LCS=0.09
 0026                 WRITE(Q,*) 'THE LIFT CURVE SLOPE=',LCS,' per deg'
 0027                 CLA=LCS*57.3
 0028                 AR=12.00
 0029                 WRITE(Q,*) 'THE ASPECT RATIO=',AR
 0030                 S=6.00
 0031                 WRITE(Q,*) 'THE SURFACE AREA=',S,'square feet'
 0032           C     WRITE(1,*) 'WHAT IS THE INCIDENCE ANGLE IN DEGREES?'
 0033           C     READ(1,*) IA
 0034                 DO 99 KK=1,15
 0035.01              IR=KK
 0036.01              IT=KK
 0037.01              ALFAR=IR/57.3
 0038.01              ALFAT=IT/57.3
 0039.01              DO 60 H=1,1
 0040.02              TR(H)=1.0
 0041.02              B=SQRT(AR*S)
 0042.02              WRITE(Q,*) ' '
 0043.02              WRITE(Q,*) '************************************************'
 0044.02              WRITE(Q,*) 'WHEN THE THE TAPER IS',TR(H)
 0045.02              WRITE(Q,*) ' '
 0046.02              WRITE(Q,*) 'b=',B,' feet'
 0047.02              CR=S/((B/2)*(1.0+TR(H)))
 0048.02              WRITE(Q,*) 'CR=',CR
 0049.02              CT=TR(H)*CR
 0050.02              WRITE(Q,*) 'Ct=',CT
 0051.02              N=4
 0052.02              WRITE(1,*) ' '
 0053.02        C
 0054.02              DO 10 J=1,N
 0055.03                 R=J*22.5
 0056.03                 THETA(J)=R/(57.3)
 0057.03                 C(J)=CR-((CR-CT)*COS(THETA(J)))
 0058.03                 GANG(J)=ALFAR-((ALFAR-ALFAT)*COS(THETA(J)))
 0059.03                 MU(J)=(C(J)*CLA)/(4*B)
 0060.03                 ALFA(J)=GANG(J)-ALO
 0061.03        C        WRITE(Q,*) C(J), GANG(J), MU(J), ALFA(J)
 0062.03                 Z(J)=MU(J)*ALFA(J)
 0063.03                 DO 20 I=1,N
 0064.04                    L=2*I-1
 0065.04                    A(J,I)=SIN(L*THETA(J))*(1.0+MU(J)*L/SIN(THETA(J)))
 0066.04           20    CONTINUE
 0067.03           10 CONTINUE
 0068.02              DEG=ALFA(1)*57.3
 0069.02              WRITE(Q,*) 'ANGLE OF ATTACK = ',KK,' DEGREES'
 0070.02        C
 0071.02              CALL INVRT(A,N,4,F,Y)
 0072.02              CALL MULT (A,Z,ANS,4,4,1,4,4,4)
 0073.02              WRITE(1,*) ' '
 0074.02        C
 0075.02              WRITE(Q,*) 'THE COEFFICIENTS ARE...'
```

```
0076.02          DO 30 K=1,N
0077.03             JJ=K*2-1
0078.03             WRITE(Q,*) 'A',JJ,'=',ANS(K)
0079.03       30 CONTINUE
0080.02          WRITE(Q,*) ' '
0081.02          SUM=0.0
0082.02          CL=3.14159*AR*ANS(1)
0083.02          DO 40 L=1,N
0084.03             SIGMA(L)=0.0
0085.03             DO 50 M=1,N
0086.04                P=2*M-1
0087.04                TAU=ANS(M)*SIN(P*(THETA(L)))
0088.04                SIGMA(L)=SIGMA(L)+TAU
0089.04       50    CONTINUE
0090.03             GAMMA(L)=2*B*VEL*SIGMA(L)
0091.03             CLS(L)=(2*GAMMA(L))/(VEL*C(L))
0092.03             RATIO(L)=CLS(L)/CL
0093.03             X=(B/2.)*COS(THETA(L))
0094.03             WRITE(Q,*) 'Y = ',X,'Cl = ',CLS(L),'Cl/CL =',RATIO(L)
0095.03   C          WRITE(Q,*) 'FOR THETA=',THETA(L),'radians.'
0096.03   C          WRITE(Q,*) 'Cl = ',CLS(L)
0097.03   C          WRITE(Q,*) 'Cl/CL=',RATIO(L)
0098.03             BETA=L*((ANS(L)/ANS(1))**2)
0099.03             SUM=SUM+BETA
0100.03       40 CONTINUE
0101.02          WRITE(Q,*) ' '
0102.02          WRITE(Q,*) 'CL =',CL
0103.02          CDi=(CL**2)*SUM/(3.14159*AR)
0104.02          WRITE(Q,*) 'CDi=',CDi
0105.02          WRITE(Q,*) ' '
0106.02       60 CONTINUE
0107.01       99 CONTINUE
0108             STOP
0109             END
```

```
************************************************
WHEN THE THE TAPER IS      1.00000

b=       8.48528       feet
CR=      0.707107
Ct=      0.707107
ANGLE OF ATTACK =                5 DEGREES
THE COEFFICIENTS ARE...
A              1=      1.419672E-02
A              3=      2.592424E-03
A              5=      7.128958E-04
A              7=      1.511579E-04

Y =        3.91974     Cl =       0.410112     Cl/CL =      0.766274
Y =        3.00017     Cl =       0.540508     Cl/CL =       1.00991
Y =        1.62393     Cl =       0.575554     Cl/CL =       1.07539
Y =       4.919211E-04 Cl =       0.583969     Cl/CL =       1.09112

CL =     0.535203
CDi=     8.165775E-03


************************************************
WHEN THE THE TAPER IS      1.00000

b=       8.48528       feet
CR=      0.707107
Ct=      0.707107
ANGLE OF ATTACK =                6 DEGREES
THE COEFFICIENTS ARE...
A              1=      1.622482E-02
A              3=      2.962771E-03
A              5=      8.147378E-04
A              7=      1.727515E-04

Y =        3.91974     Cl =       0.468700     Cl/CL =      0.766274
Y =        3.00017     Cl =       0.617723     Cl/CL =       1.00991
Y =        1.62393     Cl =       0.657777     Cl/CL =       1.07539
Y =       4.919211E-04 Cl =       0.667393     Cl/CL =       1.09112

CL =     0.611661
CDi=     1.066550E-02
```

Appendix D

Appendix D is the derivation for the roll moment created by a dihedral angle and rudder input. First of all, the change in angle of attack that the wing sees as a result of the dihedral angle is derived. Then, this is used to develop the equation for the roll moment.

Appendix D

Roll Due to Dihedral

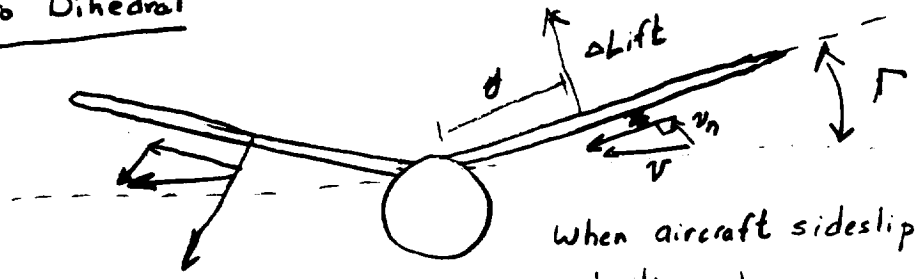

When aircraft sideslips get side velocities shown.

Wing sees velocity as shown

other side of wing sees opposite

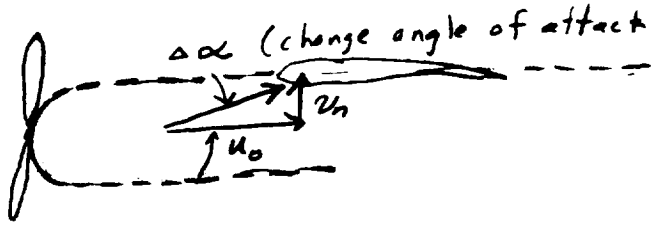

$$\Delta\alpha \approx \frac{v_n}{u_o} \qquad \text{But} \quad v_n = v \sin\Gamma$$

$$\Delta\alpha \approx \frac{v}{u_o}\sin\Gamma \qquad \text{By definition } \frac{v}{u_o} = \beta$$

$$\boxed{\Delta\alpha \approx \beta \sin\Gamma}$$

$$\Delta L\left(\begin{matrix}\text{Roll}\\ \text{moment}\end{matrix}\right) = -\Delta\text{Lift}\; y = -C_{L_\alpha}\,\Delta\alpha\, Q\, c\, y\, dy$$

$$\Delta L = C_l\, Q S b \qquad \Delta\alpha = \beta \sin\Gamma$$

$$\Delta C_l = -C_{L_\alpha}\frac{\cancel{Q} c}{\cancel{Q} S b}\beta\sin\Gamma\, y\, dy \qquad \text{assume } Q\text{'s equal}$$

$$C_l = -\frac{C_{L_\alpha}}{b^2}\beta\sin\Gamma(2)\int_0^{b/2} y\, dy = -\frac{C_{L_\alpha}}{b^2}\beta\sin\Gamma\,(2)\left[\frac{y^2}{2}\right]$$

$$C_l = -\frac{C_{L_\alpha}}{b^2}\beta\sin\Gamma\,(2)\frac{b^2}{\cancel{8}\,4}$$

Thus

$$\boxed{C_l = -\frac{C_{L_\alpha}}{4}\sin(\Gamma)\,\beta}$$